BIOINORGANIC CHEMICAL STUDIES ON COPPER COMPLEXES INVOLVING PYRROLOQUINOLINE QUINONE (PQQ) AND TRIHYDROXYPHENYLALANINE (TOPA)

Dissertation Presented by

NOBUHUMI NAKAMURA

in Partial Fulfillment of the Requirements

for the Degree of Doctor of Philosophy (Science)

Graduate School of Science

Osaka University

1993

CONTENTS

Chapter I. GENERAL INTRODUCTION

The structure of the cofactor of methanol dehydrogenase (EC 1.1.99.8) was elucidated in 1979.[1] The compound has been given the name of pyrroloquinoline quinone (PQQ) or methoxatin, as shown in Figure I-1a. After the elucidation, it appeared that many other dehydrogenases from Gram-negative bacteria contain this cofactor. By analogy with the names "flavoproteins" and "hemoproteins", this class of enzymes has been named "quinoproteins".

In 1984, the presence of covalently bound PQQ in copper-containing plasma amine oxidase (EC 1.4.3.6) was reported by two independent research groups.[2,3] Ameyama's group concluded the presence of PQQ from the spectroscopic detection of PQQ after acid hydrolysis of the enzyme.[2] On the other hand, Duine's group concluded the presence of PQQ from the HPLC-detection of PQQ (in the form of a PQQ hydrazone) after treatment of the enzyme with a hydrazine, followed by hydrolysis with proteases.[3] The latter approach, so-called "hydrazine method", established the presence of covalently bound PQQ in amine oxidases of pea seedlings[4] and pig kidney,[5] and in lysyl oxidase (EC 1.4.3.13) of human placenta.[6] Moreover, using this approach, Duine and his co-workers have reported that PQQ is present in proteins as disparate as methylamine dehydrogenase (EC 1.4.99.3) from *Thiobacillus versutus*[7] and in metalloproteins like dopamine β-hydroxylase (EC 1.14.17.1),[8] galactose oxidase (EC 1.1.3.9),[9] and lipoxygenase-1 (EC 1.13.11.12).[10] Application of resonance Raman spectroscopy to hydrazine-derivatized plasma amine oxidase[11] and lysyl oxidase from bovine aorta[12] also showed the presence of covalently bound PQQ.

However, recent investigations show that the concept of covalently bound

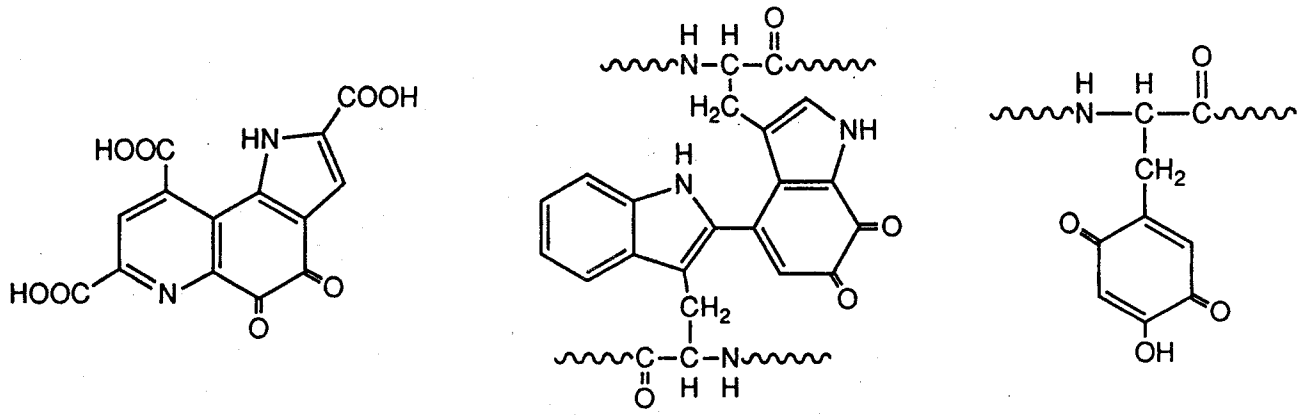

(a) pyrroloquinoline quinone (PQQ or H_4pqq) (b) tryptophan tryptophylquinone (TTQ) (c) topa quinone (TPQ)

Figure I-1. Cofactors of quinoproteins.

PQQ is not tenable in a number of cases (even perhaps in all cases). For example, although PQQ can be extracted as a derivative from methylamine dehydrogenase,[7] the X-ray diffraction patterns indicated that an active site lacks the pyridine ring present in authentic PQQ,[13] so that it was concluded that the hydrazine method is unsuited to reveal the cofactor. Evidence from structural investigations[14] and from the sequencing of the gene of the cofactor-bearing small subunit of methylamine dehydrogenase from *Methylobacterium extorquens* AM1[15] and *Thiobacillus versutus*[16] indicates that a tryptophan dimer with an *o*-quinone group (tryptophan tryptophylquinone, TTQ, see Figure I-1b) is the cofactor of this enzyme.

A similar remarkable development has taken place with respect to plasma amine oxidase. Klinman and co-workers showed a method of derivatization with hydrazines under mild conditions which is then followed by hydrolysis with thermolysin and mass spectrometry.[17] They demonstrated the presence of 6-hydroxydopa quinone (the quinone form of trihydroxyphenylalanine) or topa quinone (TPQ, see Figure I-1c) instead of PQQ.[17]

In addition, it seems that PQQ formation can even start with precursors having a much simpler structure. Several enzymes which have these precursors, such as dopamine β-hydroxylase,[18] galactose oxidase,[19,20] soybean lipoxygenase-1,[21] and dopa decarboxylase,[22] no longer belong to the category of quinoprotein. Much conflicting data have appeared in the literatures regarding the nature of the active sites of quinoproteins. As a summery, quinoproteins which contain PQQ, TPQ, or TTQ are listed in Table I-1.

As described above, recent developments show that almost metalloprotein, such as amine oxidase,[17] dopamine β-hydroxylase,[18] and galactose oxidase,[19,20]

Table I-1. Quinoproteins

enzyme	cofactor	metal ion
methanol dehydrogenase	PQQ	Ca^{2+}
alcohol dehydrogenase	PQQ	Ca^{2+}
glucose dehydrogenase	PQQ	Ca^{2+}
lupanine hydroxylase	PQQ	Ca^{2+}
methylamine dehydrogenase	TTQ	–
methylamine oxidase	TPQ	Cu^{2+}
plasma amine oxidase	TPQ	Cu^{2+}
pig kidney diamine oxidase	TPQ	Cu^{2+}
pea seedling amine oxidase	TPQ	Cu^{2+}

do not have PQQ. However, it is clear that PQQ occurs in many dehydrogenases produced by Gram-negative bacteria, although the presence of it in other organisms like plants and animals, is controversial.[23-25] In addition, despite the absence of PQQ in amine oxidases, the reactions between PQQ and amines are still attracting much attention. Ohshiro and co-workers have reported the reaction of PQQ with amines, where the effective deamination of amines by PQQ has been demonstrated.[26-28] Moreover, Suzuki and co-workers have described the preparation and characterization of ternary copper(II) complexes containing PQQ or 1-methyl PQQ and bipyridine or terpyridine.[29-31] They suggested Cu(H_2pqq)(terpy) and Cu(1-Me-Hpqq)(terpy) promote the oxidative deamination of benzylamine to benzaldehyde by factors of 15 and 5 compared with free PQQ and free 1-Me-PQQ, respectively.[29,30] Although other several studies on the complex formations of PQQ and its analogous have been reported so far,[32-34] nothing is known about the structure of the transition metal complex of PQQ by X-ray crystal analysis.

In Chapter II of this thesis, the PQQ-containing copper(II) complexes are studied in order to reveal the molecular structure. Chapter III deals with the molecular structure of tripotassium Hpqq salt in order to compare with those of the other related compounds. Besides, to know the redox properties of PQQ and the PQQ-containing complex is important for understandings of the electron transfer processes in PQQ-containing oxidoreductases. Chapter IV deals with the electrochemical properties of PQQ and the PQQ-containing copper (II) complex.

TPQ has been identified as a novel redox cofactor in bovine serum amine oxidase in 1990.[17] TPQ and TOPA (the reduced form of TPQ) are very reactive

compounds. For that reason, their properties are scarcely known, although the absorption maxima of TPQ have been reported.[35] Needless to say, no TPQ- or TOPA-containing complex is reported. In Chapter V, synthesis, characterization, and catalytic activity of the first TOPA-containing copper(II) complexes to shed light on the relationships between nonblue copper and the organic cofactor in copper-containing amine oxidases. Finally, Chapter VI deals with the molecular structure of the first TOPA-containing copper(II) complex, [Cu(DL-topa)(bpy)(H_2O)]BF_4·3H_2O.

References

(1) Salisbury, S. A.; Forrest, H. S.; Cruse, W. B. T.; Kennard, O. *Nature (London)* **1979**, *281*, 843–844.

(2) Ameyama, M.; Hayashi, M.; Matsushita, K.; Shinagawa, E.; Adachi, O. *Agric. Biol. Chem.* **1984**, *48*, 561–565.

(3) Lobenstein-Verbeek, C. L.; Jongejan, J. A.; Frank, J.; Duine, J. A. *FEBS Lett.* **1984**, *170*, 305–309.

(4) Glatz, Z.; Kovar, J.; Machola, L.; Pec, P. *Biochem. J.* **1987**, *242*, 603–606.

(5) van der Meer, R. A.; Jongejan, J. A.; Duine, J. A. *FEBS Lett.* **1986**, *206*, 111–114.

(6) van der Meer, R. A.; Duine, J. A. *Biochem. J.* **1986**, *239*, 789–791.

(7) van der Meer, R. A.; Jongejan, J. A.; Duine, J. A. *FEBS Lett.* **1987**, *221*, 299–304.

(8) van der Meer, R. A.; Jongejan, J. A.; Duine, J. A. *FEBS Lett.* **1988**, *231*, 303–307.

(9) van der Meer, R. A.; Jongejan, J. A.; Duine, J. A. *J. Biol. Chem.* **1989**, *264*, 7792–7794.

(10) van der Meer, R. A.; Duine, J. A. *FEBS Lett.* **1988**, *235*, 194–200.

(11) Moog, R. S.; McGuirl, M. A.; Cote, C. E.; Dooley, D. M. *Proc. Natl. Acad. Sci. USA* **1986**, *83*, 8435–8439.

(12) Williamson, J. R.; Moog, R. S.; Dooley, D. M.; Kagan, H. M. *J. Biol. Chem.* **1986**, *261*, 16302–16305.

(13) Vellieux, F. M. D.; Huitema, F.; Groendijk, H.; Kalk, H. H.; Frank, J.; Jongejan, J. A.; Duine, J. A.; Petratos, K.; Drenth, J.; Hol, W. G. J. *EMBO J.*

1989, *8*, 2171–2178.

(14) McIntire, W. S.; Wemmer, D. E.; Chistoserdov, A. Y.; Lidstrom, M. E. *Science* **1991**, *252* 817–824.

(15) Chistoserdov, A. Y.; Tsygankov, Y. D.; Lidstrom, M. E. *Biochem. Biophys. Res. Commun.* **1990**, *172*, 211–216.

(16) Ubbink, M.; van Kleef, M. A. G.; Kleinjan, D.-J.; Hoitink, C. W. G.; Huitema, F.; Beintema, J. J., Duine, J. A. Canters, G. W. *Eur. J. Biochem.* **1991**, *202*, 1003–1012.

(17) Janes, S. M.; Mu, D.; Wemmer, D. M.; Smith, A. J.; Kaur, S.; Maltby, D.; Burlingame, A. L.; Klinman, J. P. *Science* **1990**, *248*, 981–987.

(18) Robertson, J. G.; Kumar, A.; Mancewicz, J. A.; Villafranca, J. J. *J. Biol. Chem.* **1989**, *264*, 19916–19921.

(19) Whittaker, M. M.; Whittaker, J. *J. Biol. Chem.* **1990**, *265*, 9610–9613.

(20) Ito, N.; Keen, J. N.; Knowles, P. F.; McPherson, M. J.; Phillips, S. E. V.; Stevens, C.; Yadav, K. D. S. *Biochem. Soc. Trans.* **1990**, *18*, 931–932.

(21) Veldink, G. A.; Boelens, H.; Maccaroni, M.; van der Lecq, F.; Vliegenthart, J. F. G.; Paz, M. A.; Flueckiger, R.; Gallop, P. M. *FEBS Lett.* **1990**, *270*, 135–138.

(22) De. Biase, D.; Maras, B.; John, R. A. *FEBS Lett.* **1991**, *278*, 120–122.

(23) van der Meer, R. A.; Groen, B. W.,; Jongejan, J. A.; Duine, J. A. *FEBS Lett.* **1990**, *261*, 131–134.

(24) Paz, M. A.; Flueckiger, R.; Gallop, P. M. *FEBS Lett.* **1990**, *264*, 283.

(25) van der Meer, R. A.; Groen, B. W.; Jongejan, J. A.; Duine, J. A. *FEBS Lett.* **1990**, *264*, 284.

(26) Itoh, S.; Kitamura, Y.; Ohshiro, Y.; Agawa, T. *Bull. Chem. Soc. Jpn.* **1986**, *59*, 1907–1910.

(27) Itoh, S.; Mure, M.; Ohshiro, Y. *J. Jpn. Oil Chem. Soc.* **1987**, *36*, 882–883.

(28) Ohshiro, Y.; Itoh, S. *Bioorg. Chem.* **1991**, *19*, 169–189.

(29) Suzuki, S.; Sakurai, T.; Itoh, S.; Ohshiro, Y. *Inorg. Chem.* **1988**, *27*, 591–592.

(30) Suzuki, S.; Sakurai, T.; Itoh, S.; Ohshiro, Y. *Nippon Kagaku Kaishi* **1988**, 421–424.

(31) Suzuki, S.; Sakurai, T.; Itoh, S.; Ohshiro, Y. *Chem. Lett.* **1988**, 777–780.

(32) Noar, J. B.; Rodriguez, E. J.; Bruice, T. C. *J. Am. Chem. Soc.* **1985**, *107*, 7198–7199.

(33) Jongejan, J. A.; van der Meer, R. A.; van Zuylen, G. A.; Duine, J. A. *Recl. Trav. Chim. Pays-Bas* **1987**, *106*, 365.

(34) Schwederski, B.; Kasack, V.; Kaim, W.; Roth, E.; Jordanov, J. *Angew. Chem., Int. Ed. Engl.* **1990**, *29*, 78–79.

(35) Graham, D. G.; Jeffs, P. W. *J. Biol. Chem.* **1977**, *252*, 5729–5734.

Chapter II. SYNTHETIC AND STRUCTURAL STUDIES ON COPPER(II) COMPLEXES CONTAINING COENZYME PQQ AND TERPYRIDINE

Introduction

Since pyrroloquinoline quinone (PQQ; 1*H*-pyrrolo[2,3-*f*]quinoline-4,5-quinone-2,7,9-tricarboxylic acid) was first recognized as a coenzyme for alcohol dehydrogenases in methylotrophic bacteria,[1] it has been remarked to be also a coenzyme in numerous oxidoreductases.[2] In 1984, two research groups independently reported that copper-containing amine oxidases contain covalently bound PQQ, and accordingly the structural and the functional interactions between Cu and PQQ at the active site were of interest.[3,4] However, the most plausible candidate of an organic cofactor in the amine oxidases was demonstrated to be topa quinone (6-hydroxydopa quinone) residue, as mentioned in many recent papers.[5-11]

Ca(II) and Sr(II) ions are essential for the reconstitution of alcohol dehydrogenase from the apoenzyme plus PQQ.[12,13] Some transition metal ions are also required for the reconstitutions of membrane glycerol dehydrogenase (Co(II) and Ni(II))[14] and membrane-bound aldehyde dehydrogenase (Mn(II)).[15] Moreover, nitrile hydratase have been described to contain PQQ and Fe(III) in the active center.[16] Consequently, it is important to know about the interaction between PQQ and metal ion.

Several studies on the metal complexes of PQQ and its analogues have

been reported so far.[17-22] PQQ possesses three binding sites as a multidentate ligand (Figure II-1). Suzuki and co-workers presented the preparation and characterization of ternary Cu(II) complexes containing PQQ or 1-methyl PQQ and 2,2'-bipyridine (bpy) or 2,2':6',2"-terpyridine (terpy), in which the bindings of PQQ and its derivative to Cu(II) probably take place at their pyridine moieties (site 1 in Figure II-1).[19-21] Moreover, the binding site of PQQ with *cis*-$[Ru(bpy)_2Cl_2]$ has been demonstrated to be the *o*-quinone moiety (site 2 in Figure II-1).[22] However, there has been no report on the crystal structure of transition metal complex containing PQQ.

In this chapter, the author describes synthetic and spectroscopic investigations of the PQQ-containing mononuclear and dinuclear Cu(II) complexes ($[Cu(H_2pqq)(terpy)]$ (**1**) and $[Cu_2(\mu\text{-}pqq)(terpy)_2]$ (**2**), respectively) together with the X-ray crystal analysis of complex **2**.

Experimental Section

PQQ was purchased from Ube Industries (Tokyo, Japan). $[Cu(terpy)](NO_3)_2 \cdot H_2O$ was synthesized from Cu(II) nitrate according to a method described in the previous paper.[23] Other commercial chemicals were used without further purification. The diffuse reflectance spectra were recorded on a Hitachi U-3400 spectrophotometer.

Preparation of Complex 1: $[Cu(H_2pqq)(terpy)]$.[19] Complex **1** was obtained as follows. PQQ (30 μmol) was dissolved in about 2 cm^3 of 0.1 M KOH solution, and then the pH value of the solution was adjusted to about 7 by addition of 0.1 M

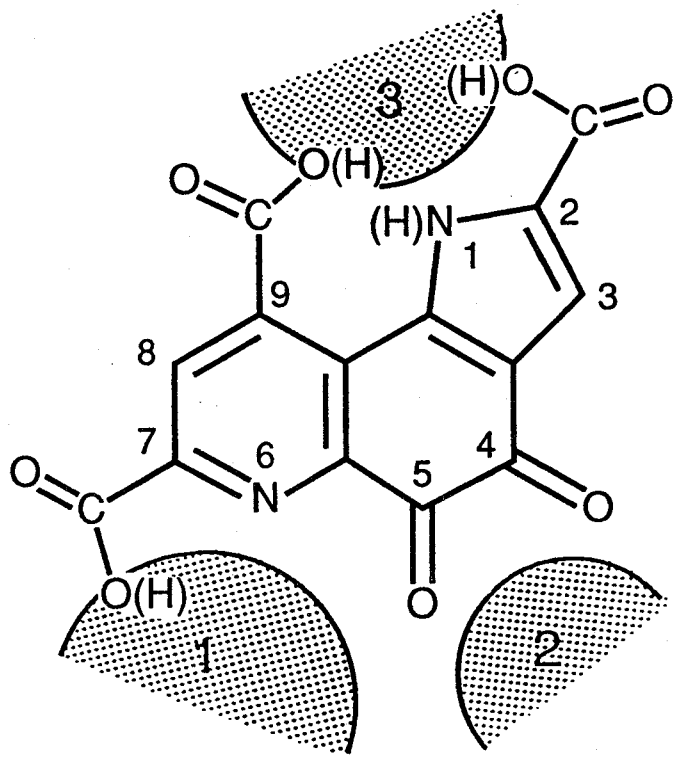

Figure II-1. Coordination sites of (H_4)pqq.

HCl solution. After the solution was added to an aqueous solution (2 cm^3) of $[Cu(terpy)](NO_3)_2 \cdot H_2O$ (60 μmol), the pH value of the mixture was adjusted to about 3 by addition of 0.1 M HCl solution. The reddish brown powder was collected by filtration, washed with water, and then dried in vacuo overnight. Anal. Calcd for $C_{29}H_{15}N_5O_8Cu \cdot 2.5H_2O$: C, 51.98; H, 3.01; N, 10.45 %. Found: C, 52.04; H, 3.06; N, 10.51 %.

Preparation of Complex 2: $[Cu_2(\mu\text{-pqq})(terpy)_2]$. PQQ (30 μmol) was dissolved in about 2 cm^3 of 0.1 M KOH solution. $[Cu(terpy)](NO_3)_2 \cdot H_2O$ (60 μmol) in 2 cm^3 of water was added to the solution. The pH value of the mixture was adjusted to 7.0 by addition of 0.1 M HCl solution. The resulting yellowish green solution was allowed to stand at room temperature. After a few days, microcrystals appeared, which were collected by filtration and washed with water. The dark-green microcrystals were powdered and then dried in vacuo overnight. Anal. Calcd for $C_{44}H_{24}N_8O_8Cu_2 \cdot 7H_2O$: C, 50.52; H, 3.66; N, 10.71 %. Found: C, 50.26; H, 3.66; N, 10.67 %.

Complex **2** could also be obtained as follows. Complex **1** (60 μmol) was dissolved in a minimum quantity of 0.1 M KOH solution and then the pH value of the solution was adjusted to 7.0 by addition of 0.1 M HCl solution. The reddish brown solution was allowed to stand at room temperature. After a few days, the resulting dark-green microcrystals were collected by filtration and washed with water. The microcrystals were dried in vacuo overnight. Anal. Calcd for $C_{44}H_{24}N_8O_8Cu_2 \cdot 6H_2O$: C, 51.41; H, 3.53; N, 10.90 %. Found: C, 51.40; H, 3.41; N, 10.86 %.

Crystallographic Structure Determination on $[Cu_2(\mu\text{-pqq})(terpy)_2]\cdot 12H_2O \cdot CH_3CN$. The crystals suitable for X-ray diffraction were obtained as follows. Complex **1** was dissolved in 0.1 M KOH solution. After the pH value of the solution was adjusted to 7.0 by the addition of 0.1 M HCl solution, a small amount of acetonitrile was added to it. The mixture was allowed to stand at room temperature. After a few weeks, dark-green crystals were obtained as needles. A needle-shaped crystal was sealed in a glass capillary to retard loss of water and acetonitrile of crystallization. Diffraction data were collected using a Rigaku AFC-5R automated four-circle diffractometer with Ni-filtered Cu $K\alpha$ radiation. The unit cell constants were refined from 12 centered reflections ($13° < 2\theta < 21°$). Intensity data in the range $2\theta < 120°$ were collected by the ω–2θ scan technique. Intensities of three reflections, chosen as standards and measured every 100 reflections, showed no significant variations (< 2 %). Data were corrected for Lorentz and polarization effects. An empirical absorption correction based on a series of ψ-scans was applied to the data.[24] The crystallographic data are summarized in Table II-1.

The structure was solved by the direct method (**MULTAN 78**)[25] and refined by a block-diagonal least squares method using the program **HBLS-V**.[26] Anisotropic temperature factors were used for non-hydrogen atoms. The position of the hydrogen atoms, except on the water and acetonitrile, were calculated based on the molecular geometry. These hydrogen atoms with isotropic temperature factors were included in further refinement. The weighting scheme used was $w = 1 / \sigma^2(F_o)$. The final R and R_w values were 0.078 and 0.062 for 2137 reflections ($|F_o| > 3\,\sigma|F_o|$), respectively. All the computations were carried out on an ACOS 2020 computer at the Computation Center, Osaka

Table II-1. Crystallographic Data for $[Cu_2(\mu\text{-pqq})(terpy)_2]\cdot 12H_2O\cdot CH_3CN$ (2)

formula	$C_{46}H_{51}N_9O_{20}Cu_2$
fw	1177.05
color and habit	dark-green needles
cryst system	triclinic
space group	$P\bar{1}$
a, Å	22.466 (3)
b, Å	10.862 (5)
c, Å	10.890 (2)
α, deg	94.93 (3)
β, deg	97.36 (2)
γ, deg	90.31 (2)
V, Å^3	2626 (1)
Z	2
cryst dimens, nm	0.10 × 0.10 × 0.31
D_{calcd}, g cm^{-3}	1.489
μ(Cu Kα), cm^{-1}	16.86
F(000)	1216
scan method	ω–2θ
2θ range, deg	0–120
no. of unique data collcd	7807
no. of data used in refinement	2137 ($\|Fo\| > 3\sigma\|Fo\|$)
R^a	0.078
$R_w{}^b$	0.062

$^aR = \Sigma\|\|Fo\|-\|Fc\|\|/\Sigma|Fo|$. $^bR_w = [\Sigma w(|Fo|-|Fc|)^2/\Sigma w(Fo)^2]^{1/2}$.

University, and on an ACOS S-850 computer at the Crystallographic Research Center, Institute for Protein Research, Osaka University.

The atomic positional parameters and equivalent isotropic temperature factors for the non-hydrogen atoms, the atomic coordinates of the hydrogen atoms, and the non-hydrogen anisotropic thermal parameters are listed in Appendix I.

Results and Discussion

Syntheses of Ternary Cu(II) Complexes Containing PQQ. The preparation of ternary Cu(II) complexes containing PQQ are shown in Scheme II-1. The mononuclear (complex **1**) and dinuclear (complex **2**) Cu(II) complexes were obtained at pH 3 and 7, respectively, regardless of the molar ratio of PQQ to $[Cu(terpy)]^{2+}$. This finding means that the binding of the second $[Cu(terpy)]^{2+}$ complex to PQQ is affected by the change of the pH value. At pH > 3, two carboxyl groups (C-7 and C-9 in Figure II-1) of the pyridine ring are dissociated, and the pyridine (N-6) and the *o*-quinone (C-4 and C-5) moieties are unprotonated.[27] On the other hand, the acid dissociation constants (pKa) of the carboxyl group (C-2) of the pyrrole ring and the pyrrole moiety (N-1) are 3.3 and 10.3, respectively.[27,28] Taking into account these pKa values, the possible binding sites of PQQ to the first and the second $[Cu(terpy)]^{2+}$ complexes seems to be site 1[19] and site 3 in Figure II-1, respectively (see *vide infra*). Therefore, complexes **1** and **2** are probably produced under acidic and neutral pH conditions, respectively.

Scheme II-1.

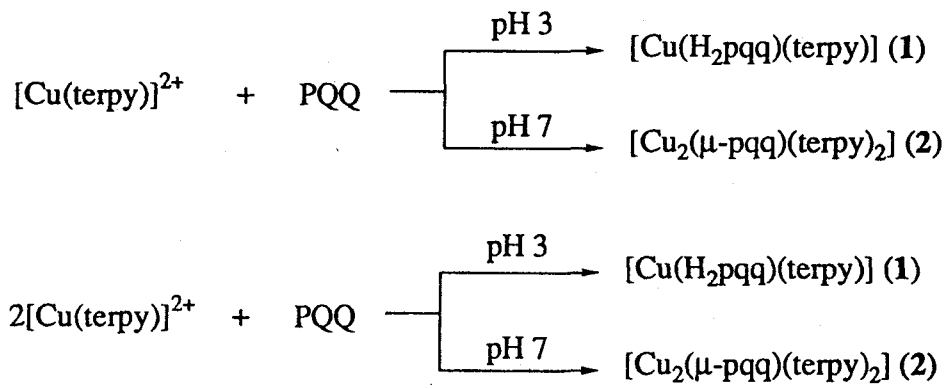
[Cu(terpy)]2+ + PQQ
pH 3
[Cu(H2pqq)(terpy)] (1)
pH 7
[Cu2(μ-pqq)(terpy)2] (2)
2[Cu(terpy)]2+ + PQQ
pH 3
[Cu(H2pqq)(terpy)] (1)
pH 7
[Cu2(μ-pqq)(terpy)2] (2)

Crystal Structure of $[Cu_2(\mu\text{-pqq})(terpy)_2]\cdot 12H_2O\cdot CH_3CN$. A view showing the features of complex **2** is given in Figure II-2. The bond lengths and the bond angles are presented in Table II-2 and Table II-3, respectively. Poor crystal quality requires that some caution must be exercised in interpreting the crystallographic results.[29] In particular, bond distances and angles should be discussed as less accurate than estimated standard deviations. The molecular structure of complex **2** consists of two six-coordinate Cu atoms bridged by pqq with two coordinating terpy ligands in the terminal positions. Each copper ion, Cu(1) and Cu(2), occupies site 1 and site 3 of pqq (Figure II-1), respectively. pqq acts as a tridentate ligand, being perpendicular to two terpyridine rings which are almost parallel to each other (Figure II-3). The dihedral angles between the pqq ring and the terpy 1 or terpy 2 ring are estimated to be 82.4° and 92.6°, respectively. On the other hand, dihedral angle between two terpy rings is estimated to be 24.3 °.

The coordination spheres of two Cu(II) ions are nearly identical, as shown in Figure II-4. Each Cu(II) ion is basically in a distorted octahedral geometry with three nitrogens of terpy and one nitrogen of pqq in the plane and with two oxygens of pqq in the remote axial positions. The long axial Cu–O bonds are due to the Jahn-Teller effect. The conformational geometries of two terpy ligands reveal the similar bond lengths and angles. The nitrogen atoms [N(2t) and N(5t)] of the central pyridine rings are bound to the Cu(II) ions at significantly shorter distances (Cu(1)–N(2t) = 1.96 (1) Å and Cu(2)–N(5t) = 1.98 (1) Å), as a result of the constrained complex formation. The constraint due to the chelation of the terpy ligands also appears in the N(1t)–Cu(1)–N(3t) and N(4t)–Cu(2)–N(6t) angles of 160.1 (6)° and 160.2 (6)°, respectively. These bond lengths and angles are

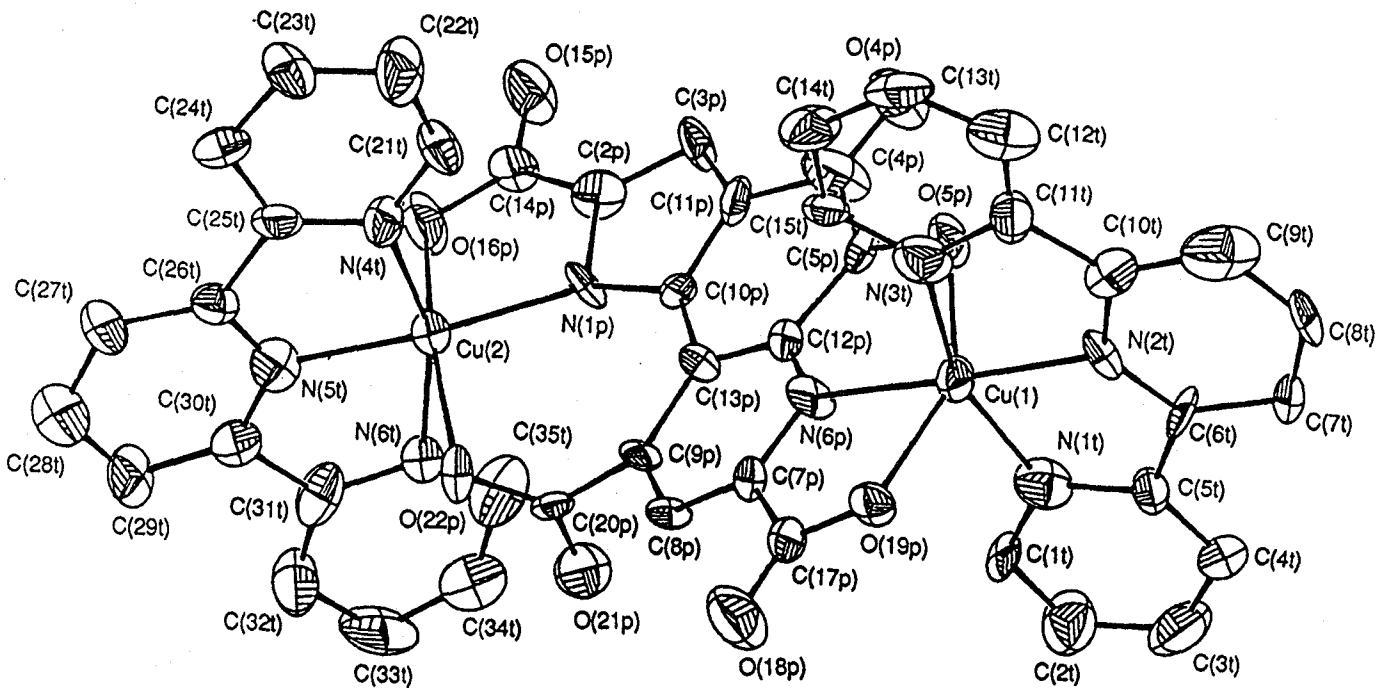

Figure II-2. Molecular structure of $[Cu_2(\mu\text{-pqq})(terpy)_2]\cdot 12H_2O\cdot CH_3CN$ (**2**) showing the 50% probability thermal ellipsoids and atom-labeling scheme. Water and acetonitrile molecules and hydrogen atoms are omitted.

Table II-2. Bond Lengths (Å) for $[Cu_2(\mu\text{-pqq})(terpy)_2]\cdot 12H_2O\cdot CH_3CN$ (2)[a]

Bond	Length	Bond	Length
Cu(1) - O(5p)	2.47(1)	Cu(1) - O(19p)	2.23(1)
Cu(1) - N(6p)	2.03(2)	Cu(1) - N(1t)	2.00(2)
Cu(1) - N(2t)	1.96(1)	Cu(1) - N(3t)	2.08(2)
Cu(2) - O(16p)	2.24(1)	Cu(2) - O(22p)	2.36(1)
Cu(2) - N(1p)	2.00(1)	Cu(2) - N(4t)	2.12(2)
Cu(2) - N(5t)	1.98(2)	Cu(2) - N(6t)	2.02(2)
O(4p) - C(4p)	1.25(2)	O(5p) - C(5p)	1.23(2)
O(15p) - C(14p)	1.22(2)	O(16p) - C(14p)	1.31(2)
O(18p) - C(17p)	1.20(2)	O(19p) - C(17p)	1.27(2)
O(21p) - C(20p)	1.23(2)	O(22p) - C(20p)	1.24(2)
N(1p) - C(2p)	1.41(2)	N(1p) - C(10p)	1.43(2)
N(6p) - C(7p)	1.33(2)	N(6p) - C(12p)	1.35(2)
N(1t) - C(1t)	1.35(2)	N(1t) - C(5t)	1.44(2)
N(2t) - C(6t)	1.37(2)	N(2t) - C(10t)	1.33(2)
N(3t) - C(11t)	1.37(2)	N(3t) - C(15t)	1.39(2)
N(4t) - C(21t)	1.34(3)	N(4t) - C(25t)	1.35(3)
N(5t) - C(26t)	1.33(2)	N(5t) - C(30t)	1.32(2)
N(6t) - C(31t)	1.35(2)	N(6t) - C(35t)	1.32(2)
C(2p) - C(3p)	1.41(3)	C(2p) - C(14p)	1.49(3)
C(3p) - C(11p)	1.40(3)	C(4p) - C(5p)	1.54(3)
C(4p) - C(11p)	1.47(3)	C(5p) - C(12p)	1.49(3)
C(7p) - C(8p)	1.36(2)	C(7p) - C(17p)	1.52(3)
C(8p) - C(9p)	1.37(2)	C(9p) - C(13p)	1.41(3)
C(9p) - C(20p)	1.54(2)	C(10p) - C(11p)	1.38(3)
C(10p) - C(13p)	1.47(3)	C(12p) - C(13p)	1.36(3)
C(1t) - C(2t)	1.38(3)	C(2t) - C(3t)	1.36(3)
C(3t) - C(4t)	1.41(3)	C(4t) - C(5t)	1.37(3)
C(5t) - C(6t)	1.48(3)	C(6t) - C(7t)	1.47(3)
C(7t) - C(8t)	1.42(3)	C(8t) - C(9t)	1.41(3)
C(9t) - C(10t)	1.44(3)	C(10t) - C(11t)	1.44(3)
C(11t) - C(12t)	1.37(3)	C(12t) - C(13t)	1.40(3)
C(13t) - C(14t)	1.40(3)	C(14t) - C(15t)	1.33(3)
C(21t) - C(22t)	1.43(3)	C(22t) - C(23t)	1.32(3)
C(23t) - C(24t)	1.41(3)	C(24t) - C(25t)	1.42(3)
C(25t) - C(26t)	1.49(3)	C(26t) - C(27t)	1.40(3)
C(27t) - C(28t)	1.43(3)	C(28t) - C(29t)	1.41(3)
C(29t) - C(30t)	1.41(3)	C(30t) - C(31t)	1.46(3)
C(31t) - C(32t)	1.43(3)	C(32t) - C(33t)	1.42(3)
C(33t) - C(34t)	1.41(3)	C(34t) - C(35t)	1.33(3)
N(1a) - C(1a)	1.09(3)	C(1a) - C(2a)	1.48(3)

[a]Estimated standard deviations are given in parentheses.

Table II-3. Bond Angles (°) for $[Cu_2(\mu\text{-pqq})(terpy)_2]\cdot 12H_2O\cdot CH_3CN$ (2)[a]

Bond	Angle	Bond	Angle
O(5p) -Cu(1) -O(19p)	149.5(4)	O(5p) -Cu(1) -N(6p)	73.5(5)
O(5p) -Cu(1) -N(1t)	86.9(5)	O(5p) -Cu(1) -N(2t)	99.9(5)
O(5p) -Cu(1) -N(3t)	92.0(5)	O(19p)-Cu(1) -N(6p)	76.5(5)
O(19p)-Cu(1) -N(1t)	94.1(5)	O(19p)-Cu(1) -N(2t)	110.4(5)
O(19p)-Cu(1) -N(3t)	96.9(5)	N(6p) -Cu(1) -N(1t)	101.8(6)
N(6p) -Cu(1) -N(2t)	172.3(6)	N(6p) -Cu(1) -N(3t)	96.9(6)
N(1t) -Cu(1) -N(2t)	81.6(6)	N(1t) -Cu(1) -N(3t)	160.1(6)
N(2t) -Cu(1) -N(3t)	79.1(6)	O(16p)-Cu(2) -O(22p)	167.6(5)
O(16p)-Cu(2) -N(1p)	80.1(5)	O(16p)-Cu(2) -N(4t)	85.0(5)
O(16p)-Cu(2) -N(5t)	98.8(6)	O(16p)-Cu(2) -N(6t)	96.0(6)
O(22p)-Cu(2) -N(1p)	96.3(5)	O(22p)-Cu(2) -N(4t)	84.4(5)
O(22p)-Cu(2) -N(5t)	86.0(5)	O(22p)-Cu(2) -N(6t)	96.2(5)
N(1p) -Cu(2) -N(4t)	104.7(6)	N(1p) -Cu(2) -N(5t)	173.6(6)
N(1p) -Cu(2) -N(6t)	94.9(6)	N(4t) -Cu(2) -N(5t)	81.5(6)
N(4t) -Cu(2) -N(6t)	160.2(6)	N(5t) -Cu(2) -N(6t)	78.9(6)
Cu(1) -O(5p) -C(5p)	108(1)	Cu(2) -O(16p)-C(14p)	111(1)
Cu(1) -O(19p)-C(17p)	113(1)	Cu(2) -O(22p)-C(20p)	107(1)
Cu(2) -N(1p) -C(2p)	112(1)	Cu(2) -N(1p) -C(10p)	137(1)
C(2p) -N(1p) -C(10p)	107(1)	C(7p) -N(6p) -C(12p)	120(2)
Cu(1) -N(6p) -C(7p)	118(1)	Cu(1) -N(6p) -C(12p)	122(1)
Cu(1) -N(1t) -C(1t)	128(1)	Cu(1) -N(1t) -C(5t)	117(1)
C(1t) -N(1t) -C(5t)	114(2)	Cu(1) -N(2t) -C(6t)	115(1)
Cu(1) -N(2t) -C(10t)	117(1)	C(6t) -N(2t) -C(10t)	128(1)
Cu(1) -N(3t) -C(11t)	113(1)	Cu(1) -N(3t) -C(15t)	127(1)
C(11t)-N(3t) -C(15t)	119(1)	Cu(2) -N(4t) -C(21t)	128(1)
Cu(2) -N(4t) -C(25t)	109(1)	C(21t)-N(4t) -C(25t)	123(2)
Cu(2) -N(5t) -C(26t)	117(1)	Cu(2) -N(5t) -C(30t)	118(1)
C(26t)-N(5t) -C(30t)	124(2)	Cu(2) -N(6t) -C(31t)	115(1)
Cu(2) -N(6t) -C(35t)	130(1)	C(31t)-N(6t) -C(35t)	115(2)
N(1p) -C(2p) -C(3p)	111(2)	N(1p) -C(2p) -C(14p)	119(2)
C(3p) -C(2p) -C(14p)	130(2)	C(2p) -C(3p) -C(11p)	103(2)
O(4p) -C(4p) -C(5p)	118(2)	O(4p) -C(4p) -C(11p)	128(2)
C(5p) -C(4p) -C(11p)	114(2)	O(5p) -C(5p) -C(4p)	118(2)
O(5p) -C(5p) -C(12p)	121(2)	C(4p) -C(5p) -C(12p)	120(2)
N(6p) -C(7p) -C(8p)	121(2)	N(6p) -C(7p) -C(17p)	116(2)
C(8p) -C(7p) -C(17p)	123(2)	C(7p) -C(8p) -C(9p)	120(2)
C(8p) -C(9p) -C(13p)	120(2)	C(8p) -C(9p) -C(20p)	116(1)
C(13p)-C(9p) -C(20p)	123(2)	N(1p) -C(10p)-C(11p)	104(2)
N(1p) -C(10p)-C(13p)	130(2)	C(11p)-C(10p)-C(13p)	125(2)
C(3p) -C(11p)-C(4p)	124(2)	C(3p) -C(11p)-C(10p)	114(2)
C(4p) -C(11p)-C(10p)	122(2)	N(6p) -C(12p)-C(5p)	115(2)
N(6p) -C(12p)-C(13p)	123(2)	C(5p) -C(12p)-C(13p)	122(2)
C(9p) -C(13p)-C(10p)	127(2)	C(9p) -C(13p)-C(12p)	116(2)
C(10p)-C(13p)-C(12p)	117(2)	O(15p)-C(14p)-O(16p)	128(2)

– to be continued –

Table II-3. – continued –

Bond	Angle	Bond	Angle
O(15p)-C(14p)-C(2p)	117(2)	O(16p)-C(14p)-C(2p)	115(2)
O(18p)-C(17p)-O(19p)	127(2)	O(18p)-C(17p)-C(7p)	117(2)
O(19p)-C(17p)-C(7p)	116(2)	O(21p)-C(20p)-O(22p)	125(2)
O(21p)-C(20p)-C(9p)	117(1)	O(22p)-C(20p)-C(9p)	118(1)
N(1t) -C(1t) -C(2t)	125(2)	C(1t) -C(2t) -C(3t)	117(2)
C(2t) -C(3t) -C(4t)	124(2)	C(3t) -C(4t) -C(5t)	115(2)
N(1t) -C(5t) -C(4t)	124(2)	N(1t) -C(5t) -C(6t)	108(2)
C(4t) -C(5t) -C(6t)	128(2)	N(2t) -C(6t) -C(5t)	119(2)
N(2t) -C(6t) -C(7t)	117(2)	C(5t) -C(6t) -C(7t)	124(2)
C(6t) -C(7t) -C(8t)	117(2)	C(7t) -C(8t) -C(9t)	122(2)
C(8t) -C(9t) -C(10t)	119(2)	N(2t) -C(10t)-C(9t)	117(2)
N(2t) -C(10t)-C(11t)	116(2)	C(9t) -C(10t)-C(11t)	126(2)
N(3t) -C(11t)-C(10t)	113(2)	N(3t) -C(11t)-C(12t)	122(2)
C(10t)-C(11t)-C(12t)	124(2)	C(11t)-C(12t)-C(13t)	118(2)
C(12t)-C(13t)-C(14t)	120(2)	C(13t)-C(14t)-C(15t)	120(2)
N(3t) -C(15t)-C(14t)	121(2)	N(4t) -C(21t)-C(22t)	116(2)
C(21t)-C(22t)-C(23t)	125(2)	C(22t)-C(23t)-C(24t)	116(2)
C(23t)-C(24t)-C(25t)	120(2)	N(4t) -C(25t)-C(24t)	119(2)
N(4t) -C(25t)-C(26t)	119(2)	C(24t)-C(25t)-C(26t)	122(2)
N(5t) -C(26t)-C(25t)	114(2)	N(5t) -C(26t)-C(27t)	121(2)
C(25t)-C(26t)-C(27t)	125(2)	C(26t)-C(27t)-C(28t)	118(2)
C(27t)-C(28t)-C(29t)	118(2)	C(28t)-C(29t)-C(30t)	120(2)
N(5t) -C(30t)-C(29t)	118(2)	N(5t) -C(30t)-C(31t)	113(2)
C(29t)-C(30t)-C(31t)	129(2)	N(6t) -C(31t)-C(30t)	115(2)
N(6t) -C(31t)-C(32t)	125(2)	C(30t)-C(31t)-C(32t)	119(2)
C(31t)-C(32t)-C(33t)	116(2)	C(32t)-C(33t)-C(34t)	117(2)
C(33t)-C(34t)-C(35t)	120(2)	N(6t) -C(35t)-C(34t)	126(2)
N(1a) -C(1a) -C(2a)	169(2)		

[a]Estimated standard deviations are given in parentheses.

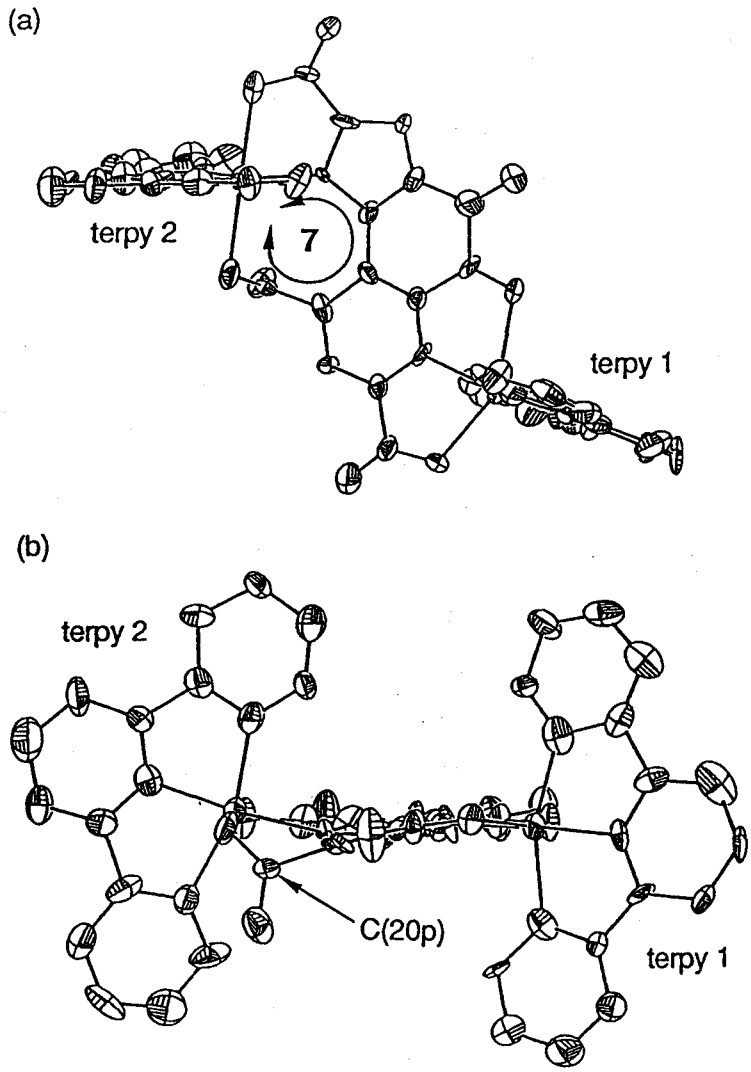

Figure II-3. Complex **2** is projected perpendicular (a) and parallel (b) to the PQQ ligand.

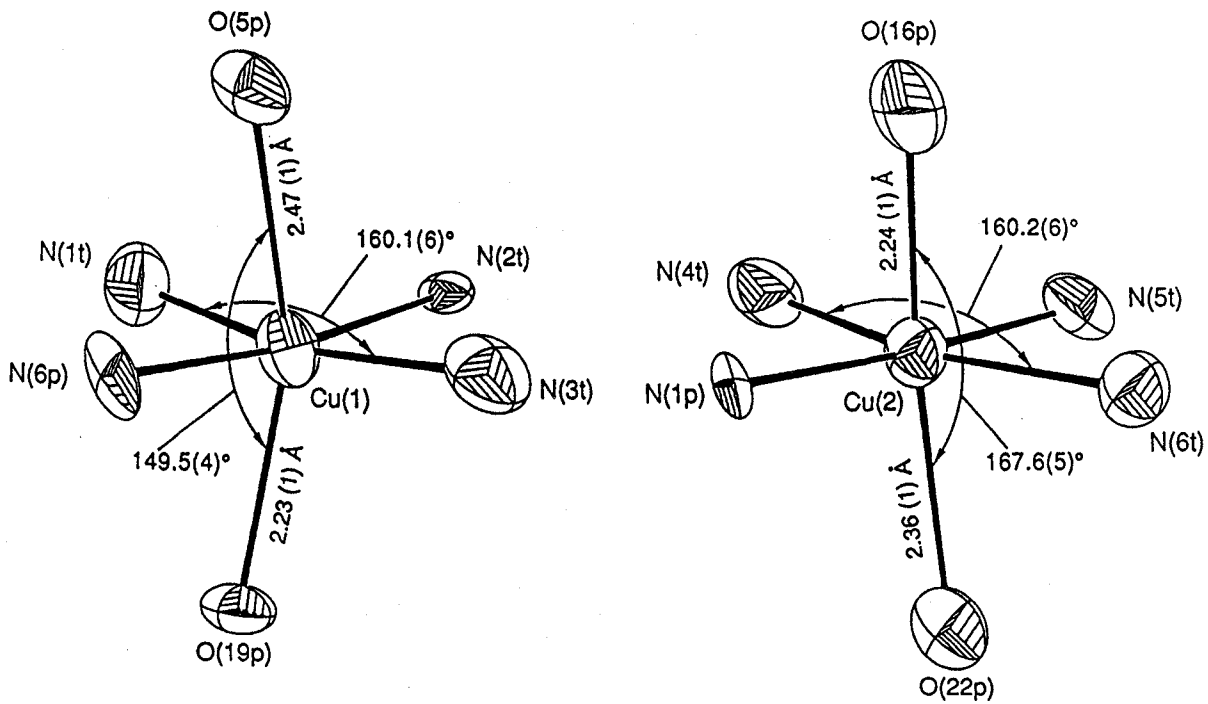

Figure II-4. Coordination spheres of two copper(II) ions in complex **2**. The letters p and t show the pqq and terpyridine, respectively.

approximately equal to those found in the structures of other terpy-containing Cu(II) complexes.[30,31] Differences between the coordination geometries around two Cu(II) ions are clear in the O–Cu–O angles (O(5p)–Cu(1)–O(19p) = 149.5 (4)° and O(16p)–Cu(2)–O(22p) = 167.6 (5)°), that is, the smaller bite angle of the Cu(1) site than that of the Cu(2) site results in larger deviations from ideal geometry. The chelate ring comprised of the Cu(2), N(1p), C(10p), C(13p), C(9p), C(20p), and O(22p) atoms is the only seven-membered ring in complex **2** (Figure II-3a), so that the O(22p)–Cu(2)–N(1p) angle of (96.3 (5)°) is larger than 90° and C(20p) deviates by 0.73 Å from the plane composed of the other six atoms (Figure II-3b). The Cu(1)–O(5p) distances of 2.47 (1) Å is longer than the other three Cu–O bond distances in this complex **2**. This is because O(5p) is carbonyl oxygen and the other three oxygens (O(16p), O(19p), and O(22p)) are carboxylate oxygens. Since the axial coordination of O(5p) is weak, Cu(1) deviates by 0.11 Å from the coordination plane (N(6p), N(1t), N(2t), and N(3t)) toward the O(19p) atom. On the other hand, Cu(2) atom lies on the plane consisting of the N(4t), N(5t), N(6t), and N(1p) atoms within the experimental error.

Although pqq has the tetraanionic form (pqq^{4-}) in complex **2**, the bond lengths and angles in the PQQ ligand are almost similar to those observed in the structures of disodium H_2pqq salt,[32] tripotassium Hpqq salt,[33] and the 5-(2-oxopropyl)[1,34] and the 5-(2,4-dinitrophenylhydrazine)[35] adducts of PQQ. However, the longer N–C lengths in the pyrrole ring (1.41 (2) and 1.43 (2) Å for N(1p)–C(2p) and N(1p)–C(10p), respectively) than the corresponding N—C lengths of the free PQQ molecule[33], are caused by the deprotonation of the N(1p) group. A noticeable structural feature of the pqq ligand is the twisting of the aromatic ring system. In the structures of PQQ and its adducts already reported, only the 5-(2-

oxopropyl) adduct has the twisted ring system to accommodate the fully substituted sp^3 C-5 atom.[1,34] In spite of absence of the sp^3 carbon atom in the aromatic ring system of complex **2**, the ring system of pqq is still twisted, which is due to the binding of Cu(2) to site 3 of pqq. The large seven-membered chelate ring causes the distortion of pqq. The dihedral angle between the pyridine and the pyrrole rings is 9.1°. The intramolecular hydrogen bond between nitrogen of the pyrrole moiety (N(1p)) and oxygen of C-9 carboxylate (O(21p) or O(22p)) is not observed in this complex **2**, although such a hydrogen bond is observed in all structures of PQQ and its adducts already reported.[1,32-35]

Finally, Figure II-5 shows the crystal packing of complex **2**. One of the most remarkable structural features observed in the crystal unit is the hydrogen bonding network. Possible hydrogen bonds and their distances are listed in Table II-4. The extensive layer of the many solvent molecules in the crystal is formed through the hydrogen bonds.

Spectroscopic Investigations of Complexes 1 and 2 and Proposed Structure of Complex 1. On the basis of the structure of complex **2**, it is considered that H_2pqq in complex **1** binds to Cu(II) with either the pyridine moiety (site 1 in Figure II-1) or the pyrrole moiety (site 3). According to the previous NMR and EPR spectroscopies, Suzuki and co-workers reported that H_2pqq in complex **1** might be coordinated to Cu(II) with N-6 and C-7 carboxylate of the pyridine moiety.[19] Additionally a comparison of the diffuse reflectance spectra between complexes **1** and **2** reveals a marked difference, as presented in Figure II-6. Complexes **1** and **2** show the absorption maxima at 490 and 640 nm, respectively. The absorption spectrum of free PQQ in a solution (pH > 9) exhibits the extremely

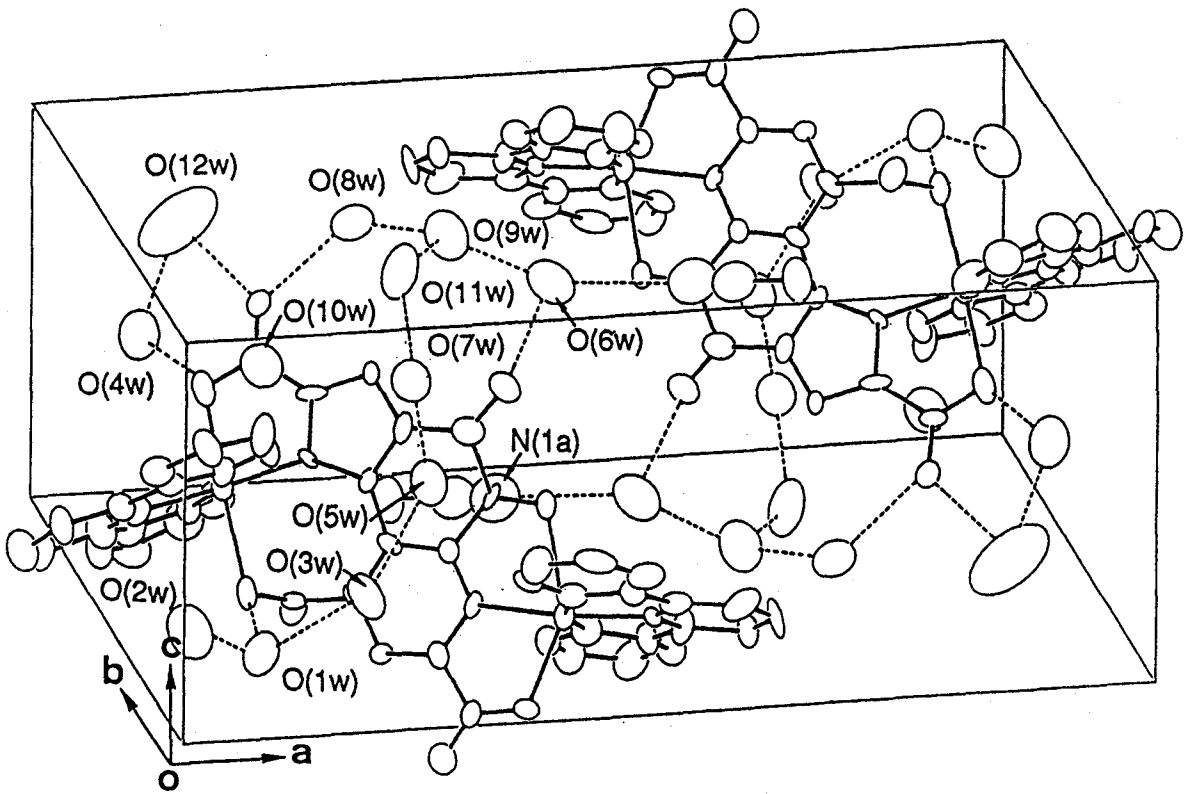

Figure II-5. Crystal structure of complex **2**. The letters w and a show the water and acetonitrile molecules, respectively. The dotted lines represent possible hydrogen bonds.

Table II-4. Possible Hydrogen Bond Distances (Å)[a-c]

O(4p) ···O(6w)	2.75(2)	O(15p)···O(8w)	2.76(2)
O(15p)···O(12w)	2.65(3)	O(16p)···O(4w)	2.80(2)
O(22p)···O(1w)	2.74(2)	O(1w) ···O(2w)	2.80(2)
O(1w) ···O(3w)	2.97(2)	O(3w) ···O(5w)	2.89(2)
O(4w) ···O(12w)	2.97(4)	O(5w) ···O(7w)	2.76(2)
O(6w) ···O(9w)	2.98(3)	O(7w) ···O(11w)	2.74(3)
O(8w) ···O(9w)	2.67(2)	O(9w) ···O(11w)	2.74(3)
O(4w) ···O(2w)^{i}	2.83(3)	O(4w) ···O(3w)^{i}	2.80(2)
O(12w)···O(10w)^{i}	2.66(4)	O(7w) ···O(18p)^{ii}	3.00(2)
O(10w)···O(1w)^{ii}	2.82(2)	O(11w)···O(21p)^{ii}	2.84(2)
O(18p)···O(8w)^{iii}	2.77(2)	O(6w) ···N(1a)^{iv}	3.13(3)
O(2w) ···O(10w)^{v}	2.77(2)		

[a]The letters p, w, and a represent the PQQ, water, and acetonitrile molecules, respectively.

[b]Symmetry code: (i) *x*, 1+*y*, *z*; (ii) *x*, *y*, 1+*z*; (iii) *x*, -1+*y*, -1+*z*; (iv) 1-*x*, 1-*y*, 1-*z*, (v) -*x*, -*y*, 1-*z*.

[c]Estimated standard deviations are given in parentheses.

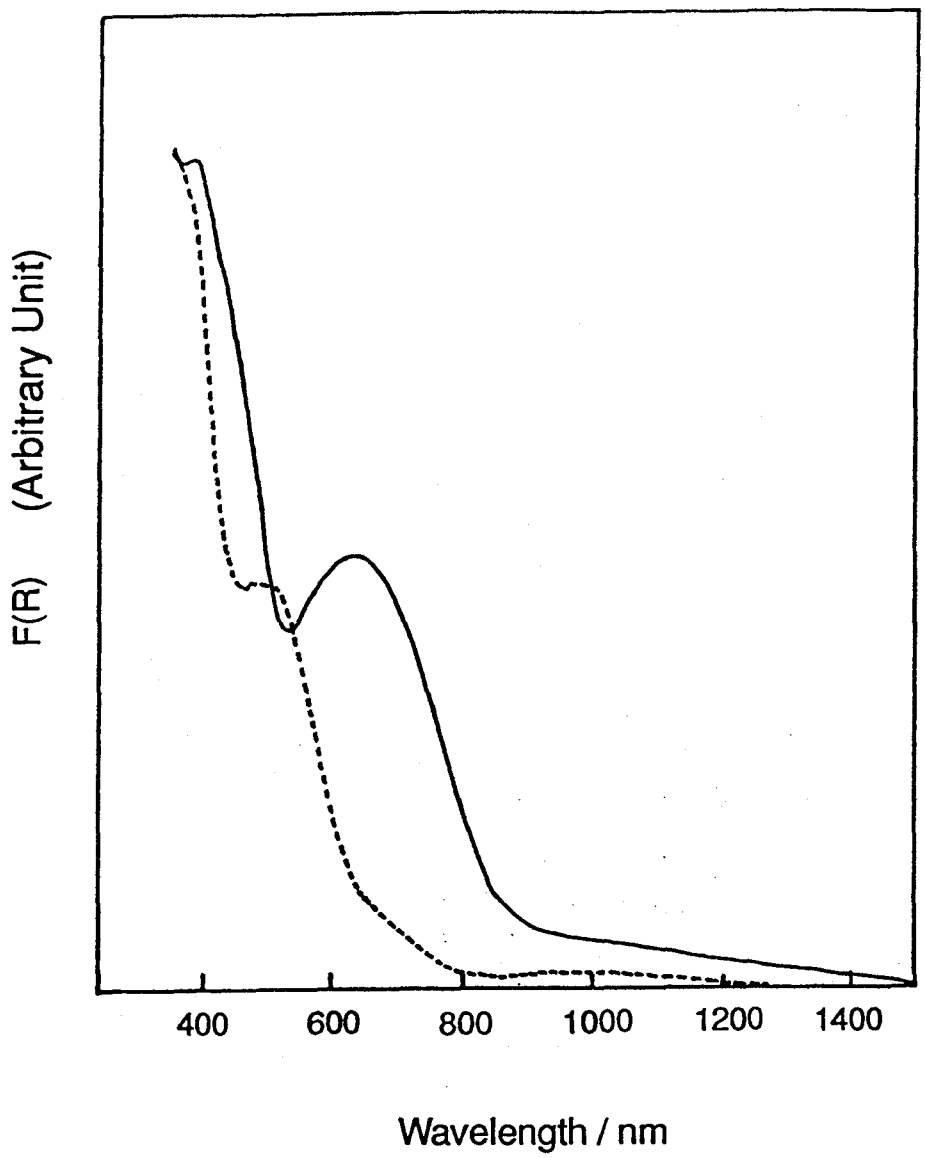

Figure II-6. Diffuse reflectance spectra of complex **1** (broken line) and complex **2** (solid line).

decreasing of the 480-nm band in order to deprotonate at the pyrrole moiety,[28] and hence the lack of the 490-nm band in complex **2** is also responsible for the deprotonation of the pyrrole moiety by the binding of N-1 to Cu(II). Since the very intense absorption band assigned to the pqq ligand at 490 nm disappears, the 640-nm band probably due to d–d transitions of Cu(II) is emphasized, as shown Figure II-6. In the spectrum of complex **1**, the absorption band at 490 nm is presumably assigned to n–π^* transitions[36] of the *o*-quinone group in H_2pqq and both the shoulder band near 700 nm and the broad band around 1000 nm are attributable to d–d transitions.

All experimental results (NMR, EPR, and diffuse reflectance spectra and the pH dependence of the complex formation) substantiate that Cu(II) in complex **1** is attached to the pyridine moiety of H_2pqq and has the binding mode similar to Cu(1) in complex **2**. In addition, the EXAFS (extended X-ray absorption fine structure) analysis of complex **1** has also supported that Cu(II) has six coordination atoms of nitrogen and/or oxygen and the average Cu – N(or O) length is 2.03 Å.[37]

The pqq ligand can be coordinated to Cu(II) with the pyridine moiety (site 1 in Figure II-1) and the pyrrole moiety (site 3), but would bind to Cu(II) through no quinone moiety (site 2). Especially site 1 seems to be predominantly occupied by Cu(II) ion. On the other hand, the complex of PQQ with *cis*-[Ru(bpy)$_2$Cl$_2$] has been described as the O,O–coordination of the quinone moiety (site 2).[22] The complexation modes of PQQ are of interest in connection with the other transition metals and the comparison with the complex formations of aromatic coenzymes such as flavin and pterin. It is known these coenzymes which have plural chelating sites are meridionally coordinated to Cu(II) like pqq.[38,39]

Finally, it is known that Ca^{2+} ions are essential for PQQ-containing quinoproteins (e.g. methanol dehydrogenase, glucose dehydrogenase, and lupanine hydroxylase). However, the binding site of the Ca^{2+} ion has been unclear. The information obtained from the PQQ-containing copper complexes might indicate that Ca^{2+} ion in the quinoproteins could be located at pyridine moiety of PQQ.

References and Notes

(1) Salisbury, S. A.; Forrest, H. S.; Cruse, W. B. T.; Kennard, O. *Nature (London)* **1979**, *281*, 843–844.

(2) Duine, J. A. *Eur. J. Biochem.* **1991**, *200*, 271–284.

(3) Lobenstein-Verbeek, C. L.; Jongejan, J. A.; Frank, J.; Duine, J. A. *FEBS Lett.* **1984**, *170*, 305–309.

(4) Ameyama, M.; Hayashi, M.; Matsushita, K.; Shinagawa, E.; Adachi, O. *Agric. Biol. Chem.* **1984**, *48*, 561–565.

(5) Janes, S. M.; Mu, D.; Wemmer, D.; Smith, A. J.; Kain, S.; Maltby, D.; Burlingame, A. L.; Klinman, J. P. *Science*, **1990**, *248*, 981–987.

(6) Kumazawa, T.; Seno, H.; Urakami, T.; Suzuki, O. *Arch. Biochem. Biophys.* **1990**, *283*, 533–536.

(7) Klinman, J. P.; Dooley, D. M.; Duine, J. A.; Knowles, P. F.; Mondovi, B.; Villafranca, J. J. *FEBS Lett.* **1991**, *282*, 1–4.

(8) Brown, D. E.; McGuirl, M. A.; Dooley, D. M.; Janes, S. M.; Mu, D.; Klinman, J. P. *J. Biol. Chem.* **1991**, *266*, 4049–4051.

(9) Maccarrone, M.; Veldink, G. A.; Vliegenthart, J. F. G. *J. Biol. Chem.* **1991**, *266*, 21014–21017.

(10) Mu, D.; Janes, S. M.; Smith, A. J.; Brown, D. E.; Dooley, D. M.; Klinman, J. P. *J. Biol. Chem.* **1992**, *267*, 7979–7982.

(11) Pedersen, J. Z.; El-Sherbini, S.; Finazzi-Agro, A.; Rotilio, G. *Biochemistry* **1992**, *31*, 8–12.

(12) Mutzel, A; Görisch, H. *Agric. Biol. Chem.* **1991**, *55*, 1721–1726.

(13) Richardson, I. W.; Anthony, C. *Biochem. J.* **1992**, *287*, 709–715.

(14) Adachi, O.; Matsushita, K.; Shinagawa, E.; Ameyama, M. *Agric. Biol. Chem.* **1988**, *52*, 2081–2082.

(15) Hommel, R.; Kleber, H. P. *J. Gen. Microbiol.* **1990**, *136*, 1705–1711.

(16) Kobayashi, M.; Yanaka, N.; Nagasawa, T.; Yamada, H. *Biochemistry* **1992**, *31*, 9000–9007.

(17) Noar, J. B.; Rodriguez, E. J.; Bruice, T. C. *J. Am. Chem. Soc.* **1985**, *107*, 7198–7199.

(18) Jongejan, J. A.; van der Meer, R. A.; van Zuylen, G. A.; Duine, J. A. *Recl. Trav. Chim. Pays-Bas* **1987**, *106*, 365.

(19) Suzuki, S.; Sakurai, T.; Itoh, S.; Ohshiro, Y. *Inorg. Chem.* **1988**, *27*, 591–592.

(20) Suzuki, S.; Sakurai, T.; Itoh, S.; Ohshiro, Y. *Nippon Kagaku Kaishi* **1988**, 421–424.

(21) Suzuki, S.; Sakurai, T.; Itoh, S.; Ohshiro, Y. *Chem. Lett.* **1988**, 777–780.

(22) Schwederski, B.; Kasack, V.; Kaim, W.; Roth, E.; Jordanov, J. *Angew. Chem., Int. Ed. Engl.* **1990**, *29*, 78–79.

(23) Morgan, G.; Burstall, F. H. *J. Chem. Soc.* **1937**, 1649.

(24) North, A. C. T.; Phillips, D. C.; Mathews, F. S. *Acta Crystallogr.* **1968**, *A24*, 351–359.

(25) Main, P; Hull, S. E.; Lessinger, L.; Germain, G.; Declercq, J. -P.; Woolfson, M. M. *MULTAN 78*, A System of Computer Programs for the Automatic Solution of Crystal Structures from X-ray Diffraction Data, Universities of York, England, and Louvain, Belgium, 1978.

(26) Ashida, T. *HBLS-V*, The Universal Crystallographic Computing System-Osaka, The Computation Center, Osaka University, Japan, 1979.

(27) Kano, K.; Mori, K.; Uno, B.; Kubota, T.; Ikeda, T.; Senda, M. *Bioelectrochemistry and Bioenergetics* **1990**, *24*, 193–201.

(28) Kano, K.; Mori, K.; Uno, B.; Kubota, T.; Ikeda, T.; Senda, M. *Bioelectrochemistry and Bioenergetics* **1990**, *23*, 227–238.

(29) The crystal was used for data collection, in spite of its poor quality, because single crystals were extremely difficult to obtain and treat, and repeated attempts by many methods over a year's time failed to produce crystals having better quality.

(30) Anderson, O. P.; Packard, A. B.; Wicholas, M. *Inorg. Chem.* **1976**, *15*, 1613–1618.

(31) Bresciani-Pahor, N.; Nardin, G.; Bonomo R. P.; Rizzarelli, E. *J. Chem. Soc., Dalton Trans.* **1984**, 2625–2630.

(32) Ishida, T.; Doi, M.; Tomita, K.; Hayashi, H.; Inoue, M.; Urakami, T. *J. Am. Chem. Soc.* **1989**, *111*, 6822–6828.

(33) Nakamura, N.; Kohzuma, T.; Kuma, H.; Suzuki, S. submitted for publication (see Chapter III).

(34) Cruse, W. B. T.; Kennard, O.; Salisbury, S. A. *Acta Crystallogr.* **1980**, *B36*, 751–754.

(35) van Koningsveld, H.; Jansen, J. C.; Jongejan, J. A.; Frank, J.; Duine, J. A. *Acta Crystallogr.* **1985**, *C41*, 89–92.

(36) Dekker, R. H.; Duine, J. A.; Frank, J.; Verwiel, J. E. P.; Westerling, J. *Eur. J. Biochem.* **1982**, *125*, 69–73.

(37) EXAFS spectra were measured at BL-6B of the Photon Factory in the National Laboratory for High Energy Physics (KEK-PF). The measurements were carried out with a beam current of about 250 mA and a storage-ring

energy of 2.5 GeV. The data were collected with a Si(111) double crystal monochromator at room temperature in the transmission mode on a pellet sample diluted with polyethylene to reduce thickness effects. Nitrogen filled ionization chambers (I_0 and I) were used. The energy was defined by assigning the first inflection point of the Cu foil spectrum to 8980.3 eV. The analysis of EXAFS was carried out by subtracting a smooth varying part estimated from a cubic spline and normalizing the spectrum to the absorption edge. Extracted EXAFS modulation was analyzed on the basis of plane-wave single-scattering theory (Sayers, D. E.; Stern, E. A.; Lytle, F. W. *Phys. Rev. Lett.* **1971**, *27*, 1204). The backscattering amplitude $F(\mathbf{k})$ and the phase shift $f(\mathbf{k})$ functions employed were the theoretical curves tabulated by Teo and Lee. The fixed reducing factors S obtained from the analysis of model compounds were used. The coordination number N, the Debye-Waller factor σ, the interatomic distance r, and the difference in threshold energy ΔE_0 are determined in the nonlinear least-squares refined curve fitting procedure. The extraction of the EXAFS, the Fourier transformation, and the curve fitting were processed by using the systematic programs **EXAFS 1** (Kosugi, N.; Kuroda, H. *EXAFS 1*, Research Center for Spectrochemistry, University of Tokyo, Japan, 1985). All calculations were performed on a HITAC M-682H computer at the Computer Center of the University of Tokyo.

(38) Garland, W. T.,Jr.; Fritchie, C. J., Jr. *J. Biol. Chem.* **1974**, *249*, 2228–2234.

(39) Kohzuma, T.; Masuda, H.; Yamauchi, O. *J. Am. Chem. Soc.* **1989**, *111*, 3431–3433.

Chapter III. STRUCTURE OF TRIPOTASSIUM HPQQ SALT

Introduction

PQQ is known as the coenzyme of a novel class of oxidoreductases[1,2]. To understand its biological behavior, it is important to reveal the molecular structure and atomic charge distribution in the molecule. The structures of the 5-(2-oxopropyl) adduct[3,4] and the 5-(2,4-dinitrophenylhydrazine) adduct of PQQ[5] and disodium H_2pqq salt[6] have already been reported. Ishida and co-workers demonstrated that H_2pqq possesses two sodium-binding sites.[6] This is the first report on the crystal structure of the trianionic form of PQQ ($Hpqq^{3-}$). It is of interest in the third metal-binding site of PQQ.

Experimental Section

Preparation of K_3Hpqq. PQQ was purchased from Ube Industries (Tokyo, Japan). PQQ was dissolved in 0.1 M KOH solution and then the pH value of the solution was adjusted to 7.0 by addition of 0.1 M HCl solution. Addition of CH_3CN to the solution yielded the dark-red crystals in a few weeks.

Crystallographic Structure Determination on $K_3Hpqq \cdot 4H_2O$. A needle-shaped crystal with approximate dimensions 0.10 × 0.12 × 0.42 mm was sealed in a glass capillary. Diffraction data were collected using a Rigaku AFC-5R

automatic diffractometer with Ni-filtered Cu $K\alpha$ radiation. Unit-cell parameters indicated a monoclinic crystal system, and systematic absences indicated the space group. Lattice constants were obtained by least-squares refinement of the setting angles of 20 reflections with $18 < \theta < 20°$. Intensity data were collected by the ω–2θ scan technique, ω–scan width $(1.50 + 0.5\tan\theta)°$, scan speed $(4.0° \text{ min}^{-1})$. The intensities of 2957 unique reflections were measured in the range $0 \leq 2\theta \leq 125°$ (hkl range: -20 to 20; 0 to 8; 0 to 18), of which 2127 had $I > 3\sigma(I)$ and were used. The intensities of three reflections, chosen as standards and measured every 100 reflections, showed no significant variations. Data were corrected for Lorentz and polarization effects and for empirical absorption;[7] maximum and minimum correction factors were 1.333 and 1.006, respectively. The crystallographic data are summarized in Table III-1.

The structure was solved by the direct method, using **MULTAN 78**[8] and refined by block-diagonal least-squares method on F using the program **HBLS-V**.[9] Anisotropic thermal parameters were allowed for non-H atoms. The positions of the H atoms of Hpqq were calculated on the basis of the molecular geometry. Difference Fourier syntheses calculated at intermediate stages of refinement showed maxima consistent with the expected positions of H atoms of water. H atoms were included with isotropic temperature factors in subsequent refinement. The refinement converged with $R = 0.056$ and $R_w = 0.060$ where $w = 1/(\sigma^2(F_o) + 0.0648|F_o| + 0.0002|F_o|^2)$; 325 parameters were refined. At the conclusion of the refinement, $(\Delta/\sigma)_{max} = 0.33$, the difference map had no peak larger than 0.88 $e\text{Å}^{-3}$, and $S = 1.23$. The atomic scattering factors for all atoms were taken from *International Tables for X-ray Crystallography* (1974, Vol. IV). All the computations were carried out on an ACOS 2020 computer at the

Table III-1. Crystallographic Data for $K_3Hpqq \cdot 4H_2O$

formula	$C_{14}H_{11}N_2O_{12}K_3$
fw	516.54
color and habit	dark-red needles
cryst system	monoclinic
space group	$P2_1/n$
a, Å	17.060 (2)
b, Å	7.088 (2)
c, Å	15.332 (2)
β, deg	91.76 (1)
V, Å^3	1853.1(7)
Z	4
cryst dimens, nm	0.10 × 0.12 × 0.42
D_{calcd}, g cm^{-3}	1.852
μ(Cu Kα), cm^{-1}	73.27
F(000)	1048
scan method	ω-2θ
2θ range, deg	0–120
no. of unique data collcd	2957
no. of data used in refinement	2127 ($\|Fo\| > 3\sigma\|Fo\|$)
R^a	0.056
$R_w{}^b$	0.060

$^aR = \Sigma\|\|Fo\|-\|Fc\|\|/\Sigma|Fo|$. $^bR_w = [\Sigma w(|Fo|-|Fc|)^2/\Sigma w(Fo)^2]^{1/2}$.

Computation Center, Osaka University, and on an ACOS S-850 computer at the Crystallographic Research Center, Institute for Protein Research, Osaka University.

The atomic positional parameters and equivalent isotropic temperature factors for the non-hydrogen atoms, the atomic coordinates of the hydrogen atoms, and the non-hydrogen anisotropic thermal parameters are listed in Appendix II.

Results and Discussion

The bond lengths and the bond angles are presented in Table III-2 and Table III-3, respectively. Figure III-1 shows a perspective drawing of the structure and indicates the atom-numbering scheme. In the earlier structural study of disodium H_2pqq salt, PQQ formed dianions (H_2pqq^{2-}).[6] The anionic charge on PQQ probably depends on the synthetic conditions. Since the present crystals have been prepared under neutral conditions, PQQ molecule has formed trianions ($Hpqq^{3-}$) with three carboxylate anion substituents. A comparison of the structure of Hpqq with that of H_2pqq reveals almost similar bond lengths and angles each other. The carboxylate C(2)—C(14) bond length of 1.498(8) Å is also significantly shorter than the other two carboxylate C—C bond lengths [1.531(8) and 1.552(8) Å for C(7)—C(17) and C(9)—C(20), respectively]. This fact presumably results from the energetic stabilization of the carboxy group through the resonance effect with the respective aromatic rings.[6] Differences between H_2pqq and Hpqq are manifest in the C(4) = O(4) bond lengths [1.204(5) and 1.205(6)

Table III-2. Bond Lengths (Å) for $K_3Hpqq \cdot 4H_2O$[a,b]

Bond	Length	Bond	Length	Bond	Length
K(1)—O(15)	2.716(5)	K(1)—O(16)	3.073(4)	K(1)—O(w4)	2.821(5)
K(1)—O(w3)^{i}	3.095(5)	K(1)—O(4)^{ii}	3.052(5)	K(1)—O(5)^{ii}	2.842(5)
K(1)—O(w2)^{ii}	2.797(5)	K(1)—O(w4)^{v}	3.158(5)	K(2)—O(22)	2.752(5)
K(2)—O(w1)	2.752(6)	K(2)—O(15)^{iii}	2.726(5)	K(2)—O(w4)^{iii}	2.841(5)
K(2)—O(4)^{iv}	2.841(5)	K(3)—O(16)	2.724(4)	K(3)—O(w3)	3.005(5)
K(3)—O(w3)^{i}	2.736(5)	K(3)—O(16)^{i}	2.794(4)	K(3)—O(5)^{ii}	3.008(5)
K(3)—O(19)^{ii}	2.913(4)	K(3)—N(6)^{ii}	2.852(5)	K(3)—O(5)^{iv}	2.781(5)
O(4)—C(4)	1.234(8)	O(5)—C(5)	1.209(8)	O(15)—C(14)	1.244(7)
O(16)—C(14)	1.250(7)	O(18)—C(17)	1.242(7)	O(19)—C(17)	1.253(7)
O(21)—C(20)	1.236(8)	O(22)—C(20)	1.248(7)	N(1)—C(2)	1.383(7)
N(1)—C(10)	1.362(7)	N(6)—C(7)	1.317(7)	N(6)—C(12)	1.339(7)
C(2)—C(3)	1.368(8)	C(2)—C(14)	1.498(8)	C(3)—C(11)	1.414(8)
C(4)—C(5)	1.544(9)	C(4)—C(11)	1.411(8)	C(5)—C(12)	1.484(8)
C(7)—C(8)	1.389(8)	C(7)—C(17)	1.531(8)	C(8)—C(9)	1.391(8)
C(9)—C(13)	1.399(7)	C(9)—C(20)	1.552(8)	C(10)—C(11)	1.385(8)
C(10)—C(13)	1.465(8)	C(12)—C(13)	1.448(8)		

[a]Symmetry code: (i) 0.5-*x*, 0.5+*y*, 1.5-*z*; (ii) 0.5+*x*, 0.5-*y*, 0.5+*z*; (iii) -0.5+*x*, 0.5-*y*, 0.5+*z*; (iv) -*x*, 1-*y*, 1-*z*; (v) 1-*x*, -*y*, 1-*z*.

[b]Estimated standard deviations are given in parentheses.

Table III-3. Bond Angles (°) for $K_3Hpqq{\cdot}4H_2O$[a,b]

Bond	Angle	Bond	Angle
O(15)—K(1)—O(16)	44.9(1)	O(15)—K(1)—O(w4)	77.4(1)
O(15)—K(1)—O(w3)^{i}	81.6(1)	O(15)—K(1)—O(4)^{ii}	169.6(2)
O(15)—K(1)—O(5)^{ii}	115.4(1)	O(15)—K(1)—O(w2)^{ii}	115.7(2)
O(15)—K(1)—O(w4)^{v}	112.9(1)	O(16)—K(1)—O(w4)	121.9(1)
O(16)—K(1)—O(w3)^{i}	66.9(1)	O(16)—K(1)—O(4)^{ii}	124.9(1)
O(16)—K(1)—O(5)^{ii}	70.8(1)	O(16)—K(1)—O(w2)^{ii}	134.0(1)
O(16)—K(1)—O(w4)^{v}	121.8(1)	O(w4)—K(1)—O(w3)^{i}	118.1(1)
O(w4)—K(1)—O(4)^{ii}	112.9(1)	O(w4)—K(1)—O(5)^{ii}	167.2(1)
O(w4)—K(1)—O(w2)^{ii}	69.4(1)	O(w4)—K(1)—O(w4)^{v}	68.9(1)
O(w3)^{i}—K(1)—O(4)^{ii}	92.3(1)	O(w3)^{i}—K(1)—O(5)^{ii}	66.4(1)
O(w3)^{i}—K(1)—O(w2)^{ii}	69.1(1)	O(w3)^{i}—K(1)—O(w4)^{v}	165.4(1)
O(4)^{ii}—K(1)—O(5)^{ii}	54.3(1)	O(4)^{ii}—K(1)—O(w2)^{ii}	69.2(1)
O(4)^{ii}—K(1)—O(w4)^{v}	73.1(1)	O(5)^{ii}—K(1)—O(w2)^{ii}	103.3(1)
O(5)^{ii}—K(1)—O(w4)^{v}	104.0(1)	O(w2)^{ii}—K(1)—O(w4)^{v}	104.1(1)
O(22)—K(2)—O(w1)	88.2(2)	O(22)—K(2)—O(15)^{iii}	118.2(2)
O(22)—K(2)—O(w4)^{iii}	87.1(1)	O(22)—K(2)—O(4)^{iv}	77.3(1)
O(w1)—K(2)—O(15)^{iii}	106.2(2)	O(w1)—K(2)—O(w4)^{iii}	175.2(2)
O(w1)—K(2)—O(4)^{iv}	96.9(2)	O(15)^{iii}—K(2)—O(w4)^{iii}	76.9(1)
O(15)^{iii}—K(2)—O(4)^{iv}	152.1(2)	O(w4)^{iii}—K(2)—O(4)^{iv}	81.2(1)
O(16)—K(3)—O(w3)	76.6(1)	O(16)—K(3)—O(w3)^{i}	77.0(1)
O(16)—K(3)—O(16)^{i}	151.7(1)	O(16)—K(3)—O(5)^{ii}	73.4(1)
O(16)—K(3)—O(19)^{ii}	133.4(1)	O(16)—K(3)—N(6)^{ii}	123.5(1)
O(16)—K(3)—O(5)^{iv}	91.6(1)	O(w3)—K(3)—O(w3)^{i}	149.5(1)
O(w3)—K(3)—O(16)^{i}	129.4(1)	O(w3)—K(3)—O(5)^{ii}	88.9(1)
O(w3)—K(3)—O(19)^{ii}	56.9(1)	O(w3)—K(3)—N(6)^{ii}	82.9(1)
O(w3)—K(3)—O(5)^{iv}	96.4(1)	O(w3)^{i}—K(3)—O(16)^{i}	80.1(1)
O(w3)^{i}—K(3)—O(5)^{ii}	68.9(1)	O(w3)^{i}—K(3)—O(19)^{ii}	147.7(1)
O(w3)^{i}—K(3)—N(6)^{ii}	99.2(1)	O(w3)^{i}—K(3)—O(5)^{iv}	99.5(1)
O(16)^{i}—K(3)—O(5)^{ii}	113.3(1)	O(16)^{i}—K(3)—O(19)^{ii}	73.2(1)
O(16)^{i}—K(3)—N(6)^{ii}	76.4(1)	O(16)^{i}—K(3)—O(5)^{iv}	76.0(1)
O(5)^{ii}—K(3)—O(19)^{ii}	105.4(1)	O(5)^{ii}—K(3)—N(6)^{ii}	54.0(1)
O(5)^{ii}—K(3)—O(5)^{iv}	162.5(1)	O(19)^{ii}—K(3)—N(6)^{ii}	57.4(1)
O(19)^{ii}—K(3)—O(5)^{iv}	91.4(1)	N(6)^{ii}—K(3)—O(5)^{iv}	143.2(1)
K(1)—O(15)—C(14)	102.5(4)	K(1)—O(16)—K(3)	96.9(1)

– to be continued –

Table III-3. – continued –

Bond	Angle	Bond	Angle
K(1)—O(16)—C(14)	85.4(3)	K(3)—O(16)—C(14)	136.8(4)
K(2)—O(22)—C(20)	129.9(4)	C(2)—N(1)—C(10)	109.9(5)
C(7)—N(6)—C(12)	118.7(5)	N(1)—C(2)—C(3)	107.9(5)
N(1)—C(2)—C(14)	120.6(5)	C(3)—C(2)—C(14)	131.4(5)
C(2)—C(3)—C(11)	107.0(5)	O(4)—C(4)—C(5)	117.0(5)
O(4)—C(4)—C(11)	127.6(6)	C(5)—C(4)—C(11)	115.3(5)
O(5)—C(5)—C(4)	119.2(5)	O(5)—C(5)—C(12)	120.9(6)
C(4)—C(5)—C(12)	119.8(5)	N(6)—C(7)—C(8)	121.6(5)
N(6)—C(7)—C(17)	118.5(5)	C(8)—C(7)—C(17)	119.9(5)
C(7)—C(8)—C(9)	122.0(5)	C(8)—C(9)—C(13)	117.6(5)
C(8)—C(9)—C(20)	114.4(5)	C(13)—C(9)—C(20)	128.0(5)
N(1)—C(10)—C(11)	106.9(5)	N(1)—C(10)—C(13)	126.0(5)
C(11)—C(10)—C(13)	127.1(5)	C(3)—C(11)—C(4)	129.5(5)
C(3)—C(11)—C(10)	108.3(5)	C(4)—C(11)—C(10)	122.2(5)
N(6)—C(12)—C(5)	114.3(5)	N(6)—C(12)—C(13)	123.7(5)
C(5)—C(12)—C(13)	122.0(5)	C(9)—C(13)—C(10)	130.2(5)
C(9)—C(13)—C(12)	116.4(5)	C(10)—C(13)—C(12)	113.5(5)
O(15)—C(14)—O(16)	127.3(6)	O(15)—C(14)—C(2)	114.7(5)
O(16)—C(14)—C(2)	118.0(5)	O(18)—C(17)—O(19)	126.2(5)
O(18)—C(17)—C(7)	115.8(5)	O(19)—C(17)—C(7)	118.0(5)
O(21)—C(20)—O(22)	124.1(6)	O(21)—C(20)—C(9)	121.0(5)
O(22)—C(20)—C(9)	114.9(5)	K(1)—O(w3)^{i}—K(3)	96.1(1)
K(1)—O(5)^{ii}—K(3)	95.8(1)	K(1)—O(5)^{ii}—C(5)^{ii}	121.3(4)
K(3)—O(5)^{ii}—C(5)^{ii}	112.2(4)	K(3)—N(6)^{ii}—C(7)^{ii}	115.2(4)
K(3)—N(6)^{ii}—C(12)^{ii}	116.1(4)	K(2)—O(15)^{iii}—C(14)^{iii}	140.8(4)
K(2)—O(4)^{iv}—C(4)^{iv}	147.6(4)	K(1)—O(4)^{ii}—C(4)^{ii}	114.7(4)
K(3)—O(16)^{i}—C(14)^{i}	139.8(4)	K(3)—O(19)^{ii}—C(17)^{ii}	119.2(4)
K(3)—O(5)^{iv}—C(5)^{iv}	145.4(4)		

[a]Symmetry code: (i) 0.5-*x*, 0.5+*y*, 1.5-*z*; (ii) 0.5+*x*, 0.5-*y*, 0.5+*z*; (iii) -0.5+*x*, 0.5-*y*, 0.5+*z*; (iv) -*x*, 1-*y*, 1-*z*; (v) 1-*x*, -*y*, 1-*z*.

[b]Estimated standard deviations are given in parentheses.

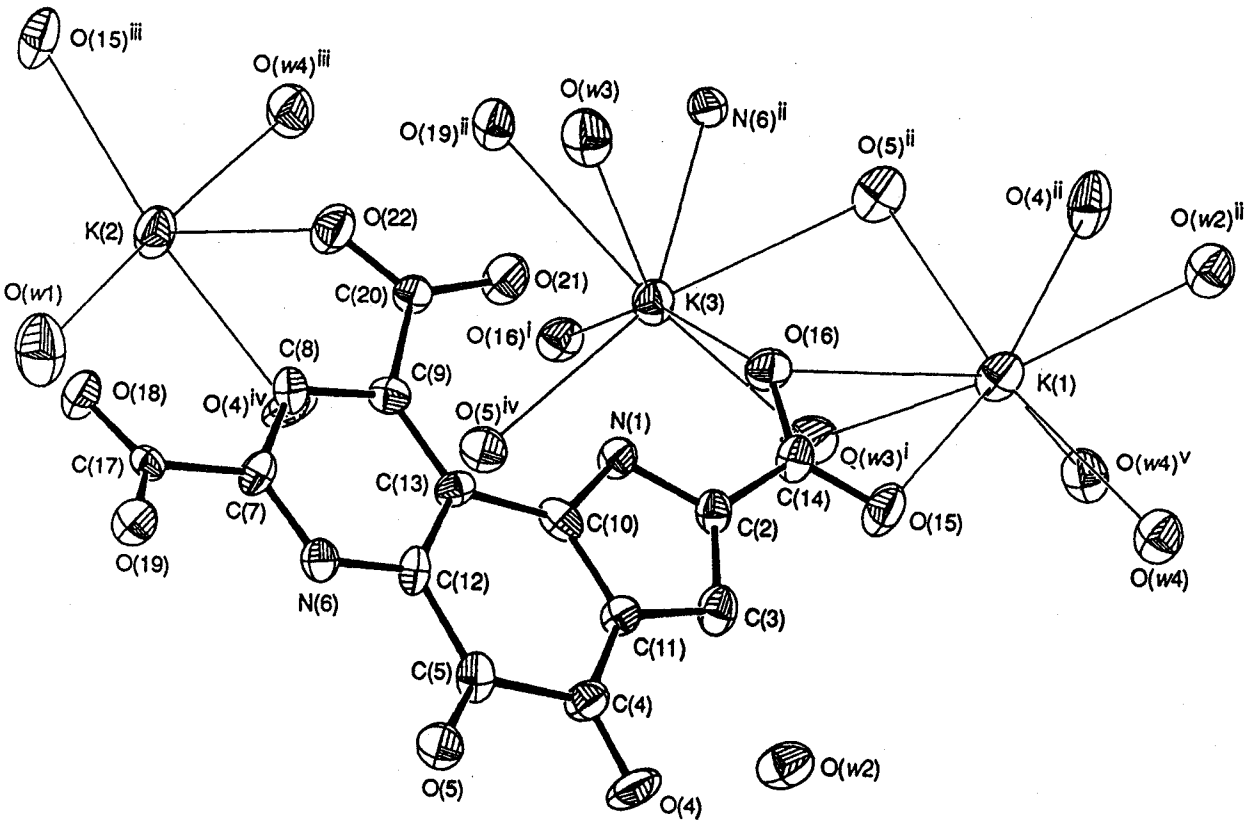

Figure III-1. Perspective view of $K_3Hpqq \cdot 4H_2O$ indicating the atom labeling. H atoms are omitted. Symmetry code: (i) 0.5-x, 0.5+y, 1.5-z; (ii) 0.5+x, 0.5-y, 0.5+z; (iii) -0.5+x, 0.5-y, 0.5+z; (iv) -x, 1-y, 1-z; (v) 1-x, -y, 1-z.

Å in H_2pqq and 1.234(8) Å in Hpqq]. The longer bond length in Hpqq is due to the coordination of O(4) atom to K(1) and K(2) ions. The crystal structure analysis of disodium H_2pqq salt demonstrated that H_2pqq possesses two metal-binding sites: a primary site in the pocket formed by the O(5), N(6), and O(19) atoms and a secondary site in the pocket formed by the O(4) and O(5) atoms.[6] In tripotassium Hpqq salt, two potassium cations (K(1) and K(3)) are also located at those sites. Another potassium cation (K(2)) is located at a novel site, which is formed by the O(4) and O(15)' atoms of two different Hpqq anions. K(2) ion is five-coordinated and two Hpqq anions bind to it as monodentate ligands. It seems that the location of K(2) ion is favorable in the view of the crystal packing. A stereoscopic view of the crystal packing is shown in Figure III-2. The most interesting features in the crystal unit are the extensive network of hydrogen-bonding interactions and the prominent stacking formation between Hpqq anions. Possible hydrogen bonds are listed in Table III-4, as judged from their bond distances. The stacking Hpqq anions form columns aligned along the crystallographic *b* axis. The closest interatomic distance between Hpqq anions is 3.416 (8) Å [C(11)···C(13)^{iv} (symmetry code: (iv) $-x$, $1-y$, $1-z$)]. The hydrogen-bonding network and the stacking interaction between Hpqq anions play an essential role in stabilizing this crystal structure.

Although the several structures of PQQ and its analogues have already been reported, this is the first report on the crystal structure of the trianionic form of PQQ ($Hpqq^{3-}$). Since PQQ seems to be the trianionic form for the ionic interaction with basic amino acid residues in the enzymes, this structural information may be useful to know the various features of PQQ in the enzymes.

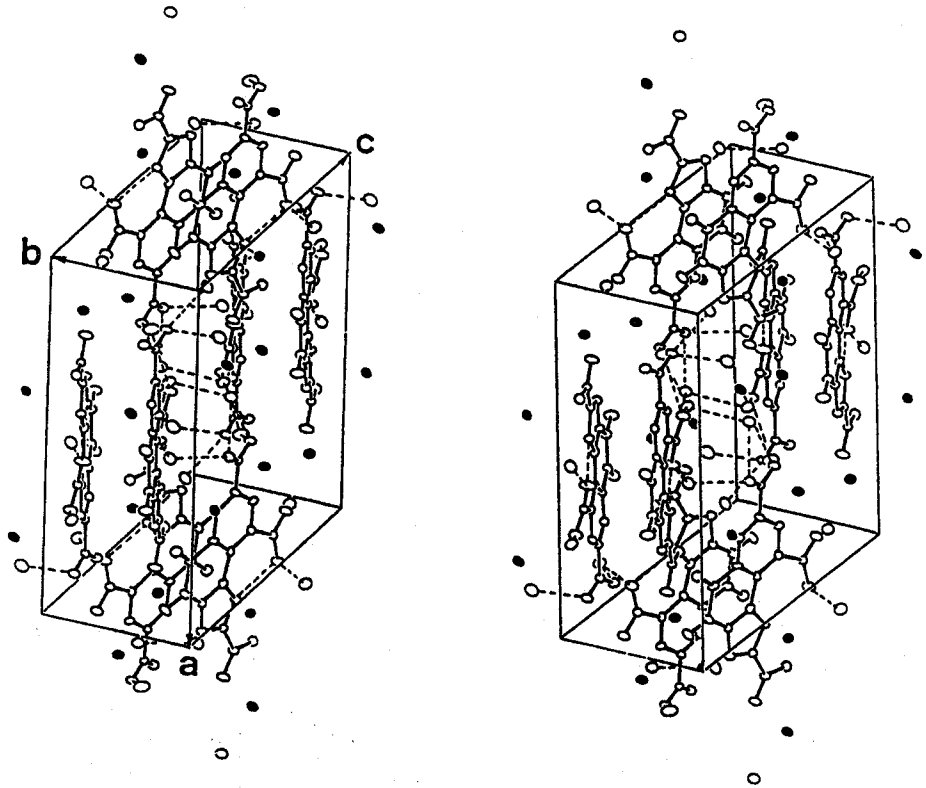

Figure III-2. Stereoscopic drawing of the crystal packing. Filled circles represent potassium ions. Broken lines indicate possible hydrogen bonds.

Table III-4. Possible Hydrogen Bond Distances (Å)[a,b]

O(18)···O(*w*1)	2.852(7)	O(21)···N(1)	2.574(7)
O(21)···O(*w*3)	2.768(7)	O(*w*3)···O(19)^{ii}	2.818(6)
O(*w*4)···O(*w*2)^{ii}	3.199(6)	O(18)···O(*w*2)^{iii}	2.813(6)
O(19)···O(*w*4)^{vi}	2.803(6)	O(*w*2)···O(*w*4)^{vii}	2.767(6)

[a]Symmetry code: (ii) 0.5+*x*, 0.5-*y*, 0.5+*z*; (iii) -0.5+*x*, 0.5-*y*, 0.5+*z*; (vi) -1+*x*, *y*, *z*; (vii) 0.5-*x*, -0.5+*y*, 0.5-*z*.

[b]Estimated standard deviations are given in parentheses.

References

(1) Duine, J. A.; Frank, J.; Verwiel, P. E. J. *Eur. J. Biochem.* **1980,** *108*, 187–192.

(2) Duine, J. A.; Frank, J. *Trends Biochem. Sci.* **1981,** *6*, 278–280.

(3) Salisbury, S. A.; Forrest, H. S.; Cruse, W. B. T.; Kennard, O. *Nature (London)* **1979,** *281*, 843–844.

(4) Cruse, W. B. T.; Kennard, O.; Salisbury, S. A. *Acta Crystallogr.* **1980,** *B36*, 751–754.

(5) van Koningsveld, H.; Jansen, J. C.; Jongejan, J. A.; Frank, J.; Duine, J. A. *Acta Crystallogr.* **1985,** *C41*, 89–92.

(6) Ishida, T.; Doi, M.; Tomita, K.; Hayashi, H.; Inoue, M.; Urakami, T. *J. Am. Chem. Soc.* **1989,** *111*, 6822–6828.

(7) North, A. C. T.; Phillips, D. C.; Mathews, F. S. *Acta Cryst.* **1968,** *A24*, 351–359.

(8) Main, P; Hull, S. E.; Lessinger, L.; Germain, G.; Declercq, J. -P.; Woolfson, M. M. *MULTAN 78*, A System of Computer Programs for the Automatic Solution of Crystal Structures from X-ray Diffraction Data, Universities of York, England, and Louvain, Belgium, 1978.

(9) Ashida, T. *HBLS-V*, The Universal Crystallographic Computing System-Osaka, The Computation Center, Osaka University, Japan, 1979.

Chapter IV. ELECTROCHEMICAL PROPERTIES OF PQQ AND A PQQ-CONTAINING COPPER COMPLEX

Introduction

A great variety of bacterial dehydrogenases (e. g., alcohol dehydrogenase from *Gluconobacter suboxydans* and glucose dehydrogenase from *Acinetobacter calcoaceticus*) have been known to contain PQQ as an organic cofactor with respect to the redox reactions of biological systems.[1-3] To know the redox properties of PQQ is important for an understanding of the electron transfer processes in these oxidoreductases. Electrochemical properties of PQQ and its analogues have been reported in recent years.[4-9] However, the electrochemical behavior of PQQ at conventional electrodes (platinum, gold, and glassy carbon) shows quasi-reversible or irreversible process.

Here we report the electrochemical behavior of PQQ in acidic solutions at a di-(4-pyridyl) disulfide (4-pyds) modified gold electrode. Various sulfur-containing promoters such as 4-pyds are generally employed for the acceleration of electron transfer between the electrodes and metalloproteins.[10,11] Spectroelectrochemistry of PQQ provides the redox potentials ($E^{\circ\prime}$), the number of electrons (n) involved in overall redox process, and the spectra of the electrogenerated species at the same time.

In this chapter, the voltammetric results of a PQQ-containing copper (II) complex ([Cu(H_2pqq)(terpy)] (**1**)), are also described.

Experimental Section

Materials. PQQ was purchased from Ube Industries (Tokyo, Japan). Other chemicals were guaranteed reagent grade and were purchased from Wako Chemical Co.

Apparatus. All electrochemical measurements were carried out with a three-electrode system consisting of an Ag/AgCl reference electrode, a platinum-wire counter electrode, and a 4-pyds modified gold working electrode. Bioanalytical Systems (BAS) CV-27 Voltammograph, BAS PA-1 low-current module, and Graphtec WX-2400 X-Y recorder were used to record the voltammograms. The optically transparent thin-layer electrode (OTTLE) cell was constructed according to the reports by Heineman and co-workers.[12,13] The size of the gold minigrid electrode was 8 mm (width) X 25 mm (height) X 0.3 mm (thickness). Electronic absorption spectra were measured with a Shimadzu MPS-2000 spectrophotometer.

Procedure. The 0.05 – 0.1 M (1 M = 1 mol dm^{-3}) CH_3COOH/HCl buffer was used for electrochemical measurements. The pH value of the buffer solution was measured before and after each measurement. The gold disk electrode (electrode surface area, A = 0.0211 cm^2) and the gold minigrid electrode were freshly modified with 4-pyds by dipping the electrode for 10 min into the saturated solution of 4-pyds before each measurement. The OTTLE cell was positioned in the Shimadzu MPS-2000 sample compartment (previously purged with nitrogen

gas) and a blanket of nitrogen gas was maintained over the sample solution throughout the experiment. After deaeration with wet argon, all electrochemical measurements were carried out at 25 °C. All of the electrode potentials in this chapter are given with respect to an Ag/AgCl electrode.

Results and Discussion

Cyclic voltammograms of PQQ were obtained under different pH conditions in the 0.1 M buffer solution. In the case of a bare gold electrode, the voltammograms exhibit no obvious peak at pH > 4.5. A couple of reduction and reoxidation peaks was observed below pH 4.5, although the electron transfer between PQQ and the electrode does not show the reversible process. Figure IV-1a depicts the voltammograms using a bare gold electrode at pH 2.70. Only one quasi-reversible response was observed with a midpoint potential, $E_{1/2}$ = +140 mV and the potential separation between the reduction peak and the oxidation one, ΔE_p = 51 mV at a scan rate (v) of 20 mV s^{-1}. These findings suggest that the electrochemically reversible response of PQQ at a bare gold electrode is difficult. The cyclic voltammetric response using a 4-pyds modified gold electrode was reversible in the region from pH 2 to pH 5, but not reversible above pH 5. The cyclic voltammograms at pH 2.70 are shown in Figure IV-1b. $E_{1/2}$ and ΔE_p were evaluated to be +144 mV and 37 mV, respectively; the ΔE_p value proved that the redox reaction proceeds in a one-step two-electron transfer process. ΔE_p was practically independent of scan rate. The peak current of the oxidation is almost the same as that of the reduction.

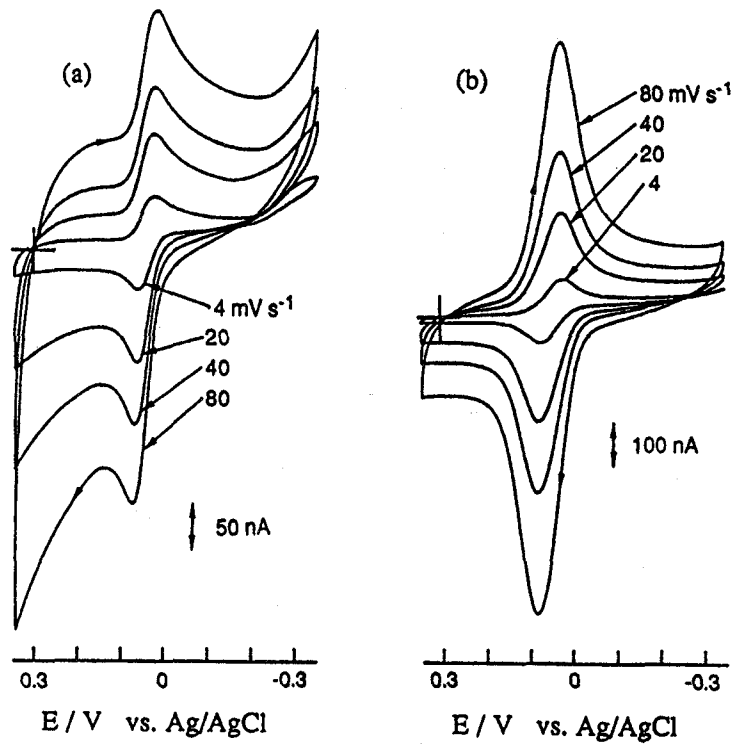

Figure IV-1. Cyclic voltammograms of PQQ using a bare gold electrode (a) and a 4-pyds modified gold electrode (b) at pH 2.70. Scan rate: 4, 20, 40, and 80 mV s^{-1}, PQQ concentration: 30 μM.

Figure IV-2 exhibits the relationships between square root of $v^{1/2}$ and cathodic peak current (i_{pc}). A scan rate dependence of the reversible couple yields linear plots of i_{pc} / C vs. $v^{1/2}$ up to v = 80 mV s^{-1} at pH 2.03 – 4.74. However, a plot of i_{pc} / C vs. $v^{1/2}$ at pH 1.52 displays to be nonlinear, which indicates that PQQ weakly adsorbs on the electrode.[14] These findings suggest that PQQ interacts with the 4-pyds modified gold electrode to receive two electrons and two protons at the *o*-quinone moiety under acidic conditions. It is considered that the pyridine moiety of 4-pyds modified gold electrode interacts with the *o*-quinone part of PQQ through hydrogen bonds, which accelerate the proton transfer as well as the electron transfer (Figure IV-3).

Electronic absorption spectra during the course of PQQ reduction were recorded by the spectroelectrochemical method using the OTTLE, as shown in Figure IV-4. The PQQ and $PQQH_2$ (two electron reduced form of PQQ) exhibit absorption maxima at 249 nm and 318 nm, respectively. The absorption band of $PQQH_2$ coincides with that of the reduction product of PQQ with $Na_2S_2O_4$.[15] The absorbance changes at a given wavelength can be related to the concentration ratio of reduced to oxidized species by equation (1),

$$[R] / [O] = (A - A_{ox}) / (A_{red} - A), \quad (1)$$

where A is the absorbance of the OTTLE at a given applied potential (E_{app}), A_{ox} is the absorbance of the fully oxidized form, and A_{red} is the absorbance of the fully reduced form. The Nernst equation (2) indicates that a plot of E_{app} vs. log([R] / [O]) should be linear

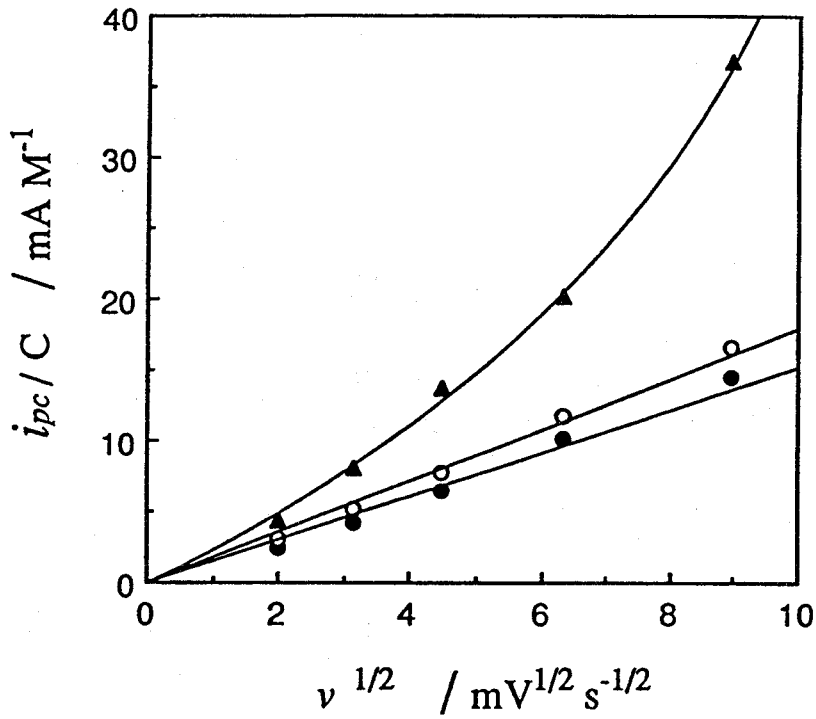

Figure IV-2. Plots of i_{pc} / C vs. $v^{1/2}$ using a 4-pyds modified gold electrode at pH 1.52 (▲), pH 2.03 (○), and pH 4.74(●). PQQ concentration (C): 30 μM.

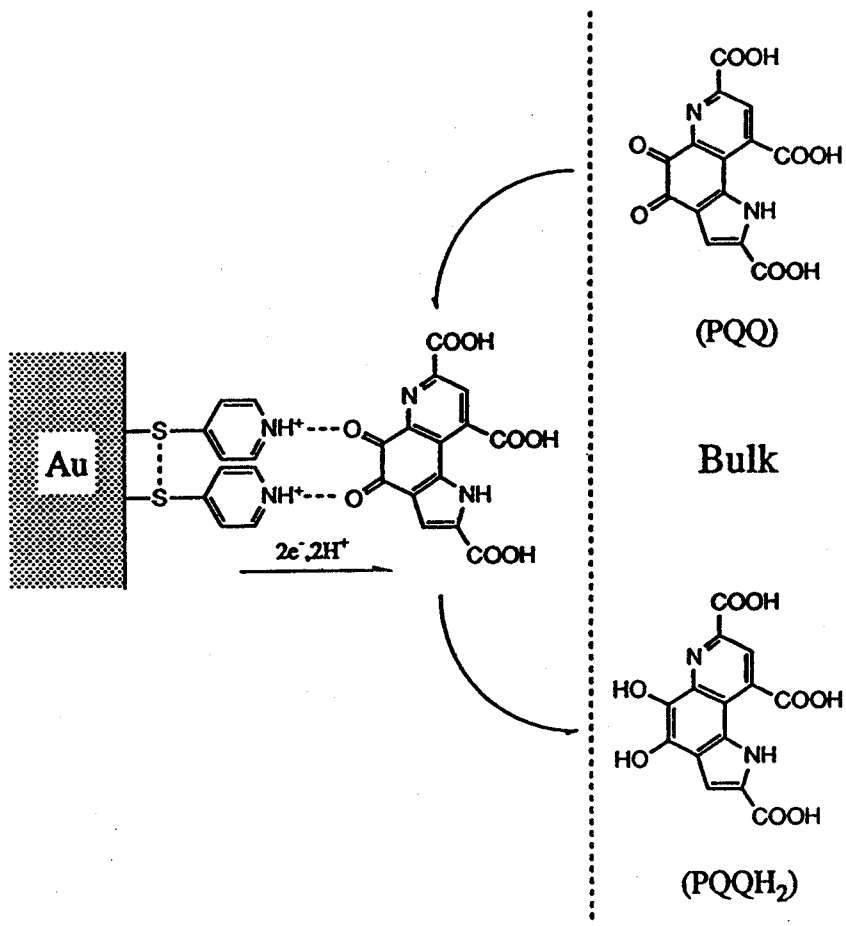

Figure IV-3. Proposed reduction mechanism of PQQ at a 4-pyds modified gold electrode.

$$E_{app} = E^{\circ\prime} - (0.059 / n) \log ([R] / [O]) \quad (2)$$

with a slope of 59 / n mV and an intercept of $E^{\circ\prime}$ (the standard redox potential), assuming Nernstian reversibility. The Nernst plot at 318 nm in Figure IV-4 gives $E^{\circ\prime}$ = +10 mV and n = 1.88 at pH 4.31.[16] The well-defined isosbestic points (at 272, 332, and 380 nm) indicate that one-electron reduced form of PQQ (pyrroloquinoline semiquinone) does not occur in this process. Therefore, this OTTLE measurement also suggests that the one-step two-electron transfer between PQQ and a 4-pyds modified gold electrode proceeds reversibly. The unclear voltammetric response was observed at pH > 5, which is presumably due to the deprotonation of pyridine moiety in 4-pyds or the hydration[17,18] of the *o*-quinone moiety in PQQ or both.

The voltammetric behavior of complex **1** using a bare gold electrode and a 4-pyds modified gold electrode under acidic conditions are also investigated. The complex **1** is not sufficiently soluble at pH < 4, so that reduction and oxidation peak can not be observed. In the case of a bare gold electrode, the electron transfer is still irreversible at pH > 4. Therefore, using a bare gold electrode, the redox reaction of complex **1** on the electrode is not smooth. In the case of a 4-pyds modified gold electrode, the electron transfer is also irreversible and complicated at pH > 4.5, and it is difficult to explain these phenomena. However, only at 4 < pH < 4.5, two redox couples were observed clearly. A typical cyclic voltammogram is shown in Figure IV-5. A scan initiated in the negative direction at +0.3 V reveals the first reduction wave at -0.006 V and the second reduction wave at -0.414 V. The first and the second reduction waves are probably attributed to the reduction of quinone (PQQ) to diol ($PQQH_2$) and of Cu(II) to

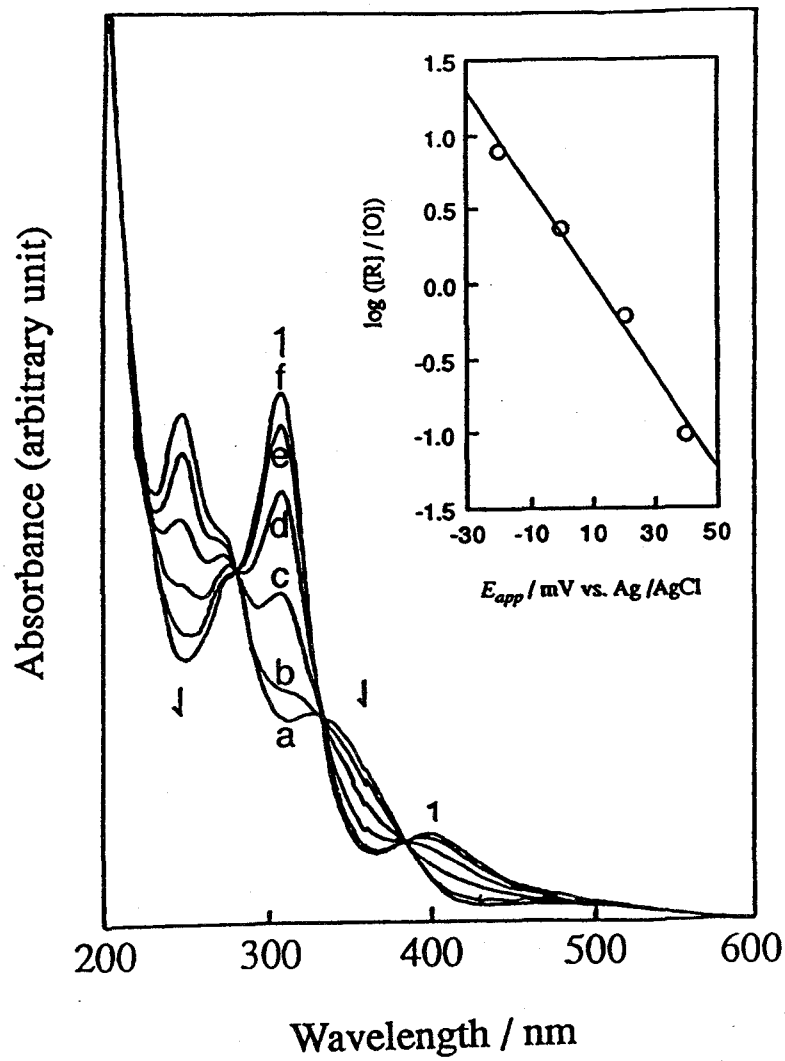

Figure IV-4. Electronic absorption spectra recorded during the OTTLE spectropotentiostatic experiment in 0.05 M CH_3COOH / HCl buffer containing 0.21 mM PQQ at pH 4.31. Applied potentials in mV vs. Ag/AgCl are follows: (a) 100, (b) 40, (c) 20, (d) 0, (e) -20, (f) -100. Inset: Nernst plot at 318 nm.

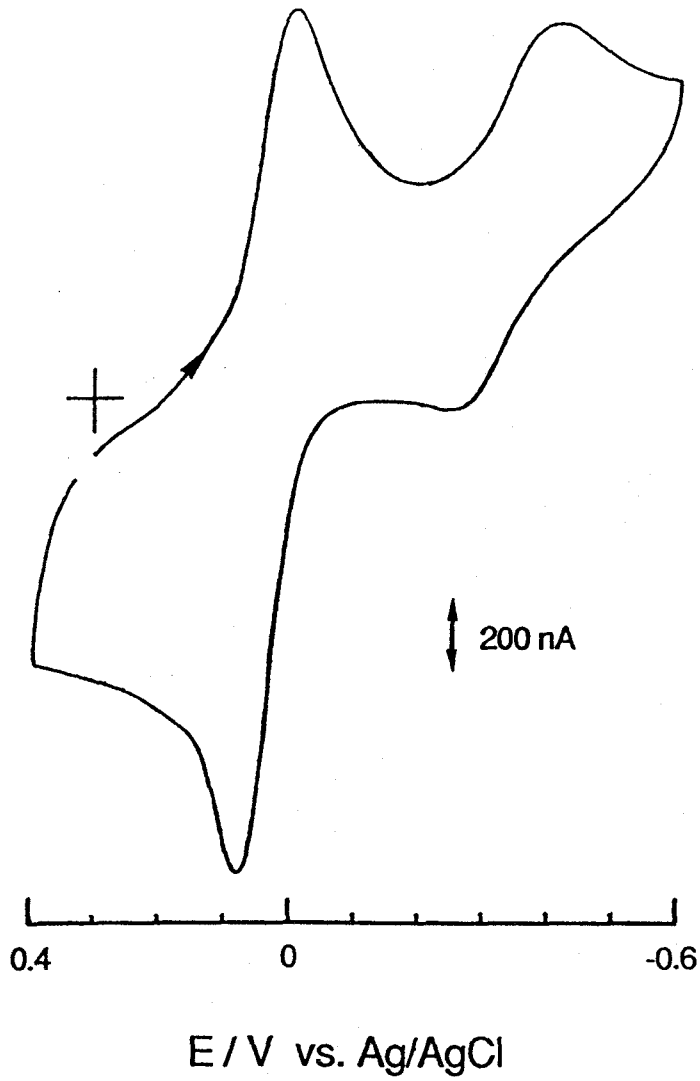

Figure IV-5. Cyclic voltammogram of [Cu(H_2pqq)(terpy)] using a 4-pyds modified gold electrode at pH 4.19. Scan rate: 80 mV/ s^{-1}.

Cu(I), respectively. Upon reversal of the scan at -0.6 V, two oxidation waves are observed at -0.247 V and +0.078 V. When the scan is reversed after the first cathodic wave at -0.006 V, a voltammogram with quasi-reversible characteristics is observed: ΔE_p of the voltammogram is 84 mV, which is apparently larger than that of the reversible cyclic voltammogram, and it increases with increasing v. Hence, this result clearly shows the difference between free PQQ and coordinated PQQ about the electron transfer modes. It might be considered that electron and proton transfer between free PQQ and a 4-pyds modified electrode is more rapid than between PQQ in the complex **1** and the electrode. A steric hindrance of the complex **1** itself probably prevents the interaction between 4-pyds on a gold electrode and PQQ in the complex **1**. Another redox couple (E_{pc} = -0.414 V and E_{pa} = -0.247 V) has large peak separation (ΔE_p = 167 mV), and the peak oxidation current is smaller than the peak reduction one, and hence the electron transfer is irreversible. In addition, application of the OTTLE method to the complex **1** were not success. Perhaps, the main problem is the solubility of the complex, because precipitate was observed soon.

In this chapter, it is revealed that hydrogen bonds between the *o*-quinone moiety of PQQ and the 4-pyds modified electrode are important to accelerate the proton and the electron transfer. Therefore, in the active site of PQQ-containing enzymes, PQQ might carry out redox reaction with a substrate through hydrogen bonds.

References and Notes

(1) Duine, J. A.; Frank, J.; Jongejan, J. A. In *Advances in Enzymology*; Meister, A. Ed.; Wiley: New York 1987; Vol. 59, pp. 169–212.

(2) Salisbury, S. A.; Forrest, H. S.; Cruse, W. B. T.; Kennard, O. *Nature*, **1979**, *280*, 843–844.

(3) Ameyama, M.; Matsushita, K.; Ohno, Y.; Shinagawa, E.; Adachi, O. *FEBS Lett.* **1981**, *130*, 179–183.

(4) Eckert, T. S.; Bruice, T. C.; Gainor, J. A.; Weinreb, S. M. *Proc. Natl. Acad. Sci. USA* **1982**, *79*, 2533–2536.

(5) Sleath, P. R.; Noar, J. B.; Eberlein, G. A.; Bruice, T. C. *J. Am. Chem. Soc.* **1985**, *107*, 3328–3338.

(6) Kano, K.; Mori, K.; Uno, B.; Kubota, T.; Ikeda, T.; Senda, M. *Bioelectrochemistry and Bioenergetics* **1990**, *23*, 227–238.

(7) Kano, K.; Mori, K.; Uno, B.; Goto, M. *J. Electroanal. Chem.* **1990**, *293*, 177–184.

(8) Kano, K.; Mori, K.; Uno, B.; Kubota, T.; Ikeda, T.; Senda, S. *Bioelectrochemistry and Bioenergetics*, **1990**, *24*, 193–201.

(9) Shinohara, H.; Khan, G. F.; Ikariyama, Y.; Aizawa, M. *J. Electroanal. Chem, 1991,* **304**, 75–84.

(10) Eddows, M. J.; Hill, H. A. O. *J. Chem. Soc., Chem. Commun.* **1977**, 771.

(11) Taniguchi, I.; Toyosawa, K.; Yamaguchi, H.; Yasukouchi, K. *J. Chem. Soc., Chem. Commun.* **1982**, 1032.

(12) Murray, R. W.; Heineman, W. R.; O'Dom, G. W. *Anal. Chem.* **1967**, *39*, 1666–1668.

(13) DeAngelis, T. P.; Heineman, W. R. *J. Chem. Educ.* **1976**, *53*, 594–597.

(14) Wopschall, R. H.; Shain, I. *Anal. Chem,* **1967**, *39*, 1514–1527.

(15) Itoh, S.; Ohshiro, Y.; Agawa, T. *Bull. Chem. Soc. Jpn.* **1986**, *59*, 1911–1914.

(16) At pH 4.31 $E_{1/2}$ was estimated to be +21 mV by the cyclic voltammetry. This value is close to $E^{o'}$ by the OTTLE method.

(17) Dekker, R. H.; Duine, J. A.; Frank, J.; Verwiel, P. E. J.; Westerling, J. *Eur. J. Biochem.* **1982**, *125*, 69–73.

(18) Rodrignez, E. J.; Bruice, T. C.; Edmondson, D. E. *J. Am. Chem. Soc.* **1987**, *109*, 532–537.

Chapter V. SYNTHESES AND CHARACTERIZATION OF TOPA-CONTAINING COPPER COMPLEXES

Introduction

Copper-containing amine oxidases (EC 1.4.3.6) are very widely distributed in plants, mammals, and microorganisms, being believed to play critical roles in the metabolism of biogenic primary amines.[1-4] Generally, these enzymes are composed of two subunits that appear to be similar, if not identical, to a total molecular weight of 170,000–190,000. They catalyze the oxidative deamination of amines by accepting two electrons from amines and transferring them to molecular oxygen, as expressed by the equation.

$$RCH_2NH_2 + O_2 + H_2O \longrightarrow RCHO + NH_3 + H_2O_2$$

They are known to contain nonblue and electron paramagnetic resonance (EPR) detectable copper and an organic cofactor responsible for their yellowish pink color. In fairly recent studies, Ameyama et al.[5] and Lobenstein-Verbeek et al.[6] proposed that the active site cofactor in bovine serum amine oxidase (BSAO) was a pyrroloquinoline quinone (PQQ). However, the most recent studies by Janes et al. show clearly that the active site cofactor of BSAO is a dihydroxy derivative of tyrosine, referred to as 6-hydroxydopa or topa.[7]

On the other hand, all the copper-containing amine oxidases contain two copper ions per protein molecule.[1,2] The Cu(II) site structure was derived from

X-ray absorption[8,9] and pulsed EPR spectroscopy.[10] It was indicated that the Cu(II) sites are tetragonal geometry. Besides, NMR[11] and fluorescence-quenching studies[12] on porcine plasma amine oxidase derivatized with substituted phenylhydrazines have placed the Cu(II) ions and the quinone groups within several angstroms of each other. A proposed structure for the Cu(II) site is displayed in Figure V-1. Recently, using the room-temperature EPR measurements, the evidence for the generation of a Cu(I) semiquinone state have been presented.[13]

In this chapter, the details for the synthesis and characterization of the first topa-containing copper(II) complexes are reported as the model for the active sites of copper-containing amine oxidases. Studies of the oxidative deamination of benzylamine to benzaldehyde by molecular oxygen in the presence of these copper complexes are also described.

Experimental Section

The treatments of DL-topa, [Cu(DL-topa)(bpy)]NO3, and [Cu(DL-topa)(phen)]NO_3 were carried out by standard Schlenk techniques under an argon atmosphere.

Material. DL-topa was purchased from Sigma, and other amino acids were from Nacalai Tesque. Other chemicals were procured from commercial sources and used without further purification. [Cu(bpy)$(H_2O)_2$]$(NO_3)_2$ and [Cu(phen)]$(NO_3)_2$ were synthesized from copper(II) nitrate according to a method

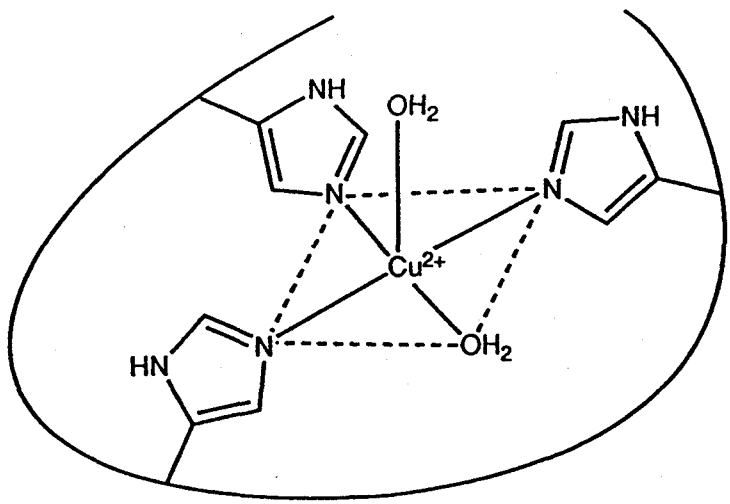

Figure V-1. Proposed structure for the Cu(II) sites in copper-containing amine oxidases.

described in the previous paper.[14]

Preparation of the Ternary Complexes. The complex, [Cu(DL-topa)(bpy)]NO_3·$4H_2O$ was prepared according to the following procedures. [Cu(bpy)$(H_2O)_2$]$(NO_3)_2$ (50 μmol) was dissolved in 3 cm^3 of distilled water under Ar atmosphere. DL-topa (50 μmol) was anaerobically added to the solution, and then the mixture was stirred to dissolve topa completely at room temperature. The solution was concentrated to about one-fourth of the volume and permitted to stand at 4 °C until the bluish green crystals separated out. Anal. Calcd for $C_{19}H_{26}N_4O_{12}Cu$: C, 40.32; H, 4.63; N, 9.90 %. Found: C, 40.55; H, 4.58; N, 9.92 %.

[Cu(DL-topa)(phen)]NO_3·$0.5H_2O$ was prepared according to the above procedure by substituting [Cu(phen)]$(NO_3)_2$ for [Cu(bpy)$(H_2O)_2$]$(NO_3)_2$. Anal. Calcd for $C_{21}H_{19}N_4O_{8.5}Cu$: C, 47.87; H, 3.63; N, 10.63 %. Found: C, 47.86; H, 3.57; N, 10.69 %.

Other ternary Cu(II) complexes comprised of bpy and amino acids were prepared in a similar manner to those above.

Physical Measurements. EPR, diffuse reflectance, and electronic absorption spectra were obtained on a JEOL JES-FE1X EPR spectrometer, a Hitachi U-3400 spectrophotometer, and a Shimadzu MPS-2000 spectrophotometer, respectively.

Difference spectra were measured with Shimadzu MPS-2000 spectrophotometer in dual compartment cells with path lengths of 1.0 cm. One side of the reference cell was filled with the solution of 1.31 mM $[Cu(bpy)]^{2+}$ (0.5 cm^3) and 1.31 mM DL-alanine (0.5 cm^3). Another side of the reference cell was

filled with the solution of 0.655 mM aromatic amino acids (1 cm^3). One side of the sample cell was filled with the solution of 1.31 mM $[Cu(bpy)]^{2+}$ (0.5 cm^3) and 1.31 mM aromatic amino acids (0.5 cm^3). Another side of the sample cell was filled with the solution of 0.655 mM DL-alanine (1 cm^3).

Cyclic voltammetry experiments were performed with a Bioanalytical Systems (BAS) CV-27 voltammograph equipped with a Graphtec WX-2400 X-Y recorder. A three-electrode configuration was used, comprised of a glassy-carbon working electrode, a platinum-wire counter electrode, and a Ag/AgCl reference electrode.

pH Titration. pH titrations were carried out for DL-topa and [Cu(DL-topa)(bpy)]NO_3 at 25 °C and I = 0.1 M (KNO_3) under a nitrogen atmosphere. The concentrations of the DL-topa and [Cu(DL-topa)(bpy)]NO_3 were 0.5 and 1.0 mM, respectively. The pH values were measured with a TOA Auto Titrator AUT-301 equipped with a TOA HS-205C electrode and a TOA HGS-4005 glass electrode. The protonation constant (pKa) values for DL-topa and [Cu(DL-topa)(bpy)]NO_3 were determined by the method of non-linear least-squares with the computer program MINIQUAD.[15]

Oxidative Deamination of Benzylamine. The complex [Cu(DL-topa)(bpy)]NO_3 (1.0 mM) was treated with 53-fold excess of benzylamine under aerobic conditions at pH 7.0 (0.01 M HEPES buffer) and 27 °C. The yield of benzaldehyde was determined by HPLC. HPLC was performed on a IRICA-LC500 system equipped with a IRICA-RC18 reverse phase column under the following conditions: the eluent, 54.5/45.0/0.5 H_2O/MeOH/H_3PO_4 v/v/v; flow rate,

0.7 ml min^{-1}; monitor, 254 nm. The reactions with other catalysts (DL-tyr, DL-dopa, DL-topa, [Cu(DL-tyr)(bpy)]NO_3, [Cu(DL-dopa)(bpy)]NO_3, and [Cu(DL-topa)(phen)]NO_3) were carried out under the same conditions.

Results and Discussion

Physical Properties of the Ternary Complexes. The absorption spectra for DL-topa, [Cu(DL-topa)(bpy)]$^+$, and [Cu(DL-topa)(phen)]$^+$ are shown in Figure V-2. The absorption spectra for [Cu(bpy)]$^{2+}$, [Cu(phen)]$^{2+}$, and the ternary systems are summarized Table V-1. The ternary complexes show a d–d absorption maximum at 600–630 nm with ε = 30–104. The diffuse reflectance spectra of [Cu(DL-topa)(bpy)]NO_3·4H_2O and [Cu(DL-topa)(phen)]NO_3·0.5H_2O are shown in Figure V-3. The d–d transition peaks of [Cu(DL-topa)(bpy)]NO_3·4H_2O and [Cu(DL-topa)(phen)]NO_3·0.5H_2O are observed at 601 nm and 606 nm, respectively. Since the d–d absorption bands of these complexes in aqueous solution corresponds well with those in the solid state, the structures in aqueous solution are similar to those established in the crystal state. The EPR spectra for these systems at 77 K show that the Cu(II) environments are of typical axial symmetry (Figure V-4) with the parameters in Table V-2. Additionally, seven superhyperfine lines (A_N = 1.2–1.9 mT) due to nitrogens bound to the Cu(II) ion were observed in $g_\perp$ regions of the signals of the all ternary complexes. Since the absorption bands of d–d transitions and EPR spectral parameters for these ternary complexes are very similar to each other, it may be concluded the glycine-like mode of coordination by amino acids in the ternary complexes.

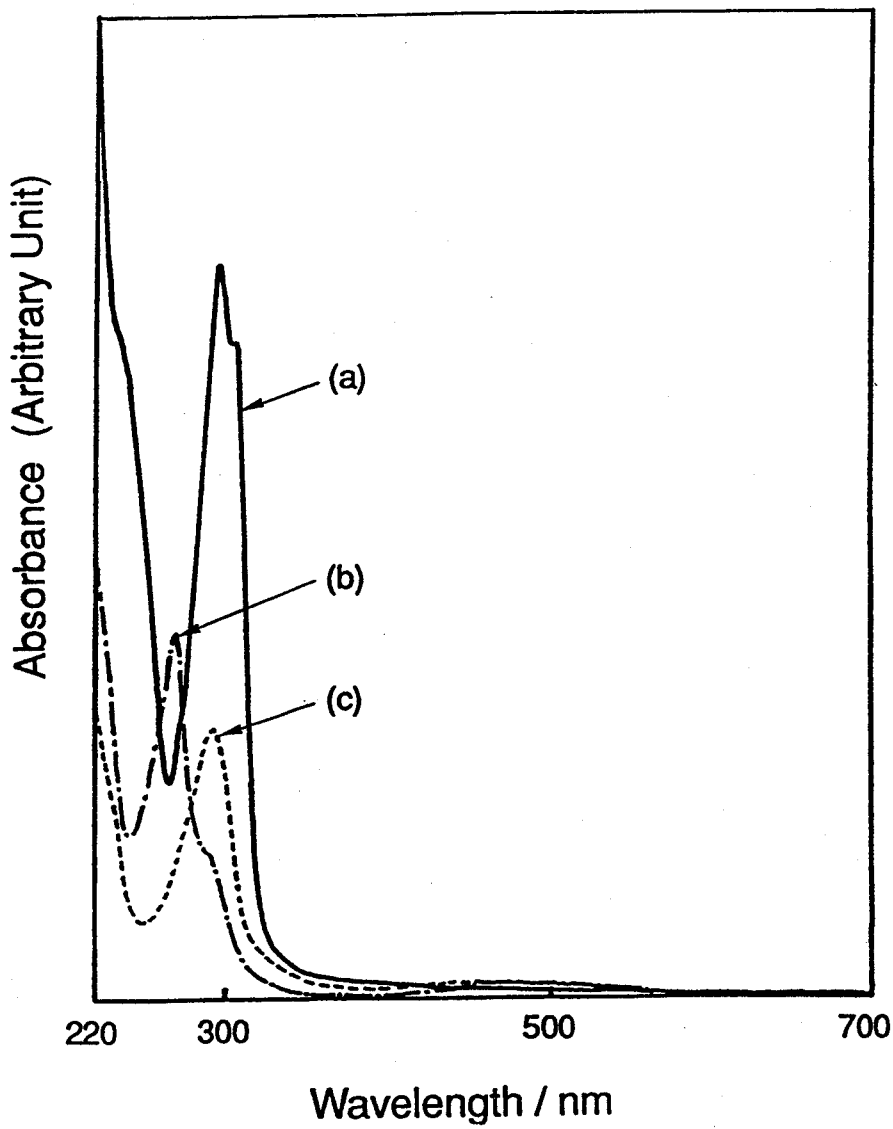

Figure V-2. Electronic absorption spectra of (a) [Cu(DL-topa)(bpy)]$^+$, (b) [Cu(DL-topa)(phen)]$^+$, and (c) DL-topa in aqueous solution.

Table V-1. Electronic Absorption Spectroscopic Data of Cu(II) Complexes in Aqueous Solution

complex	λ_{max} / nm (ε / $M^{-1}cm^{-1}$)		
$[Cu(bpy)]^{2+}$	300 (14000),	310 (14200),	699 (30)
[Cu(DL-ala)(bpy)]$^{+}$	299 (12900),	309 (12900),	601 (51)
[Cu(DL-phe)(bpy)]$^{+}$	300 (13200),	311 (12900),	601 (72)
[Cu(DL-tyr)(bpy)]$^{+}$	300 (13300),	310 (13000),	601 (74)
[Cu(DL-dopa)(bpy)]$^{+}$	300 (13400),	309 (13100),	628 (44)
[Cu(DL-topa)(bpy)]$^{+}$	300 (16700),	314 (14300),	601 (104)
$[Cu(phen)]^{2+}$	272 (31700),	294 (9300),	709 (27)
[Cu(DL-topa)(phen)]$^{+}$	272 (32200),	295[a] (13700),	606 (95)

[a] Shoulder.

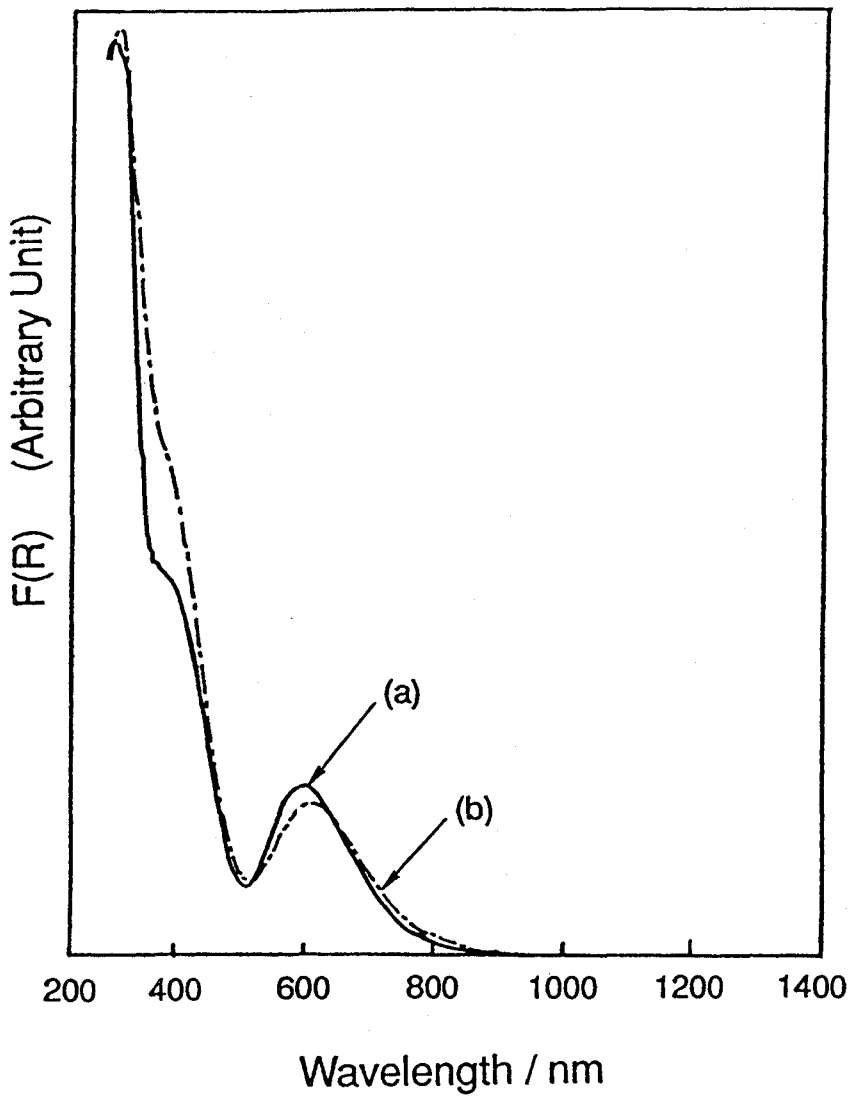

Figure V-3. Diffuse reflectance spectra of (a) [Cu(DL-topa)(bpy)]NO_3 and (b) [Cu(DL-topa)(phen)]NO_3.

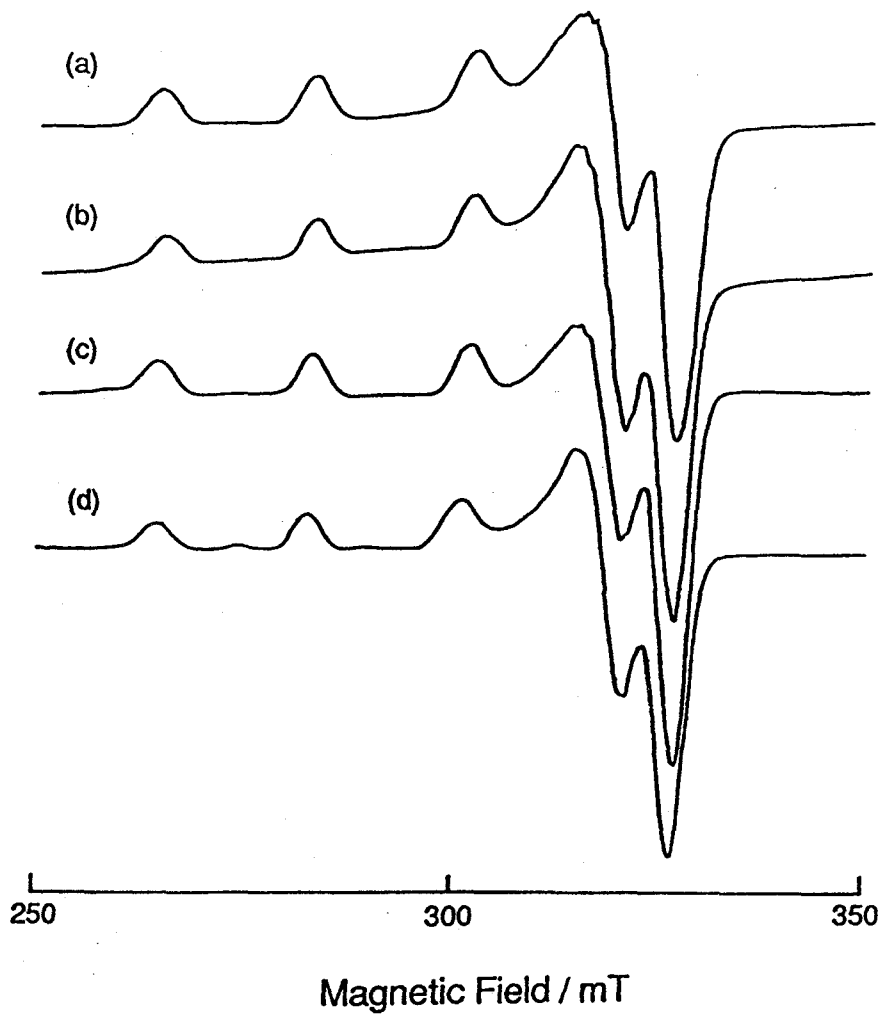

Figure V-4. EPR spectra of (a) [Cu(DL-tyr)(bpy)]$^+$, (b) [Cu(DL-dopa)(bpy)]$^+$, (c) [Cu(DL-topa)(bpy)]$^+$, and (d) [Cu(DL-topa)(phen)]$^+$ in frozen water–ethylene glycol at 77K.

Table V-2. EPR Parameters for Ternary Complexes in Frozen Water–Ethylene Glycol at 77K

complex	$g_{\perp}$	$g_{//}$	$A_{//}$ / mT	A_N / mT
[Cu(DL-ala)(bpy)]$^+$	2.06	2.23	18.7	1.3
[Cu(DL-phe)(bpy)]$^+$	2.06	2.23	18.7	1.2
[Cu(DL-tyr)(bpy)]$^+$	2.06	2.24	18.7	1.9
[Cu(DL-dopa)(bpy)]$^+$	2.06	2.24	18.3	1.8
[Cu(DL-topa)(bpy)]$^+$	2.06	2.24	18.6	1.2
[Cu(DL-topa)(phen)]$^+$	2.06	2.24	18.2	1.8

Table V-3 summarizes the pKa values for five amino acids and the [Cu(DL-topa)(bpy)]$^+$ complex. The species distributions are demonstrated in Figure V-5. The first proton dissociation constant (8.56) of the hydroxyl group of topa is lower than those of tyr and dopa. This phenomenon is consistent with the fact that the constant depends on the number of hydroxyl group in a series of phenol derivatives; phenol 9.82, catechol 9.23, and pyrogallol 8.98.[16] Further, the constant of the [Cu(DL-topa)(bpy)]$^+$ complex is much lower than that of free topa and the difference of these values is presumably due to the decreasing of π-electron density of topa by coordinating to the copper(II) ion.

Electrochemical Properties of the Ternary Systems. The results of cyclic voltammetric measurements are given in Table V-4 for [Cu(bpy)]$^{2+}$ and the ternary complexes. [Cu(bpy)]$^{2+}$, [Cu(DL-ala)(bpy)]$^+$, [Cu(DL-phe)(bpy)]$^+$, and [Cu(DL-tyr)(bpy)]$^+$ showed quasi-reversible cyclic voltammograms with a pair of cathodic and anodic waves of Cu(II)/Cu(I). In the case of [Cu(DL-topa)(bpy)]$^+$ and [Cu(DL-topa)(phen)]$^+$, cyclic voltammograms showed two redox couples. The cyclic voltammogram of [Cu(DL-topa)(bpy)]$^+$ is shown in Figure V-6. A positive potential scan initiated at the open circuit potential (-0.1 V vs. Ag/AgCl) gives an oxidation wave which is probably attributed to the reduction of diol to quinone. A coupled reduction wave is present on the subsequent negative scan. Continuing the scan in the negative direction results in a reduction wave which is probably attributed to the reduction of Cu(II) to Cu(I). After scan reversal, a coupled oxidation wave is observed. The large peak separation of the first redox couple may be due to the complex adsorption on the electrode surface or to the reduction of another species arising from rapid decomposition of the copper(II) complex

Table V-3. pKa Constants of Amino Acids and [Cu(DL-topa)(bpy)]NO_3

compound	$-NH_3^+$	-COOH	-OH
ala[a]	9.69	2.30	
phe[a]	9.11	2.18	
tyr[a]	9.04	2.17	10.14
dopa[a]	9.74	2.31	8.71, 13.40
topa	9.91	–[b]	8.56, 11.14, –[b]
[Cu(DL-topa)(bpy)]NO_3			7.54, 8.85, –[b]

[a] Reference 3. [b] Not observed.

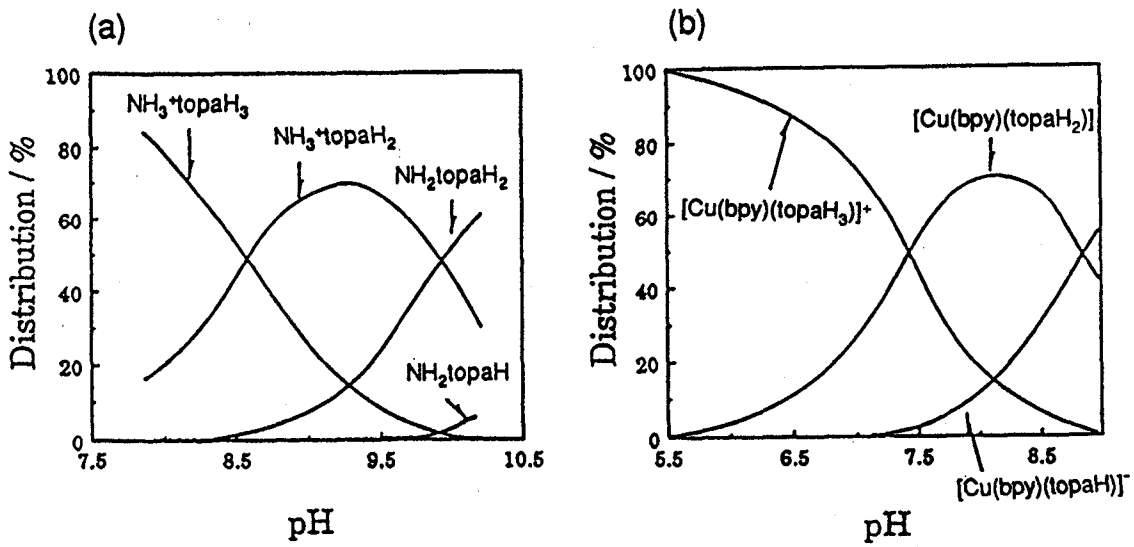

Figure V-5. Species distributions as a function of pH for (a) DL-topa and (b) [Cu(DL-topa)(bpy)]$^+$.

Table V-4. Cyclic Voltammetric Data for Copper Complexes in Aqueous Solution at 25°C[a,b]

complex	pH	diol / quinone			Cu(II) / Cu(I)			
		E_{pc} / V	E_{pa} / V	ΔE / mV	E_{pc} / V	E_{pa} / V	ΔE / mV	$E_{1/2}$ / V
$[Cu(bpy)]^{2+}$	5.4	–	–	–	-0.208	-0.043	165	-0.126
$[Cu(DL\text{-}ala)(bpy)]^{+}$	5.2	–	–	–	-0.200	-0.074	126	-0.137
$[Cu(DL\text{-}phe)(bpy)]^{+}$	5.2	–	–	–	-0.390	-0.048	342	-0.219
$[Cu(DL\text{-}tyr)(bpy)]^{+}$	5.4	–	–	–	-0.388	-0.176	212	-0.282
$[Cu(DL\text{-}topa)(bpy)]^{+}$	5.4	-0.002	0.398	400	-0.438	-0.232	206	-0.335
$[Cu(DL\text{-}topa)(phen)]^{+}$	5.1	-0.015	0.378	393	-0.342	-0.184	158	-0.263

[a]Electrolyte, 0.05 M KNO_3. [b]Scan rate, 20 mV/s.

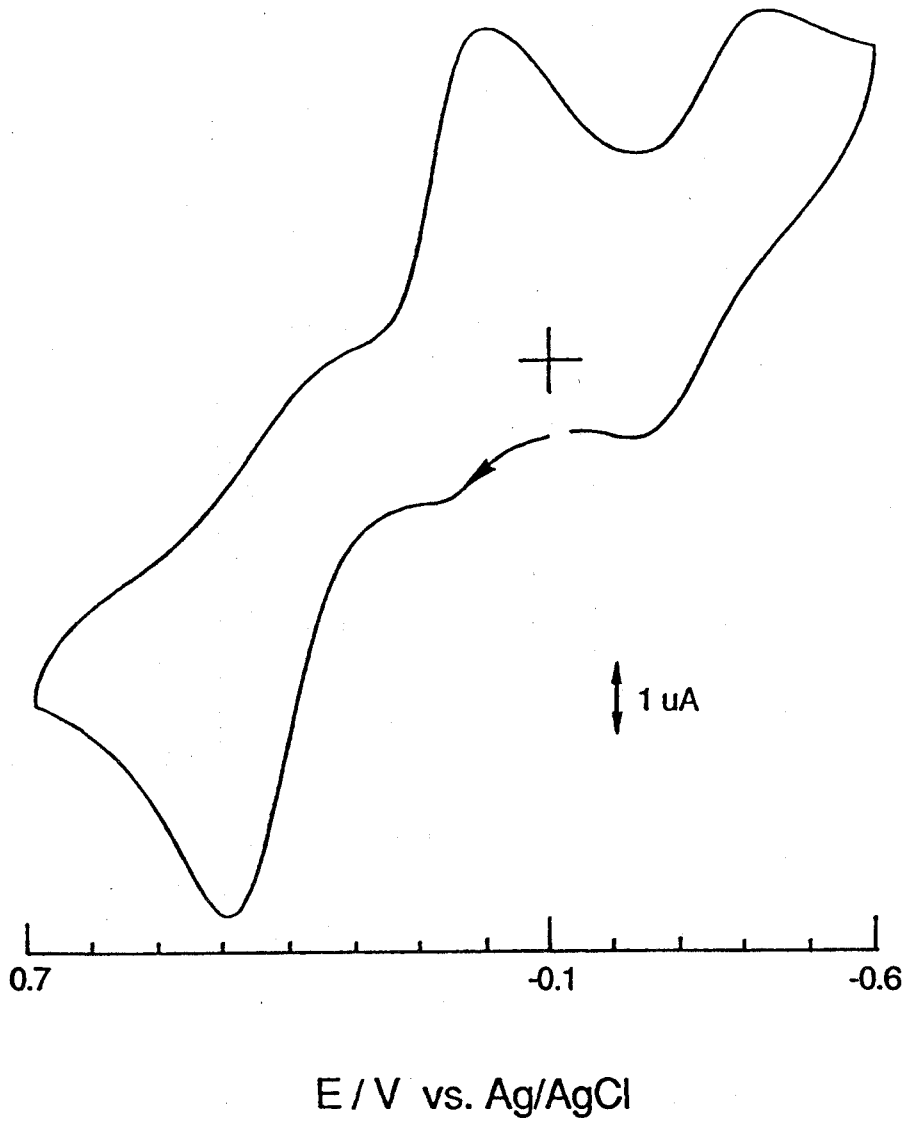

Figure V-6. Cyclic voltammogram of $[Cu(DL\text{-topa})(bpy)]^+$ in 0.05 M KNO_3 (pH 5.4) at 25°C. Scan rate: 20 mV s^{-1}.

whose ligand are oxidized, or both. A negative scan initiated at -0.1 V gives a reduction wave. A coupled oxidation wave is present on the subsequent positive scan. When the scan was reversed after the anodic wave, a voltammogram with quasi-reversible characteristics was observed.

The Stacking Interaction of the Ternary Complexes. The stacking interaction generally arises from the interaction between the π-orbitals of two aromatic rings. It often gives rise to charge transfer (CT) absorption bands in the near UV region. For the ternary systems containing Cu(II), an aromatic amine, and a nucleotide, a CT band has been reported to appear in this region.[17] Yamauchi and co-workers have also reported the presence of the CT absorption bands for the ternary Cu(II) complexes involving aromatic amines and L-tryptophan.[18] The difference absorption spectra of the ternary Cu(II) complexes are shown in Figure V-7. The difference absorption spectra of the topa-containing complexes exhibit strong CT absorption bands in the near UV region. The intramolecular stacking interaction in the topa-containing complexes may be stronger than those in dopa- and tyr-containing complexes.

The stacked structure would allow the electron flow from the phenol moiety to the electron-deficient bpy or phen. This phenomenon tends to increase the electron density on the Cu(II) ion and must reflect the redox potential of the Cu(II)/Cu(I) process. Figure V-8 demonstrates that the charge transfer magnitudes at 360 nm for the $[Cu(DL\text{-}AA)(bpy)]^+$ (DL-AA = DL-amino acid) systems correlate well with the redox potentials of the Cu(II)/Cu(I) processes, supporting that the increasing electron densities on the Cu(II) ions owes to aromatic ring stacking. Thus, the redox potential of the central metal could be

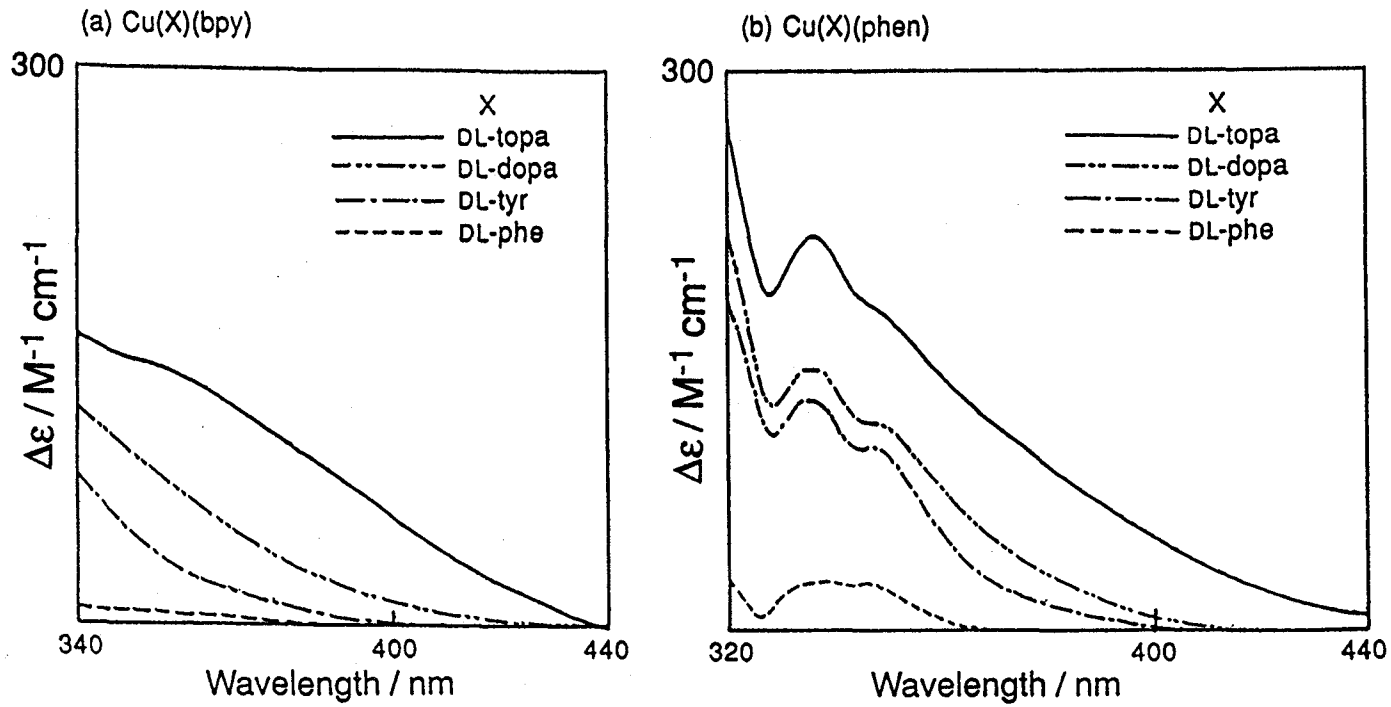

Figure V-7. Difference absorption spectra indicating charge transfer between aromatic diamines (DA; bpy and phen) and aromatic rings of amino acids (X) in water. Curves: {Cu(X)(DA) + (DL-ala)} - {Cu(DL-ala)(DA) + (X)}. Copper concentration: 0.655 mM.

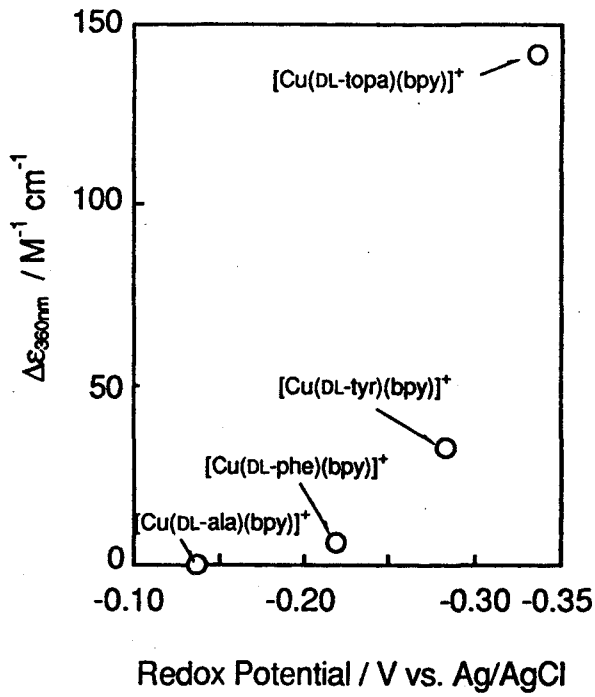

Figure V-8. Relationship between $\Delta\varepsilon$ at 360 nm and redox potentials of stacked species.

given as an indication of the strength of the intramolecular stacking interaction.

Oxidative Deamination of Benzylamine. The oxidation of benzylamine (4.9 mM) with tyr, dopa, topa, or their ternary Cu(II) complexes (2.4 mM) was carried out in 0.01 M HEPES buffer (pH 7.0) at 27 °C. No reaction with these catalysts occur under anaerobic conditions. DL-tyr and [Cu(DL-tyr)(bpy)]$^+$ show no oxidation activity of benzylamine even under aerobic conditions. On the other hand, benzylamine are oxidized to benzaldehyde in the reaction with DL-dopa, DL-topa, [Cu(DL-dopa)(bpy)]$^+$, [Cu(DL-topa)(bpy)]$^+$, or [Cu(DL-topa)(phen)]$^+$. The progress of the reaction was followed by monitoring the amount of benzaldehyde by HPLC, as shown in Figure V-9. The pseudo-first-order rate constants are listed in Table V-5. These findings suggest that dopa or topa is essential to oxidize benzylamine. Since the oxidation of benzylamine requires dioxygen, dopa quinone or topa quinone (oxidized form of dopa or topa, respectively) seems to be an activated form. DL-topa and [Cu(DL-topa)(bpy)]$^+$ have the greater activities than DL-dopa and [Cu(DL-dopa)(bpy)]$^+$. Although topa is oxidized to topa quinone immediately (Figure V-10), dopa turns to dopa quinone slowly. Since the proportion of dopa quinone, which is the activated form, is very small, the rate of reaction is slow. In comparison with the reaction with free DL-topa, [Cu(DL-topa)(bpy)]$^+$ and [Cu(DL-topa)(phen)]$^+$ promote the reaction. This result seems to be due to the decreasing of π-electron density of the aromatic ring of topa by the binding to copper(II) ion and the stacking interaction. Difference of the rate constants between free DL-dopa and [Cu(DL-dopa)(bpy)]$^+$ may be interpreted in the same way. Furthermore, benzaldehyde was obtained in 23.1 % yield based on the complex (in the case of [Cu(DL-topa)(bpy)]$^+$) after 10 h, and the concentration of

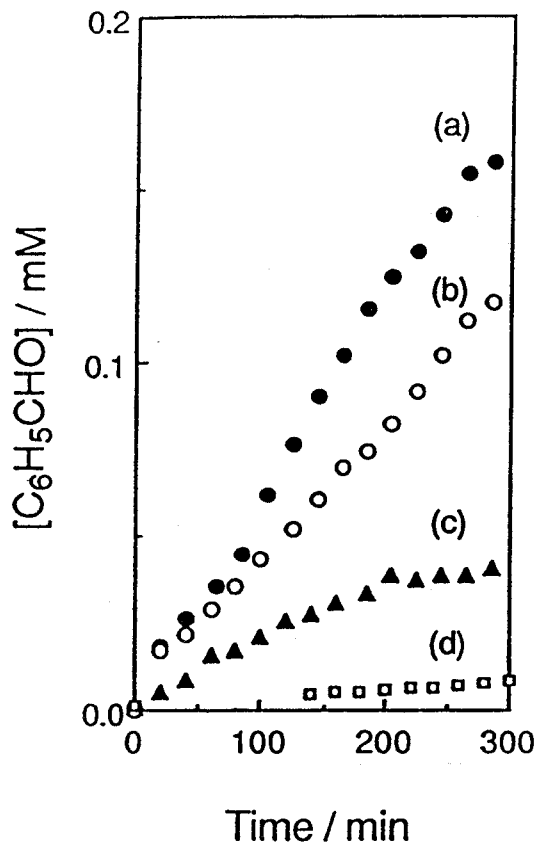

Figure V-9. Oxidation of benzylamine with (a) [Cu(DL-topa)(bpy)]$^+$, (b) [Cu(DL-topa)(phen)]$^+$, (c) DL-topa, and (d) [Cu(DL-dopa)(bpy)]$^+$ under aerobic conditions in 0.01 M HEPES buffer (pH 7.0) at 27°C. Conditions: [catalyst] = 1.0 mM, [benzylamine] = 53.0 mM.

Table V-5. Pseudo-First-Order Rate Constants (k_1 / s^{-1}) for Oxidative Deamination of Benzylamine in 0.01 M HEPES Buffer (pH 7.0) at 27°C[a]

compound	$10^7 k_1$ / s^{-1}	relative rate
DL-dopa	0.75	1
[Cu(DL-dopa)(bpy)]$^+$	3.86	5
DL-topa	19.6	26
[Cu(DL-topa)(bpy)]$^+$	91.0	122
[Cu(DL-topa)(phen)]$^+$	62.7	84

[a] [catalyst] = 1.0 mM, [benzylamine] = 53.0 mM.

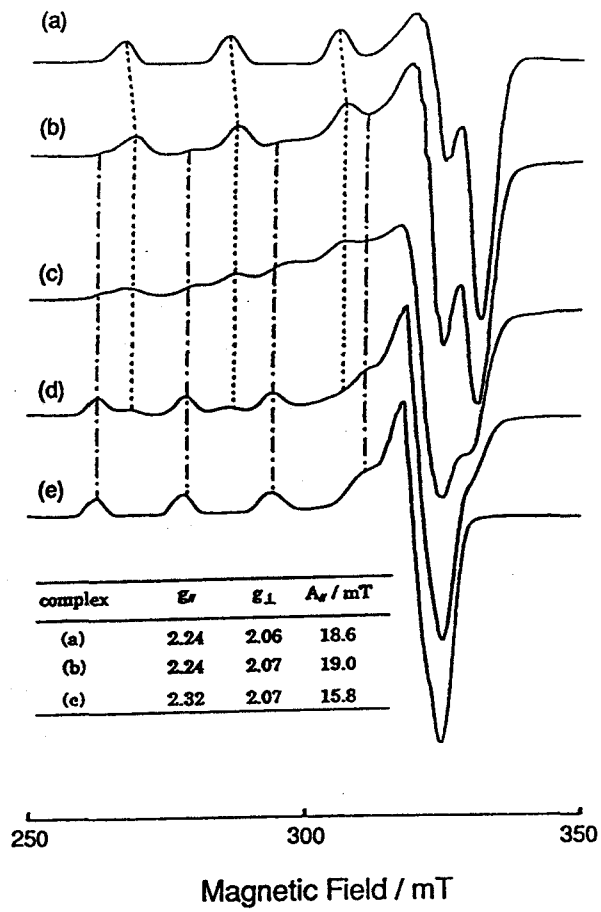

Figure V-10. EPR spectral change of $[Cu(DL\text{-topa})(bpy)]^{+}$. The complex solution is allowed to stand under aerobic conditions at room temperature. After (a) 0 min, (b) 1.0 h, (c) 1 day, and (d) 2 days, the EPR spectrum is measured at 77K. EPR spectrum of $[Cu(bpy)]^{2+}$ (e) is shown for a reference. Inset: EPR parameters of (a), (b) and (e).

benzaldehyde showed saturation phenomenon. The decrease of the reaction rate seems to be due to the deactivation of the catalyst, because the dark-brown precipitate was observed gradually. In general, dopa and topa are known to the intermediates in melanin synthesis (Figure V-11).[19] Parallel to oxidation of benzylamine, the polymerization occurs and then the catalyst may lose the activity.

In this chapter, the several properties of the topa-containing Cu(II) complex are revealed. These findings will give us vital information about the active sites of topa-containing enzymes. For example, the strong intramolecular stacking between bpy and the aromatic ring of topa indicates that the stacking interaction between the rings of topa and the aromatic amino acid residues might be expected at active site of enzymes. In addition, the acceleration of the oxidation of benzylamine owing to coordination of the Cu(II) ion predicts the presence of the close interaction between topa and the Cu(II) ion at the active site of enzymes.

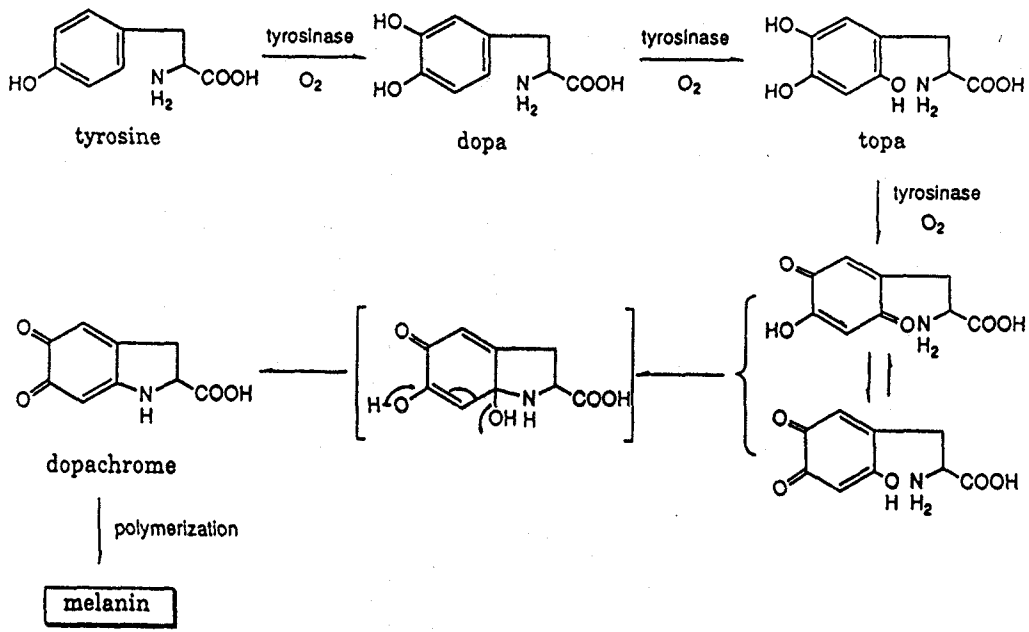

Figure V-11. Proposed pathway from tyrosine to melanin.[19]

References

(1) Knowles, P. F.; Yadav, K. D. S. In *Copper Proteins and Copper Enzymes*; Lontie, R., Ed.; CRC Press: Boca Raton, FL, 1984; pp 103–129.

(2) Mondovi, B. In *Structure and Functions of Amine Oxidases*; CRC Press: Boca Raton, FL, 1985.

(3) Suzuki, S.; Sakurai, T.; Nakahara, A.; Manabe, T.; Okuyama, T. *Biochemistry* **1983**, *22*, 1630–1635.

(4) Suzuki, S.; Sakurai, T.; Nakahara, A.; Manabe, T.; Okuyama, T. *Biochemistry* **1986**, *25*, 338–341.

(5) Ameyama, M.; Hayashi, M.; Matsushita, K.; Shinagawa, E.; Adachi, O. *Agric. Biol. Chem.* **1984**, *48*, 561–565.

(6) Lobenstein-Verbeek, C. L.; Jongejan, J. A.; Frank, J.; Duine, J. A. *FEBS Lett.* **1984**, *170*, 305–309.

(7) Janes, S. M.; Mu, D.; Wemmer, D.; Smith, A. J.; Kain, S.; Maltby, D.; Burlingame, A. L.; Klinman, J. P. *Science* **1990**, *248*, 981–987.

(8) Scott, R. A.; Dooley, D. M. *J. Am. Chem. Soc.* **1985**, *107*, 4348–4350.

(9) Knowles, P. F.; Strange, R. W.; Blackburn, N. J.; Hasnain, S. *J. Am. Chem. Soc.* **1989**, *111*, 102–107.

(10) MaCracken, J.; Peisach, J.; Dooley, D. M. *J. Am. Chem. Soc.* **1987**, *109*, 4064–4072.

(11) Williams, T. J.; Falk, M. C. *J. Biol. Chem.* **1986**, *261*, 15949–15954.

(12) Lamkin, M. S.; Williams, T. J.; Falk, M. C. *Arch. Biochem. Biophys.* **1988**, *261*, 72–79.

(13) Dooley, D. M.; McGuirl, M. A.; Brown, D. E.; Turowski, P. N.; McIntire, W. S.; Knowles, P. F. *Nature* **1991**, *349*, 262–264.

(14) Jaeger, F. A.; Dijk, J. A. *Z. Anorg. Chem.* **1936**, *227*, 273.

(15) Sabatini, A.; Vacca, A.; Gans, P. *Talanta* **1974**, *21*, 53–77.

(16) Martell, A. E.; Smith, R. M. In *Critical Stability Constants*; Plenum Press: New York, 1974.

(17) Naumann, C. F.; Sigel, H. *J. Am. Chem. Soc.* **1974**, *96*, 2750–2756.

(18) Masuda, H.; Sugimori, T.; Odani, A.; Yamauchi, O. *Inorg. Chim. Acta* **1991**, *180*, 73–79.

(19) Graham, D. G.; Jeffs, P. W. *J. Biol. Chem.* **1977**, *252*, 5729–5734.

Chapter VI. X-RAY CRYSTAL STRUCTURE ANALYSIS OF A TOPA-CONTAINING COPPER COMPLEX

Introduction

Copper-containing amine oxidases are distributed widely in plants, mammals, and microorganisms. They contain "nonblue" copper and an organic cofactor which is covalently bound to the proteins.[1-4] In 1984 Duine's[5] and Ameyama's[6] groups independently reported that the covalently bound organic cofactor was pyrroloquinoline quinone (PQQ). However, the evidence for PQQ in copper-containing amine oxidases has not been universally accepted. Recently, topa quinone (6-hydroxydopa quinone) residue has been identified as the cofactor in bovine serum amine oxidase.[7] The cupric site indicated a square pyramidal geometry with three imidazoles and two water molecules.[8-10] Dooley and co-workers presented the evidence for the generation of a Cu(I) semiquinone state by room-temperature electron paramagnetic resonance (EPR) measurements and suggested that the Cu(I) semiquinone may be the catalytic intermediate which reacts directly with dioxygen.[11]

In this chapter, the structure of the first topa-containing ternary Cu(II) complex ([Cu(DL-topa)(bpy)(H_2O)]BF_4·3H_2O (**1**)) has been revealed in order to shed light on the structural and the functional relationships between nonblue copper and the organic cofactor in copper-containing amine oxidases.

Experimental Section

Preparation of [Cu(DL-topa)(bpy))]BF_4. The complex 1 was prepared according to the following procedures. $[Cu(bpy)(H_2O)_2](BF_4)_2$ (47 μmol) was dissolved in 3 cm^3 of distilled water under an Ar atmosphere. DL-topa (47 μmol) was anaerobically added to the solution, and then the mixture was stirred to dissolve topa completely at room temperature. The solution was concentrated to about one-fourth of the volume and permitted to stand at 4 °C until the bluish green crystals separated out. Anal. Calcd for $C_{19}H_{20}N_3O_6BF_4Cu \cdot 2H_2O$: C, 41.13; H, 3.99; N, 7.57 %. Found: C, 40.80; H, 4.01; N, 7.60 %. The crystals suitable for X-ray studies were obtained by recrystallization from water under Ar atmosphere.

Crystallographic Structure Determination on [Cu(DL-topa)(bpy)(H_2O)]-$BF_4 \cdot 3H_2O$. Intensity data in the range $2\theta < 120°$ were collected by the ω–2θ scan technique using a Rigaku AFC-5R automated four-circle diffractometer with Ni-filtered Cu $K\alpha$ radiation. Intensities were corrected for Lorentz and polarization effects. An empirical absorption correction based on a series of ψ-scans was applied to the data. The crystallographic data are summarized in Table VI-1. The structure was solved by direct methods, MULTAN 78,[12] and refined by a block-diagonal least squares method using the program HBLS-V[13] Anisotropic temperature factors were used for non-hydrogen atoms. The positions of the hydrogen atoms, except on the water and hydroxyl groups of topa, were calculated on the basis of the molecular geometry. These hydrogen atoms with isotropic temperature factors were included in further refinement. The

Table VI-1. Crystallographic Data for [Cu(DL-topa)(bpy)(H_2O)]BF_4·3H_2O (1)

formula	$C_{19}H_{26}N_3O_9BF_4Cu$
fw	590.78
color and habit	bluish green plates
cryst system	monoclinic
space group	$P2_1/a$
a, Å	16.259 (8)
b, Å	10.007 (1)
c, Å	16.241 (4)
β, deg	114.12 (3)
V, Å^3	2412 (1)
Z	4
cryst dimens, nm	0.10 × 0.12 × 0.21
D_{calcd}, g cm^{-3}	1.627
μ(Cu Kα), cm^{-1}	20.30
F(000)	1212
scan method	ω–2θ
2θ range, deg	0–120
no. of unique data collcd	3579
no. of data used in refinement	2209 ($\|F_o\| > 3\sigma\|F_o\|$)
R^a	0.078
$R_w{}^b$	0.099

$^aR = \Sigma||F_o|-|F_c||/\Sigma|F_o|$. $^bR_w = [\Sigma w(|F_o|-|F_c|)^2/\Sigma w(F_o)^2]^{1/2}$.

weighting scheme used was $w = 1/(\sigma(F_o)^2 + 0.3542(F_o) + 0.0002(F_o)^2)$. The final R and R_w values were 0.078 and 0.099 for 2209 reflections ($|F_o| > 3\sigma|F_o|$), respectively. All the computations were carried out on an ACOS 2020 computer at the Computation Center, Osaka University, and on an ACOS S-850 computer at the Crystallographic Research Center, Institute for Protein Research, Osaka University.

The atomic positional parameters and equivalent isotropic temperature factors for the non-hydrogen atoms, the atomic coordinates of the hydrogen atoms, and the non-hydrogen anisotropic thermal parameters are listed in Appendix III. The bond lengths and the bond angles are presented in Table VI-2 and Table VI-3,respectively.

Results and Discussion

The topa ligand has two potential chelating sites for a metal ion: the formation of an {N,O} complex with the amino and carboxyl groups and an {O,O} complex with the phenolic dihydroxyl group. The molecular structure of complex **1** is shown in Figure VI-1. In the present synthetic conditions, the {N,O} complex was formed. The Cu(II) ion has a square pyramidal structure with two nitrogen atoms (N(1) and N(2) numbered according to Figure VI-1) of bpy and one nitrogen (N(3)) and one oxygen (O(1)) atom of topa coordinated in the equatorial plane and one water oxygen (O(6)) atom occupying a remote axial position, as shown in Figure VI-2. The Cu(II)···O(6) distance, 2.317 (9) Å, is

Table VI-2. Bond Lengths (Å) for [Cu(DL-topa)(bpy)(H_2O)]$BF_4 \cdot 3H_2O$ (1)[a]

Bond	Length	Bond	Length
Cu - O(1)	1.946(8)	Cu - O(6)	2.317(9)
Cu - N(1)	1.984(8)	Cu - N(2)	1.981(8)
Cu - N(3)	2.007(8)	O(1) - C(11)	1.271(13)
O(2) - C(11)	1.238(13)	O(3) - C(15)	1.374(13)
O(4) - C(17)	1.368(12)	O(5) - C(18)	1.394(13)
N(1) - C(1)	1.337(14)	N(1) - C(5)	1.349(13)
N(2) - C(6)	1.333(13)	N(2) - C(10)	1.335(15)
N(3) - C(12)	1.494(13)	C(1) - C(2)	1.392(17)
C(2) - C(3)	1.372(18)	C(3) - C(4)	1.370(18)
C(4) - C(5)	1.388(16)	C(5) - C(6)	1.472(14)
C(6) - C(7)	1.375(17)	C(7) - C(8)	1.376(20)
C(8) - C(9)	1.368(20)	C(9) - C(10)	1.400(18)
C(11) - C(12)	1.539(15)	C(12) - C(13)	1.533(15)
C(13) - C(14)	1.515(14)	C(14) - C(15)	1.384(14)
C(14) - C(19)	1.390(14)	C(15) - C(16)	1.390(14)
C(16) - C(17)	1.376(14)	C(17) - C(18)	1.410(14)
C(18) - C(19)	1.398(15)	B - F(1)	1.364(18)
B - F(2)	1.344(18)	B - F(3)	1.358(18)
B - F(4)	1.367(18)		

[a]Estimated standard deviations are given in parentheses.

Table VI-3. Bond Angles (°) for [Cu(DL-topa)(bpy)(H_2O)]BF_4·3H_2O (1)[a]

Bond	Angle	Bond	Angle
O(1) -Cu -O(6)	97.1(3)	O(1) -Cu -N(1)	168.0(3)
O(1) -Cu -N(2)	91.5(3)	O(1) -Cu -N(3)	83.3(4)
O(6) -Cu -N(1)	92.9(4)	O(6) -Cu -N(2)	92.9(4)
O(6) -Cu -N(3)	97.3(4)	N(1) -Cu -N(2)	81.3(3)
N(1) -Cu -N(3)	102.0(4)	N(2) -Cu -N(3)	169.1(4)
Cu -O(1) -C(11)	114.1(7)	Cu -N(1) -C(1)	126.2(7)
Cu -N(1) -C(5)	114.3(7)	C(1) -N(1) -C(5)	119.2(9)
Cu -N(2) -C(6)	115.2(7)	Cu -N(2) -C(10)	125.1(8)
C(6) -N(2) -C(10)	119.7(9)	N(1) -C(1) -C(2)	121.0(10)
C(1) -C(2) -C(3)	119.9(11)	C(2) -C(3) -C(4)	119.1(12)
C(3) -C(4) -C(5)	119.2(11)	N(1) -C(5) -C(4)	121.7(10)
N(1) -C(5) -C(6)	114.5(9)	C(4) -C(5) -C(6)	123.9(10)
N(2) -C(6) -C(5)	114.5(9)	N(2) -C(6) -C(7)	121.2(10)
C(5) -C(6) -C(7)	124.3(10)	C(6) -C(7) -C(8)	119.4(12)
C(7) -C(8) -C(9)	120.2(14)	C(8) -C(9) -C(10)	117.5(13)
N(2) -C(10)-C(9)	122.1(11)	O(1) -C(11)-O(2)	124.7(10)
O(1) -C(11)-C(12)	116.8(9)	O(2) -C(11)-C(12)	118.3(10)
N(3) -C(12)-C(11)	108.3(8)	N(3) -C(12)-C(13)	110.5(8)
C(11)-C(12)-C(13)	111.3(9)	C(12)-C(13)-C(14)	114.7(9)
C(13)-C(14)-C(15)	122.0(9)	C(13)-C(14)-C(19)	120.0(9)
C(15)-C(14)-C(19)	118.0(9)	O(3) -C(15)-C(14)	118.4(9)
O(3) -C(15)-C(16)	120.6(9)	C(14)-C(15)-C(16)	121.0(9)
C(15)-C(16)-C(17)	121.2(9)	O(4) -C(17)-C(16)	123.2(9)
O(4) -C(17)-C(18)	117.9(9)	C(16)-C(17)-C(18)	118.9(9)
O(5) -C(18)-C(17)	117.7(9)	O(5) -C(18)-C(19)	123.3(9)
C(17)-C(18)-C(19)	119.0(9)	C(14)-C(19)-C(18)	121.9(10)
F(1) -B -F(2)	107.4(11)	F(1) -B -F(3)	108.3(12)
F(1) -B -F(4)	110.1(12)	F(2) -B -F(3)	112.4(12)
F(2) -B -F(4)	109.2(12)	F(3) -B -F(4)	109.4(12)

[a]Estimated standard deviations are given in parentheses.

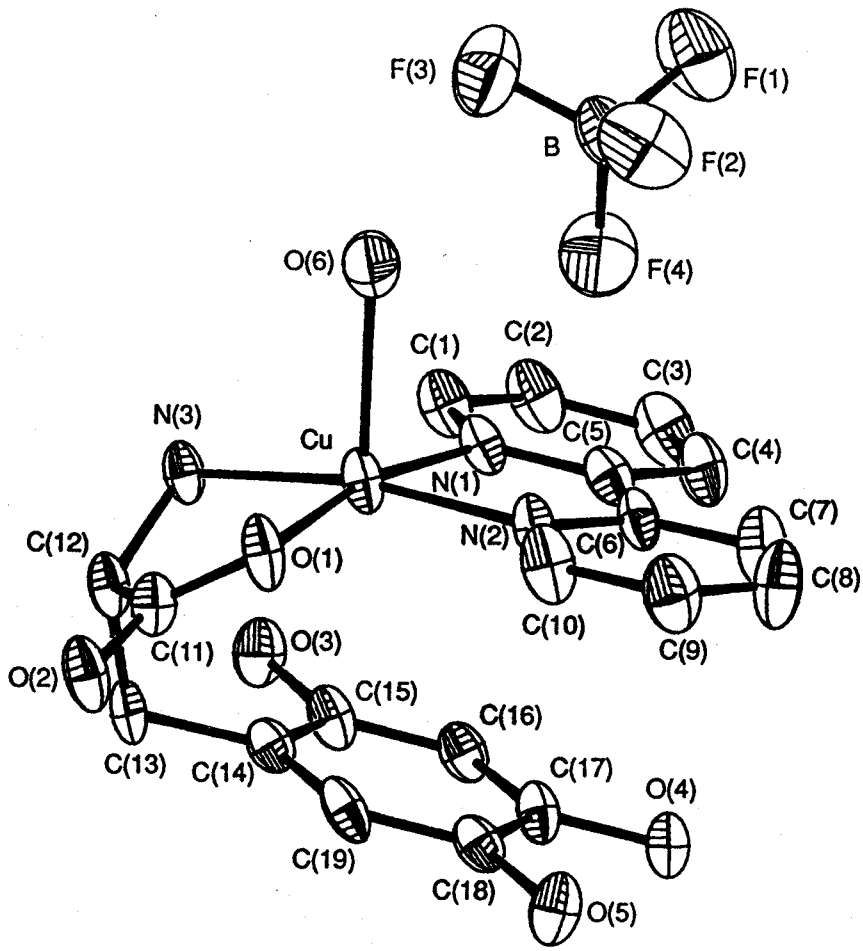

Figure VI-1. Molecular structure of [Cu(DL-topa)(bpy)(H_2O)]BF_4·3H_2O (1) showing the 30% probability thermal ellipsoids and atom-labeling scheme. Non-coordinated water molecules and hydrogen atoms are omitted.

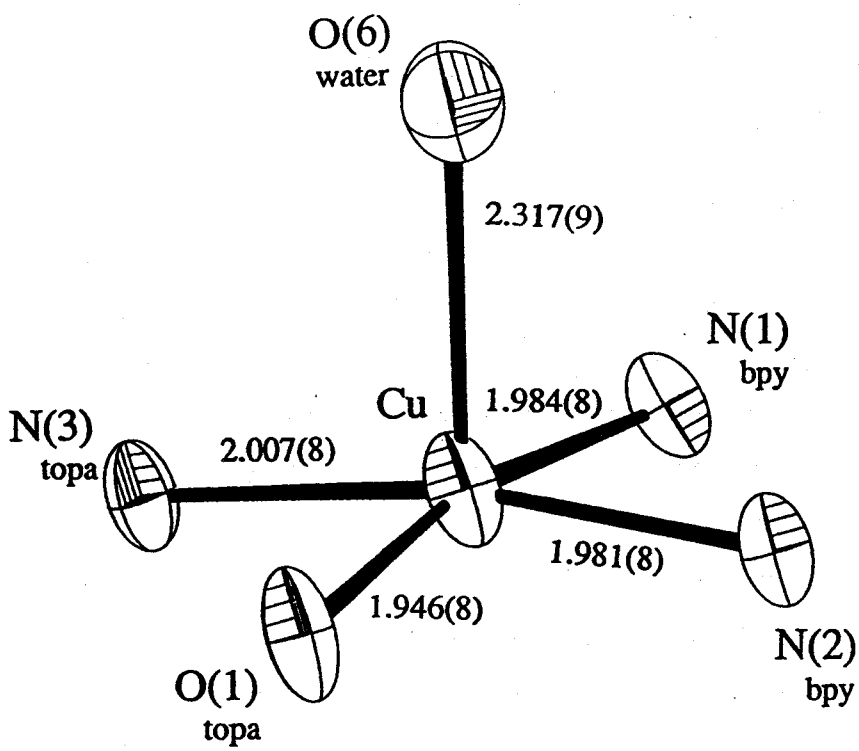

Figure VI-2. Coordination sphere of the copper(II) site in [Cu(DL-topa)(bpy)(H_2O)]BF_4·3H_2O (**1**).

within the range of axial Cu–O bond lengths (2.2–2.9 Å).[14] The three nitrogen atoms and one oxygen (O(1)) atom are planar to within experimental error, and the copper atom deviates by 0.17 Å from the coordination plane (N(1), N(2), N(3), and O(1)) toward the axial oxygen atom (O(6)). The opposite site of the axial O(6) position is occupied by the aromatic ring of the intramolecular topa group, which is approximately parallel to the Cu(II) coordination plane (Figure VI-3). The closest approach between Cu(II) and the aromatic ring of topa is 3.135 (13) Å (Cu(II)···C(14)).[15] Moreover, the aromatic ring of topa is intramolecularly stacked with the bpy ring. The shortest distance between two rings of topa and bpy is 3.308 (13) Å (C(15)···N(1)). The dihedral angle between the rings in complex **1** is estimated to be 9.73°. Similar intramolecular stacking is also found in the other ternary Cu(II) complexes comprised of aromatic diamines and aromatic amino acids.[15-19]

An additional noticeable structural feature within a crystal unit is an extensive network of hydrogen-bonding interactions, as shown Figure VI-4. The amino and three hydroxyl groups of topa and oxygen atoms of all crystal water molecules are involved in the hydrogen-bonding network. The fluorine atoms ($F(1)^{v}$ and $F(2)^{iv}$)[20] are also located within the hydrogen-bonding distance to the coordinated water oxygen atom (O(6)). Possible hydrogen bonds and their distances are displayed in Table VI-4. The stacking interaction between aromatic rings and the hydrogen-bonding network may play an essential role in stabilizing this crystal structure. X-ray crystallographic analysis of nonblue copper-containing galactose oxidase reveals that the indole ring of trp is stacked on tyr, the phenol group of which is coordinated to copper at the active center.[21] The stacking trp presumably aids stabilization of the free radical. The stacking

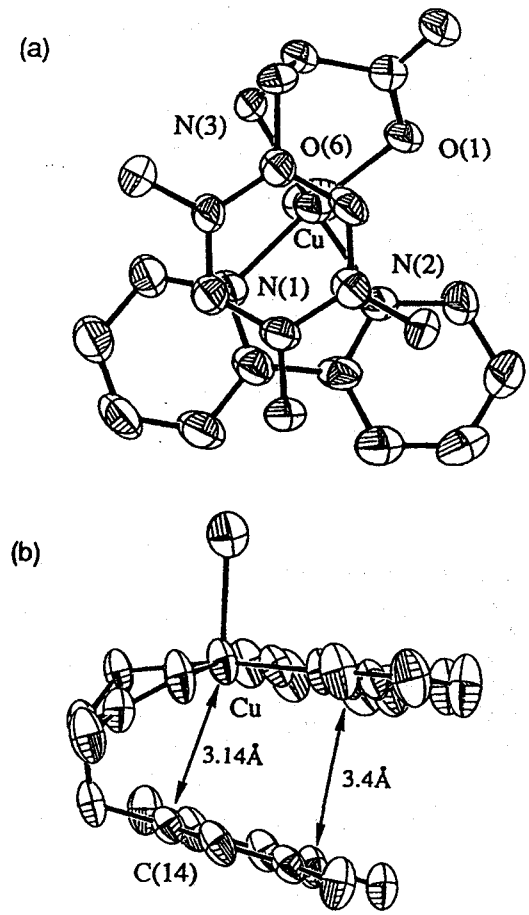

Figure VI-3. Stacking interaction between bpy and phenyl rings in [Cu(DL-topa)(bpy)(H_2O)]BF_4·3H_2O (**1**) as shown upright to the mean plane of bpy ligand (a) and parallel to the same plane (b).

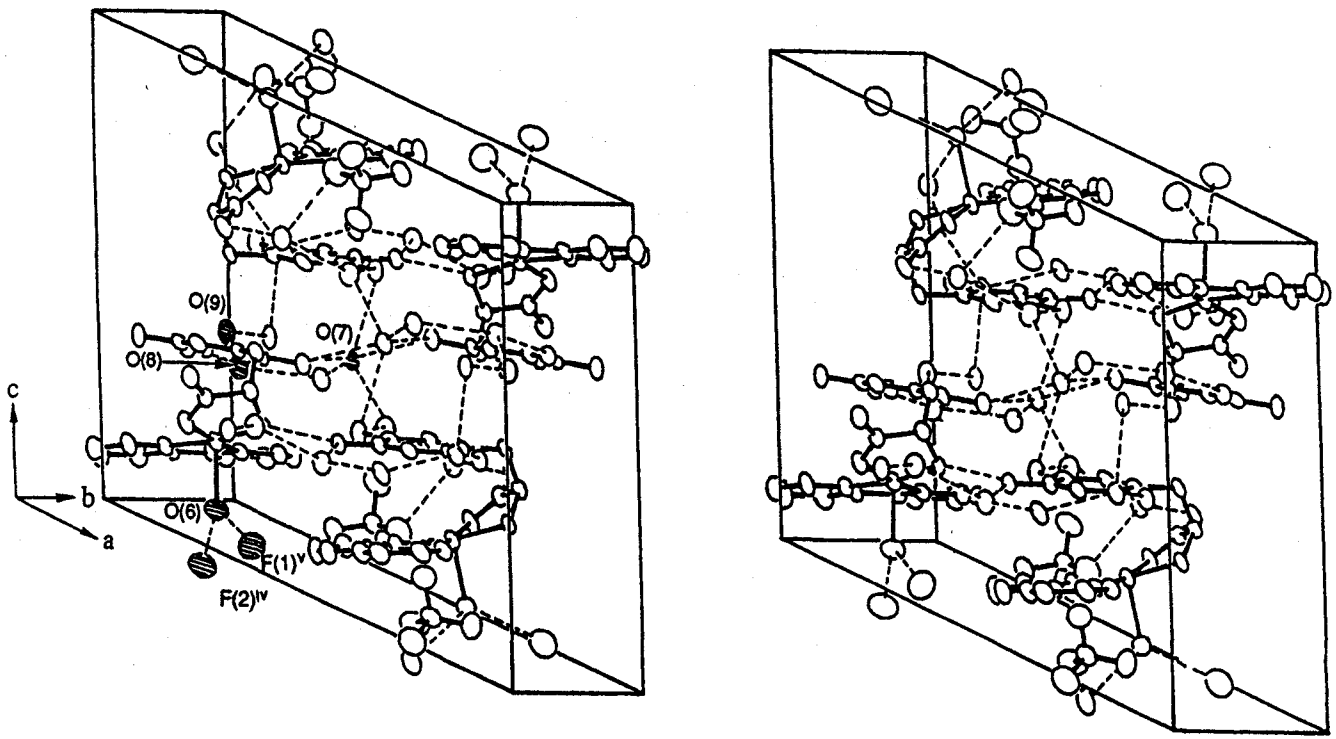

Figure VI-4. A stereoscopic view of the molecular packing for [Cu(DL-topa)(bpy)(H_2O)]BF_4·3H_2O (**1**). Hydrogen atoms are omitted. Broken lines show hydrogen bonds.

Table VI-4. Possible Hydrogen Bond Distances (Å) for $[Cu(DL\text{-}topa)(bpy)(H_2O)]BF_4 \cdot 3H_2O$ (1)[a,b]

O(3) ···O(7)	2.774(11)	O(4)···O(8)	2.781(14)
O(8)···O(9)	2.835(15)	O(4)···N(3)^{i}	3.071(14)
O(3)···O(7)^{ii}	3.007(11)	O(5)···O(7)^{iii}	3.079(11)
O(6)···F(2)^{iv}	2.696(12)	O(6)···F(1)^{v}	2.868(12)
O(2)···O(7)^{v}	2.667(11)	O(2)···O(8)^{v}	2.753(13)
O(5)···O(9)^{v}	2.672(12)	O(7)···O(9)^{vi}	2.794(13)
F(3)···O(8)^{vi}	2.909(14)		

[a]Symmetry code: (i) -0.5+*x*, 0.5-*y*, *z*; (ii) 1-*x*, 1-*y*, 2-*z*; (iii) 0.5-*x*, -0.5+*y*, 2-*z*; (iv) 0.5-*x*, -0.5+*y*, 1-*z*; (v) *x*, -1+*y*, *z*; (vi) 0.5+*x*, 1.5-*y*, *z*.

[b]Estimated standard deviations are given in parentheses.

interaction between the rings of topa and aromatic amino acid residues might also be of consequence at the active sites of amine oxidases.

Recently, it has been reported that copper is about 3.0 Å distant from the C-2 hydroxyl group of topa (O(3) shown in Figure VI-1) in copper-containing amine oxidase by use of molecular modeling and energy minimization techniques.[22] The distance of 4.073 (8) Å between copper and the C-2 hydroxyl oxygen (O(3)) of topa in complex **1** is longer than the above value, but Cu(II) can promote the oxidation of benzylamine (see Chapter V). Although these preliminary experiments are not sufficiently extensive to be able to define the mechanism, the finding that Cu(II) is particularly essential for the acceleration of the oxidation of benzylamine is of interest in connection with the mechanism of amine oxidases. Complex **1** might provide significant information of the catalytic roles on topa residue and copper in copper-containing amine oxidases.

References and Notes

(1) Knowles, P. F.; Yadav, K. D. S. In *Copper Proteins and Copper Enzymes*; Lontie, R., Ed.; CRC Press: Boca Raton, FL, 1984; pp103–129.

(2) Mondovi, B. In *Structure and Functions of Amine Oxidases*; CRC Press: Boca Raton, FL, 1985.

(3) Suzuki, S.; Sakurai, T.; Nakahara, A.; Manabe, T.; Okuyama, T. *Biochemistry* **1983**, *22*, 1630–1635.

(4) Suzuki, S.; Sakurai, T.; Nakahara, A.; Manabe, T.; Okuyama, T. *Biochemistry* **1986**, *25*, 338–341.

(5) Lobenstein-Verbeek, C. L.; Jongejan, J. A.; Frank, J.; Duine, J. A. *FEBS Lett.* **1984**, *170*, 305–309.

(6) Ameyama, M.; Hayashi, M.; Matsushita, K.; Shinagawa, E.; Adachi, O. *Agric. Biol. Chem.* **1984**, *48*, 561–565.

(7) Janes, S. M.; Mu, D.; Wemmer, D.; Smith, A. J.; Kain, S.; Maltby, D.; Burlingame, A. L.; Klinman, J. P. *Science* **1990**, *248*, 981–987.

(8) Scott, R. A.; Dooley, D. M. *J. Am. Chem. Soc.* **1985**, *107*, 4348–4350.

(9) MaCracken, J.; Peisach, J.; Dooley, D. M. *J. Am. Chem. Soc.* **1987**, *109*, 4064–4072.

(10) Dooley, D. M.; McGuirl, M. A.; Cote, C. E.; Knowles, P. F.; Singh, I.; Spiller, M.; Brown, R. D.,III; Koenig, S. H. *J. Am. Chem. Soc.* **1991**, *113*, 754–761.

(11) Dooley, D. M.; McGuirl, M. A.; Brown, D. E.; Turowski, P. N.; McIntire, W. S.; Knowles, P. F. *Nature* **1991**, *349*, 262–264.

(12) Main, P.; Hull, S. E.; Lessinger, L.; Germain, G.; Declercq, J. P.; Woolfson,

M. M. *MULTAN 78*, A System of Computer Programs for the Automatic Solution of Crystal Structures from X-Ray Diffraction Data, Universities of York, England, and Louvain, Belgium, 1978.

(13) Ashida, T. *HBLS-V*, The Universal Crystallographic Computing System-Osaka, The Computation Center, Osaka University, Japan, 1979.

(14) Procter, I. M.; Hathaway, B. J.; Nicholls, P. *J. Chem. Soc. A* **1968**, 1678–1684.

(15) In the ternary Cu(II) complex containing L-tyrosine, [Cu(L-tyr)(bpy)-(ClO_4)]·$2H_2O$, there is a close approach of 3.24 Å between Cu(II) and the corresponding carbon atom (C(14)) of the phenol ring (Yamauchi, O.; Odani, A.; Masuda, H. *Inorg. Chim. Acta*, **1992**, *198–200*, 749–761).

(16) Fischer, B. E.; Sigel, H. *J. Am. Chem. Soc.* **1980**, *102*, 2998–3008.

(17) Yamauchi, O.; Odani, A. *J. Am. Chem. Soc.* **1985**, *107*, 5938–5945.

(18) Aoki, K.; Yamazaki, H. *J. Chem. Soc., Dalton Trans.* **1987**, 2017–2021.

(19) Yamauchi, O.; Odani, A.; Kohzuma, T.; Masuda, H.; Toriumi, K.; Saito, K. *Inorg. Chem.* **1989**, *28*, 4066–4068.

(20) Symmetry operations: v x, -1.0 + y, z; iv 0.5 - x, -0.5 + y, 1.0 - z.

(21) Ito, N.; Phillips, S. V. E.; Stevens, C.; Ogel, Z. B.; McPherson, M. J.; Keen, J. N.; Yadav, K. D. S.; Knowles, P. F. *Nature* **1991**, *350*, 87–90.

(22) McGuirl, M. A.; Brown, D. E.; McCahon, C. D.; Turowski, P. N.; Dooley, D. M. *J. Inorg. Biochem.* **1991**, *43*, 186.

Chapter VII. GENERAL CONCLUSION

In the present thesis, the author has attempted to synthesize and characterize the PQQ- and topa-containing copper(II) complexes in order to obtain the fundamental information on the interaction between copper and the organic redox cofactors.

In Chapter II, the synthesis and characterization of the mononuclear and dinuclear ternary copper(II) complexes of PQQ and terpyridine were described. The structure of the dinuclear copper(II) complex, $[Cu_2(\mu\text{-pqq})(terpy)_2]$, was determined by X-ray diffraction methods. The molecular structure consists of two six-coordinate copper atoms bridged by a pqq ligand. Each of the copper(II) ions occupies the pyridine moiety and the pyrrole moiety of pqq. PQQ had the tetraanionic form with deprotonation of three carboxyl groups and a pyrrole group. Furthermore, as judged from the pH values of the complex syntheses and a comparison of the diffuse reflectance spectrum of the dinuclear complex with that of the mononuclear complex, the H_2pqq ligand in the mononuclear complex ($[Cu(H_2pqq)(terpy)]$) seemed to be coordinated to the copper(II) ion with pyridine moiety only.

In Chapter III, the crystal structure of the trianionic form of PQQ (K_3Hpqq) was determined for the first time. A comparison of the structure of Hpqq with that of H_2pqq revealed almost similar bond lengths and angles each other. The crystal structure analysis of disodium H_2pqq salt demonstrated that H_2pqq possesses two metal-binding sites: a primary site in the pocket formed by the O(5), N(6), and O(19) atoms and a secondary site in the pocket formed by the O(4) and O(5) atoms. It was clear that in tripotassium Hpqq salt, two potassium

cations are also located at those sites and the third potassium cation is located a novel site, which was formed by the O(4) and O(15)' atoms of the two different Hpqq anions.

In Chapter IV, the electrochemical properties of PQQ and the PQQ-containing copper(II) complex, [Cu(H_2pqq)(terpy)], were described. The reversible electron transfer behavior of PQQ using a 4-pyds modified gold electrode was observed by cyclic voltammetry and OTTLE method under acidic conditions. OTTLE measurement also suggested that the one-step two-electron transfer between PQQ and a 4-pyds modified gold electrode proceeded reversibly. In the cases of [Cu(H_2pqq)(terpy)], the cyclic voltammograms showed only quasi-reversible behaviors in a limited pH region.

In Chapter V, the first topa-containing copper(II) complexes were synthesized and investigated on physicochemical properties of the interaction by means of spectroscopy, cyclic voltammetry, and potentiometric titration. Moreover, studies of the oxidative deamination of benzylamine to benzaldehyde by molecular oxygen in the presence of these copper complexes were also described. In comparison with the reaction with free DL-topa, [Cu(DL-topa)(bpy)]$^+$ and [Cu(DL-topa)(phen)]$^+$ promoted the reaction. This result seemed to be due to the decreasing of π-electron density in the aromatic ring of topa by the binding to copper(II) ion and the stacking interaction.

In Chapter VI, the crystal and molecular structure of the first topa-containing copper(II) complex, [Cu(DL-topa)(bpy)(H_2O)]BF_4, was determined by X-ray diffraction methods. The Cu(II) ion has a square-pyramidal structure with nitrogen atoms of bpy and amino nitrogen and carboxyl oxygen atoms of topa coordinated in the equatorial plane and with one water oxygen occupying a

remote axial position. The aromatic ring of topa is located about 3 Å apart from Cu(II) over the opposite site of the axial O (water) position, but neither of three hydroxyl groups bound to Cu(II) ion. The distance of 4.073 (8) Å between Cu(II) and the C-2 hydroxyl oxygen (O(3)) of topa in the complex is longer than the estimated value in amine oxidase, but the presence of Cu(II) was able to promote the oxidation of benzylamine to benzaldehyde. This finding is of interest in connection with the mechanism of amine oxidases.

Bioinorganic studies consist of both metalloprotein and their model studies. The studies on Cu complexes involving PQQ and topa fall under the latter. There are some purposes of biochemical model studies. The first is to help elucidate biochemical structures, functions, and mechanisms. Secondly, there are biochemical model studies which are unique to models and which elevate the field somewhat by a lesser but important supportive role. The third point of model studies is the discovery of new chemical facts and principles; new chemical reactions or new processes which are inspired in a sense by the biochemical system, might be invented. This thesis presents the syntheses and properties of the PQQ- and topa-containing Cu(II) complexes for the first time. Although the present investigations do not deal with quinoproteins directly, the author believes that the findings form a contribution to the significant information of the active sites in the enzymes.

ACKNOWLEDGMENTS

The author would like to express his grateful acknowledgment to Professor Shinnichiro Suzuki (College of General Education, Osaka University) for his constant encouragement and guidance throughout this study. He also wishes to express his sincere gratitude to Professors Yoshihiko Kushi (College of General Education, Osaka University) and Sumio Kaizaki (Faculty of Science, Osaka University) for their encouragement and helpful advice.

He would like to acknowledge Dr. Takamitsu Kohzuma (College of General Education, Osaka University) for his guidance, instructive discussions, and encouragement. He is deeply indebted to Dr. Hiro Kuma (College of General Education, Osaka University) for his kindly instruction in X-ray crystallography. Grateful acknowledgement is made to Mr. Shuhei Deguchi (Fujisawa Pharmaceutical Co., Ltd.) for his encouragement and guidance in pH titration.

It is a great pleasure to thank Professor Takeshi Yamamura (Science University of Tokyo) for his guidance, encouragement, and helpful discussions.

Acknowledgments are also made to Mr. Deligeer and Mr. Seiji Takase (the members of the Bioinorganic Chemistry Laboratory) for their encouragement and friendship.

February, 1993

Nobuhumi Nakamura

Appendix I

Table A$_I$-1. Atomic Coordinates and Equivalent Isotropic Thermal Parameters (Å^2) for Non-Hydrogen Atoms in $[Cu_2(\mu\text{-pqq})(terpy)_2]\cdot 12H_2O\cdot CH_3CN$ (**2**)[a]

Atom	*x/a*	*y/b*	*z/c*	B_{eq}[b]
Cu(1)	0.4014(2)	0.0683(3)	0.2168(3)	2.64
Cu(2)	0.1197(2)	0.5095(3)	0.3074(3)	2.52
O(4p)	0.3933(6)	0.412(2)	0.573(2)	4.74
O(5p)	0.4090(5)	0.233(2)	0.390(2)	3.37
O(15p)	0.1939(6)	0.749(2)	0.610(2)	5.05
O(16p)	0.1256(6)	0.674(2)	0.448(2)	4.56
O(18p)	0.2626(7)	-0.022(2)	-0.067(2)	6.21
O(19p)	0.3454(5)	-0.044(1)	0.062(2)	2.57
O(21p)	0.1851(6)	0.458(2)	0.030(2)	4.30
O(22p)	0.1226(5)	0.367(2)	0.133(2)	3.56
N(1p)	0.2081(6)	0.514(2)	0.363(2)	1.65
N(6p)	0.3214(7)	0.155(2)	0.203(2)	3.21
N(1t)	0.3910(7)	-0.050(2)	0.343(2)	3.98
N(2t)	0.4836(6)	0.006(2)	0.239(2)	1.95
N(3t)	0.4432(7)	0.179(2)	0.106(2)	3.61
N(4t)	0.1068(6)	0.642(2)	0.174(2)	3.08
N(5t)	0.0312(6)	0.495(2)	0.269(2)	2.99
N(6t)	0.1008(6)	0.385(2)	0.425(2)	3.08
C(2p)	0.2227(9)	0.590(2)	0.475(2)	3.47
C(3p)	0.2805(8)	0.563(2)	0.532(2)	3.26
C(4p)	0.353(1)	0.395(2)	0.481(2)	4.78
C(5p)	0.3609(8)	0.287(2)	0.383(2)	3.07
C(7p)	0.2813(7)	0.120(2)	0.106(2)	2.37
C(8p)	0.2342(8)	0.193(2)	0.073(2)	1.63
C(9p)	0.2242(8)	0.297(2)	0.148(2)	2.43
C(10p)	0.2577(8)	0.435(2)	0.349(2)	2.85
C(11p)	0.2969(8)	0.462(2)	0.456(2)	2.79
C(12p)	0.3125(7)	0.257(2)	0.277(2)	2.46
C(13p)	0.2634(8)	0.329(2)	0.258(2)	2.37
C(14p)	0.1788(8)	0.683(2)	0.514(2)	2.76
C(17p)	0.2965(8)	0.006(2)	0.026(2)	3.20
C(20p)	0.1726(7)	0.380(2)	0.098(2)	1.86
C(1t)	0.3418(8)	-0.070(2)	0.399(2)	2.43
C(2t)	0.3385(9)	-0.151(2)	0.488(2)	4.57
C(3t)	0.389(1)	-0.211(2)	0.528(2)	4.17
C(4t)	0.443(1)	-0.201(2)	0.476(2)	4.36
C(5t)	0.4425(8)	-0.121(2)	0.386(2)	3.44
C(6t)	0.4936(8)	-0.080(2)	0.324(2)	3.01
C(7t)	0.554(2)	-0.131(2)	0.343(2)	5.87
C(8t)	0.5972(8)	-0.085(2)	0.273(2)	4.39
C(9t)	0.5827(8)	0.005(2)	0.189(2)	3.15

– to be continued –

Table A_I-1. – continued –

Atom	*x/a*	*y/b*	*z/c*	B_{eq} [b]
C(10t)	0.5233(8)	0.055(2)	0.176(2)	2.94
C(11t)	0.5010(8)	0.147(2)	0.095(2)	2.65
C(12t)	0.5361(9)	0.209(2)	0.024(2)	3.66
C(13t)	0.508(1)	0.296(3)	-0.050(2)	5.43
C(14t)	0.4482(9)	0.326(2)	-0.041(2)	5.02
C(15t)	0.4165(7)	0.265(2)	0.030(2)	2.46
C(21t)	0.1472(9)	0.721(2)	0.144(2)	4.65
C(22t)	0.127(1)	0.796(3)	0.046(2)	5.83
C(23t)	0.071(1)	0.796(3)	-0.010(2)	5.77
C(24t)	0.0283(9)	0.725(2)	0.039(2)	4.73
C(25t)	0.0476(9)	0.646(2)	0.133(2)	4.06
C(26t)	0.0048(9)	0.566(2)	0.185(2)	4.02
C(27t)	-0.0568(9)	0.554(2)	0.144(2)	3.97
C(28t)	-0.091(1)	0.474(3)	0.207(3)	6.37
C(29t)	-0.0611(9)	0.410(2)	0.303(2)	4.76
C(30t)	0.0021(8)	0.421(2)	0.332(2)	2.85
C(31t)	0.0420(8)	0.358(2)	0.421(2)	3.05
C(32t)	0.0168(9)	0.282(2)	0.503(2)	3.46
C(33t)	0.0588(8)	0.225(2)	0.588(2)	3.64
C(34t)	0.1200(9)	0.258(2)	0.591(2)	4.94
C(35t)	0.1369(8)	0.330(2)	0.508(2)	3.09
O(1w)	0.0982(7)	0.120(2)	0.138(2)	6.43
O(2w)	0.0101(8)	0.024(2)	0.265(2)	8.75
O(3w)	0.1915(7)	0.026(2)	0.324(2)	7.48
O(4w)	0.0990(8)	0.925(2)	0.436(2)	8.99
O(5w)	0.2767(6)	0.161(2)	0.508(2)	5.95
O(6w)	0.4671(8)	0.579(2)	0.727(2)	9.96
O(7w)	0.2593(7)	0.174(2)	0.756(2)	8.20
O(8w)	0.2929(8)	0.770(2)	0.789(2)	8.04
O(9w)	0.3599(8)	0.581(2)	0.863(2)	8.48
O(10w)	0.0911(7)	0.084(2)	0.877(2)	6.60
O(11w)	0.2825(7)	0.394(2)	0.896(2)	9.66
O(12w)	0.142(2)	0.947(3)	0.706(3)	22.21
N(1a)	0.401(1)	0.515(2)	0.234(2)	8.68
C(1a)	0.368(1)	0.581(2)	0.201(3)	5.73
C(2a)	0.315(1)	0.654(2)	0.160(3)	5.47

[a]Estimated standard deviations are given in parentheses.
[b]$B_{eq} = 4/3\Sigma_i\Sigma_j B_{ij}a_i a_j$.

Table A_I-2. Final Positional Parameters and Isotropic Temperature Factors ($Å^2$) for Hydrogen Atoms in $[Cu_2(\mu\text{-pqq})(terpy)_2]\cdot 12H_2O\cdot CH_3CN$ (2)[a]

Atom	*x/a*	*y/b*	*z/c*	*B*
H(3p)	0.308(8)	0.61(2)	0.61(2)	3(5)
H(8p)	0.205(7)	0.17(2)	-0.02(2)	3(5)
H(1t)	0.303(8)	-0.01(2)	0.37(2)	3(5)
H(2t)	0.297(7)	-0.16(2)	0.52(2)	3(5)
H(3t)	0.391(7)	-0.27(2)	0.60(2)	3(5)
H(4t)	0.484(8)	-0.26(2)	0.50(2)	3(5)
H(7t)	0.564(8)	-0.21(2)	0.40(2)	3(5)
H(8t)	0.644(8)	-0.12(2)	0.29(2)	3(5)
H(9t)	0.617(8)	0.03(2)	0.13(2)	3(5)
H(12t)	0.584(7)	0.19(2)	0.02(2)	3(5)
H(13t)	0.532(8)	0.35(2)	-0.11(2)	3(5)
H(14t)	0.424(7)	0.39(2)	-0.09(2)	3(5)
H(15t)	0.370(7)	0.28(2)	0.04(2)	3(5)
H(21t)	0.194(7)	0.73(2)	0.20(2)	3(5)
H(22t)	0.158(7)	0.86(2)	0.01(2)	3(5)
H(23t)	0.061(8)	0.84(2)	-0.10(2)	3(5)
H(24t)	-0.019(7)	0.74(2)	0.00(2)	3(5)
H(27t)	-0.074(8)	0.60(2)	0.07(2)	3(5)
H(28t)	-0.140(7)	0.47(2)	0.18(2)	3(5)
H(29t)	-0.087(7)	0.35(2)	0.36(2)	3(5)
H(32t)	-0.031(7)	0.27(2)	0.51(2)	3(5)
H(33t)	0.044(7)	0.16(2)	0.65(2)	3(5)
H(34t)	0.151(8)	0.22(2)	0.66(2)	3(5)
H(35t)	0.185(8)	0.34(2)	0.51(2)	3(5)

[a]Estimated standard deviations are given in parentheses.

Table A_I-3. Anisotropic Temperature Factors[a] for Non-Hydrogen Atoms in $[Cu_2(\mu\text{-pqq})(terpy)_2]\cdot 12H_2O\cdot CH_3CN$ (2)[b]

Atom	B_{11}	B_{22}	B_{33}	B_{12}	B_{13}	B_{23}
Cu(1)	0.00094(6)	0.0069(4)	0.0061(3)	0.0014(3)	0.0010(3)	0.0029(6)
Cu(2)	0.00092(6)	0.0069(4)	0.0053(3)	0.0005(3)	0.0004(3)	0.0017(5)
O(4p)	0.0020(4)	0.011(2)	0.010(2)	0.001(2)	-0.002(2)	-0.003(3)
O(5p)	0.0010(3)	0.009(2)	0.008(2)	0.003(2)	-0.001(2)	-0.002(3)
O(15p)	0.0016(4)	0.014(2)	0.010(2)	0.005(2)	-0.001(2)	-0.011(3)
O(16p)	0.0011(4)	0.013(2)	0.011(2)	0.002(2)	-0.001(2)	0.001(4)
O(18p)	0.0021(4)	0.019(3)	0.011(2)	0.006(2)	-0.002(2)	-0.007(4)
O(19p)	0.0013(3)	0.006(2)	0.005(2)	-0.000(2)	-0.000(2)	-0.003(3)
O(21p)	0.0021(4)	0.010(2)	0.008(2)	0.005(2)	0.001(2)	0.004(3)
O(22p)	0.0007(3)	0.011(2)	0.009(2)	0.001(2)	0.001(2)	0.002(3)
N(1p)	0.0009(4)	0.001(2)	0.006(2)	0.000(2)	-0.003(2)	-0.002(3)
N(6p)	0.0015(4)	0.009(3)	0.005(2)	0.006(2)	-0.001(2)	0.000(3)
N(1t)	0.0022(5)	0.010(3)	0.006(2)	0.002(2)	-0.000(2)	-0.003(4)
N(2t)	0.0008(4)	0.003(2)	0.006(2)	0.001(2)	-0.002(2)	-0.003(3)
N(3t)	0.0022(5)	0.006(2)	0.007(2)	0.002(2)	0.000(2)	0.003(4)
N(4t)	0.0011(4)	0.009(3)	0.006(2)	0.001(2)	0.001(2)	0.002(4)
N(5t)	0.0016(4)	0.005(2)	0.008(2)	0.002(2)	0.001(2)	-0.001(3)
N(6t)	0.0011(4)	0.008(2)	0.007(2)	0.002(2)	0.002(2)	-0.000(4)
C(2p)	0.0019(6)	0.008(3)	0.006(3)	-0.001(2)	0.001(2)	-0.010(4)
C(3p)	0.0008(5)	0.009(3)	0.008(3)	0.003(2)	-0.001(2)	-0.007(4)
C(4p)	0.0027(7)	0.011(3)	0.008(3)	0.004(3)	-0.002(3)	-0.003(5)
C(5p)	0.0009(5)	0.011(3)	0.005(3)	0.003(2)	0.003(2)	-0.002(4)
C(7p)	0.0007(4)	0.007(3)	0.006(3)	-0.000(2)	0.001(2)	0.002(4)
C(8p)	0.0013(5)	0.002(2)	0.003(2)	0.001(2)	0.000(2)	0.002(3)
C(9p)	0.0011(5)	0.008(3)	0.003(2)	-0.001(2)	-0.001(2)	0.007(4)
C(10p)	0.0010(5)	0.011(3)	0.003(3)	0.003(2)	0.001(2)	-0.001(4)
C(11p)	0.0007(5)	0.008(3)	0.007(3)	0.001(2)	0.002(2)	0.002(4)
C(12p)	0.0008(5)	0.008(3)	0.005(3)	0.001(2)	0.001(2)	0.000(4)
C(13p)	0.0010(5)	0.007(3)	0.004(2)	-0.001(2)	-0.001(2)	-0.001(4)
C(14p)	0.0015(5)	0.005(3)	0.006(3)	-0.000(2)	-0.000(2)	-0.006(4)
C(17p)	0.0010(5)	0.011(3)	0.005(3)	0.003(2)	0.001(2)	-0.001(4)
C(20p)	0.0012(5)	0.005(3)	0.002(2)	-0.000(2)	0.001(2)	-0.000(4)
C(1t)	0.0013(5)	0.007(3)	0.003(2)	-0.002(2)	-0.000(2)	0.001(4)
C(2t)	0.0025(7)	0.012(4)	0.007(3)	0.004(3)	0.003(3)	0.010(5)
C(3t)	0.0031(7)	0.010(3)	0.004(3)	-0.004(3)	0.001(3)	0.000(4)
C(4t)	0.0033(7)	0.006(3)	0.007(3)	0.002(3)	0.000(3)	-0.002(4)
C(5t)	0.0012(5)	0.009(3)	0.007(3)	-0.000(2)	0.001(2)	-0.003(5)
C(6t)	0.0018(6)	0.005(3)	0.006(3)	-0.003(2)	0.002(2)	-0.002(4)
C(7t)	0.0042(9)	0.012(4)	0.008(3)	0.008(3)	0.003(3)	0.000(5)
C(8t)	0.0006(4)	0.016(4)	0.009(3)	0.002(2)	-0.001(2)	0.008(5)
C(9t)	0.0007(4)	0.010(3)	0.007(3)	-0.000(2)	0.001(2)	0.004(4)
C(10t)	0.0008(5)	0.008(3)	0.008(3)	-0.000(2)	0.004(2)	0.005(4)
C(11t)	0.0008(5)	0.007(3)	0.006(3)	-0.000(2)	0.000(2)	0.004(4)
C(12t)	0.0016(6)	0.012(3)	0.005(3)	-0.000(2)	0.002(2)	0.002(5)
C(13t)	0.0027(7)	0.015(4)	0.009(3)	0.002(3)	0.005(3)	0.007(5)
C(14t)	0.0019(6)	0.012(4)	0.013(4)	-0.001(3)	0.002(3)	0.009(5)
C(15t)	0.0008(5)	0.006(3)	0.007(3)	-0.002(2)	0.002(2)	0.003(4)
C(21t)	0.0025(7)	0.006(3)	0.014(4)	-0.002(2)	0.005(3)	0.004(5)
C(22t)	0.0029(8)	0.016(4)	0.009(3)	0.000(3)	0.003(3)	0.004(6)
C(23t)	0.0039(8)	0.013(4)	0.008(3)	0.003(3)	-0.001(3)	0.012(5)
C(24t)	0.0014(6)	0.012(3)	0.013(4)	0.000(2)	0.001(3)	0.004(5)
C(25t)	0.0017(6)	0.008(3)	0.012(3)	-0.002(2)	0.004(3)	0.002(5)
C(26t)	0.0017(6)	0.012(3)	0.006(3)	-0.000(3)	0.001(2)	0.007(5)
C(27t)	0.0014(5)	0.009(3)	0.011(3)	0.004(2)	0.001(2)	-0.001(5)

– to be continued –

Table A_I-3. – continued –

Atom	B_{11}	B_{22}	B_{33}	B_{12}	B_{13}	B_{23}
C(28t)	0.0021(7)	0.021(4)	0.011(4)	0.002(3)	-0.000(3)	0.004(6)
C(29t)	0.0014(6)	0.016(4)	0.008(3)	0.004(3)	-0.001(2)	0.005(5)
C(30t)	0.0015(5)	0.007(3)	0.005(3)	-0.000(2)	0.000(2)	0.003(4)
C(31t)	0.0017(6)	0.009(3)	0.003(3)	0.002(2)	0.001(2)	-0.000(4)
C(32t)	0.0022(6)	0.008(3)	0.005(3)	-0.000(2)	0.002(2)	0.004(4)
C(33t)	0.0016(6)	0.007(3)	0.010(3)	-0.000(2)	-0.002(2)	0.009(5)
C(34t)	0.0015(6)	0.011(3)	0.014(4)	0.004(3)	0.002(3)	0.006(5)
C(35t)	0.0011(5)	0.006(3)	0.009(3)	0.000(2)	-0.001(2)	0.005(4)
O(1w)	0.0027(5)	0.013(3)	0.017(3)	0.002(2)	0.004(2)	0.002(4)
O(2w)	0.0034(6)	0.021(3)	0.021(3)	-0.004(2)	0.001(3)	0.015(5)
O(3w)	0.0026(5)	0.018(3)	0.018(3)	0.000(2)	-0.004(2)	0.005(4)
O(4w)	0.0037(6)	0.016(3)	0.026(4)	0.004(2)	0.001(3)	0.001(5)
O(5w)	0.0023(5)	0.013(3)	0.016(3)	-0.001(2)	0.002(2)	0.010(4)
O(6w)	0.0044(7)	0.022(3)	0.022(3)	-0.000(3)	-0.004(3)	-0.004(5)
O(7w)	0.0032(6)	0.022(3)	0.016(3)	0.003(2)	0.001(2)	-0.002(5)
O(8w)	0.0043(6)	0.017(3)	0.015(3)	0.004(2)	0.001(2)	-0.009(4)
O(9w)	0.0039(6)	0.023(3)	0.015(3)	0.002(3)	0.000(2)	0.016(5)
O(10w)	0.0032(5)	0.012(3)	0.017(3)	-0.002(2)	0.002(2)	0.007(4)
O(11w)	0.0028(6)	0.024(3)	0.027(4)	0.003(2)	0.009(3)	0.008(5)
O(12w)	0.016(2)	0.032(5)	0.044(6)	0.021(5)	0.022(6)	0.007(8)
N(1a)	0.0051(9)	0.015(4)	0.019(4)	0.001(3)	0.003(3)	0.006(5)
C(1a)	0.0035(8)	0.009(3)	0.013(4)	-0.004(3)	0.005(3)	0.008(5)
C(2a)	0.0020(6)	0.011(4)	0.015(4)	0.003(3)	0.000(3)	0.012(6)

[a]Temperature factor is expressed in the formura,
$T=1/exp(B_{11}\times h\times h+B_{22}\times k\times k+B_{33}\times 1\times 1+2B_{12}\times h\times k+2B_{13}\times h\times 1+2B_{23}\times k\times 1)$.

[b]Estimated standard deviations are given in parentheses.

Appendix II

Table A_{II}-1. Atomic Coordinates and Equivalent Isotropic Thermal Parameters ($Å^2$) for Non-Hydrogen Atoms in $K_3Hpqq{\cdot}4H_2O$[a]

Atom	*x/a*	*y/b*	*z/c*	B_{eq}[b]
K(1)	0.41995(7)	0.1700(3)	0.60593(8)	2.75
K(2)	-0.14302(7)	0.3644(3)	0.84090(8)	2.83
K(3)	0.23923(7)	0.3705(2)	0.77651(8)	2.36
O(4)	0.0340(3)	0.4260(7)	0.2566(3)	3.41
O(5)	-0.1207(3)	0.3875(7)	0.2823(3)	2.90
O(15)	0.2987(3)	0.2586(7)	0.4944(3)	3.21
O(16)	0.2408(3)	0.1914(6)	0.6194(3)	2.36
O(18)	-0.3297(2)	0.2069(7)	0.5826(3)	2.53
O(19)	-0.3417(2)	0.2014(6)	0.4377(3)	2.51
O(21)	0.0268(3)	0.0846(8)	0.6673(3)	3.77
O(22)	-0.0886(3)	0.0998(7)	0.7261(3)	3.07
N(1)	0.0940(3)	0.2340(7)	0.5360(3)	1.98
N(6)	-0.1822(3)	0.2693(7)	0.4301(3)	1.91
C(2)	0.1632(3)	0.2718(8)	0.4949(4)	1.86
C(3)	0.1447(3)	0.3298(9)	0.4117(4)	2.28
C(4)	0.0135(3)	0.3713(9)	0.3289(4)	2.21
C(5)	-0.0754(3)	0.3499(9)	0.3419(4)	2.11
C(7)	-0.2134(3)	0.2193(8)	0.5042(4)	1.94
C(8)	-0.1671(3)	0.1723(8)	0.5771(4)	2.01
C(9)	-0.0856(3)	0.1798(8)	0.5765(4)	1.83
C(10)	0.0317(3)	0.2656(8)	0.4801(4)	1.96
C(11)	0.0620(3)	0.3279(8)	0.4024(4)	1.76
C(12)	-0.1041(3)	0.2835(8)	0.4270(4)	1.90
C(13)	-0.0511(3)	0.2402(8)	0.4998(4)	1.71
C(14)	0.2408(3)	0.2384(9)	0.5408(4)	1.98
C(17)	-0.3028(3)	0.2094(8)	0.5083(4)	1.60
C(20)	-0.0442(3)	0.1191(8)	0.6636(4)	1.78
O(w1)	-0.2705(3)	0.4165(8)	0.7291(3)	4.48
O(w2)	0.0408(3)	0.0637(7)	0.1189(3)	3.07
O(w3)	0.1360(3)	0.0329(7)	0.8025(3)	3.33
O(w4)	0.4944(3)	0.2074(7)	0.4450(3)	3.04

[a]Estimated standard deviations are given in parentheses.

[b]$B_{eq} = 4/3\Sigma_i\Sigma_j B_{ij}a_i a_j$.

Table A_{II}-2. Final Positional Parameters and Isotropic Temperature Factors ($Å^2$) for Hydrogen Atoms in $K_3Hpqq \cdot 4H_2O$[a]

Atom	*x/a*	*y/b*	*z/c*	*B*
H(3p)	0.308(8)	0.61(2)	0.61(2)	3(5)
H(8p)	0.205(7)	0.17(2)	-0.02(2)	3(5)
H(1t)	0.303(8)	-0.01(2)	0.37(2)	3(5)
H(2t)	0.297(7)	-0.16(2)	0.52(2)	3(5)
H(3t)	0.391(7)	-0.27(2)	0.60(2)	3(5)
H(4t)	0.484(8)	-0.26(2)	0.50(2)	3(5)
H(7t)	0.564(8)	-0.21(2)	0.40(2)	3(5)
H(8t)	0.644(8)	-0.12(2)	0.29(2)	3(5)
H(9t)	0.617(8)	0.03(2)	0.13(2)	3(5)
H(12t)	0.584(7)	0.19(2)	0.02(2)	3(5)
H(13t)	0.532(8)	0.35(2)	-0.11(2)	3(5)
H(14t)	0.424(7)	0.39(2)	-0.09(2)	3(5)
H(15t)	0.370(7)	0.28(2)	0.04(2)	3(5)
H(21t)	0.194(7)	0.73(2)	0.20(2)	3(5)
H(22t)	0.158(7)	0.86(2)	0.01(2)	3(5)
H(23t)	0.061(8)	0.84(2)	-0.10(2)	3(5)
H(24t)	-0.019(7)	0.74(2)	0.00(2)	3(5)
H(27t)	-0.074(8)	0.60(2)	0.07(2)	3(5)
H(28t)	-0.140(7)	0.47(2)	0.18(2)	3(5)
H(29t)	-0.087(7)	0.35(2)	0.36(2)	3(5)
H(32t)	-0.031(7)	0.27(2)	0.51(2)	3(5)
H(33t)	0.044(7)	0.16(2)	0.65(2)	3(5)
H(34t)	0.151(8)	0.22(2)	0.66(2)	3(5)
H(35t)	0.185(8)	0.34(2)	0.51(2)	3(5)

[a]Estimated standard deviations are given in parentheses.

Table A_{II}-3. Anisotropic Temperature Factors[a] of Non-Hydrogen Atoms $K_3Hpqq\text{-}4H_2O$[b]

Atom	B(11)	B(22)	B(33)	B(12)	B(13)	B(23)
K(1)	0.00185(4)	0.0206(4)	0.00206(5)	-0.0018(2)	-0.00029(7)	0.0000(3)
K(2)	0.00202(5)	0.0211(4)	0.00202(5)	0.0016(3)	0.00055(8)	-0.0011(3)
K(3)	0.00188(4)	0.0143(3)	0.00213(5)	0.0010(2)	0.00003(7)	-0.0009(3)
O(4)	0.0025(2)	0.027(2)	0.0021(2)	-0.0016(8)	0.0008(3)	0.0075(9)
O(5)	0.0021(2)	0.022(2)	0.0019(2)	0.0031(7)	-0.0010(3)	0.0023(8)
O(15)	0.0014(2)	0.029(2)	0.0023(2)	0.0003(7)	0.0006(3)	0.0025(9)
O(16)	0.0021(2)	0.015(1)	0.0017(2)	0.0004(6)	-0.0003(3)	0.0002(7)
O(18)	0.0015(2)	0.021(2)	0.0018(2)	0.0001(7)	0.0004(3)	-0.0005(7)
O(19)	0.0015(2)	0.019(2)	0.0021(2)	-0.0010(6)	-0.0008(3)	0.0010(7)
O(21)	0.0014(2)	0.035(2)	0.0028(2)	0.0029(8)	-0.0003(3)	0.0073(9)
O(22)	0.0016(2)	0.025(2)	0.0025(2)	0.0005(7)	0.0005(3)	0.0034(8)
N(1)	0.0011(2)	0.014(2)	0.0019(2)	-0.0005(7)	-0.0004(3)	0.0006(8)
N(6)	0.0014(2)	0.010(2)	0.0021(2)	0.0000(7)	-0.0001(3)	-0.0014(8)
C(2)	0.0014(2)	0.011(2)	0.0018(3)	0.0007(8)	0.0000(4)	-0.0019(9)
C(3)	0.0013(2)	0.015(2)	0.0024(3)	-0.0005(9)	0.0000(4)	-0.002(1)
C(4)	0.0016(2)	0.013(2)	0.0022(3)	-0.0013(9)	0.0001(4)	0.002(1)
C(5)	0.0014(2)	0.016(2)	0.0015(3)	0.0012(9)	-0.0006(3)	-0.003(1)
C(7)	0.0013(2)	0.012(2)	0.0021(3)	-0.0022(8)	0.0008(4)	-0.0017(9)
C(8)	0.0014(2)	0.011(2)	0.0023(3)	0.0013(8)	0.0003(4)	-0.002(1)
C(9)	0.0016(2)	0.009(2)	0.0020(3)	-0.0007(8)	-0.0004(4)	0.0006(9)
C(10)	0.0015(2)	0.010(2)	0.0022(3)	0.0004(8)	-0.0019(4)	-0.001(1)
C(11)	0.0013(2)	0.011(2)	0.0017(3)	-0.0011(8)	-0.0002(3)	0.0004(9)
C(12)	0.0010(2)	0.012(2)	0.0023(3)	-0.0000(8)	0.0006(4)	-0.0030(9)
C(13)	0.0021(2)	0.008(2)	0.0012(3)	-0.0005(8)	0.0006(4)	-0.0012(8)
C(14)	0.0012(2)	0.013(2)	0.0021(3)	-0.0012(8)	-0.0000(4)	-0.003(1)
C(17)	0.0011(2)	0.009(2)	0.0018(3)	0.0014(7)	-0.0005(3)	0.0008(9)
C(20)	0.0015(2)	0.011(2)	0.0016(3)	0.0001(8)	-0.0003(3)	-0.0002(9)
O(w1)	0.0025(2)	0.031(2)	0.0046(3)	0.0023(9)	-0.0005(4)	-0.006(2)
O(w2)	0.0025(2)	0.019(2)	0.0026(2)	-0.0032(7)	-0.0007(3)	0.0023(8)
O(w3)	0.0025(2)	0.022(2)	0.0029(2)	0.0022(7)	-0.0010(3)	-0.0021(8)
O(w4)	0.0019(2)	0.020(2)	0.0030(2)	-0.0011(7)	-0.0005(3)	-0.0006(8)

[a] Temperature factor is expressed in the formura,
$T=1/exp(B_{11}\times h\times h+B_{22}\times k\times k+B_{33}\times l\times l+2B_{12}\times h\times k+2B_{13}\times h\times l+2B_{23}\times k\times l)$.
[b] Estimated standard deviations are given in parentheses.

Appendix III

Table A_{III}-1. Atomic Coordinates and Equivalent Isotropic Thermal Parameters ($Å^2$) for Non-Hydrogen Atoms in $[Cu(DL\text{-topa})(bpy)(H_2O)]BF_4 \cdot 3H_2O$ (**1**)[a]

Atom	x/a	y/b	z/c	B_{eq}[b]
Cu	0.24051(9)	0.12814(13)	0.71115(9)	3.85
O(1)	0.2276(4)	-0.0549(6)	0.7445(5)	4.42
O(2)	0.2862(4)	-0.1950(7)	0.8602(5)	5.15
O(3)	0.3854(4)	0.3591(7)	0.9289(5)	4.76
O(4)	0.0697(4)	0.4518(6)	0.8374(4)	4.27
O(5)	0.0362(4)	0.1900(6)	0.8490(5)	4.86
O(6)	0.2541(5)	0.0793(9)	0.5778(5)	6.95
O(7)	0.4167(4)	0.6320(6)	0.9507(5)	4.72
O(8)	0.1132(5)	0.7138(7)	0.8141(5)	5.82
O(9)	0.0161(5)	0.9251(7)	0.8495(6)	6.10
N(1)	0.2363(5)	0.3236(8)	0.6893(5)	3.93
N(2)	0.1081(5)	0.1501(7)	0.6495(5)	3.80
N(3)	0.3702(5)	0.1002(7)	0.7946(5)	3.47
C(1)	0.3071(7)	0.4057(10)	0.7136(7)	4.61
C(2)	0.2955(7)	0.5435(10)	0.7039(8)	5.31
C(3)	0.2102(8)	0.5965(10)	0.6683(8)	5.56
C(4)	0.1376(7)	0.5120(10)	0.6418(8)	5.22
C(5)	0.1524(6)	0.3753(9)	0.6530(6)	4.06
C(6)	0.0797(6)	0.2755(9)	0.6282(6)	3.80
C(7)	-0.0105(7)	0.3048(11)	0.5846(8)	5.91
C(8)	-0.0726(7)	0.2029(13)	0.5635(9)	6.93
C(9)	-0.0447(7)	0.0738(12)	0.5855(8)	5.99
C(10)	0.0481(7)	0.0511(10)	0.6301(8)	5.23
C(11)	0.2888(6)	-0.0917(9)	0.8194(7)	4.00
C(12)	0.3684(6)	0.0047(9)	0.8645(7)	3.92
C(13)	0.3603(6)	0.0803(9)	0.9429(6)	3.86
C(14)	0.2843(6)	0.1812(9)	0.9150(6)	3.36
C(15)	0.2992(6)	0.3167(9)	0.9104(6)	3.65
C(16)	0.2287(6)	0.4077(9)	0.8861(6)	3.83
C(17)	0.1415(6)	0.3662(9)	0.8640(6)	3.81
C(18)	0.1247(6)	0.2290(9)	0.8693(6)	3.80
C(19)	0.1968(7)	0.1392(9)	0.8949(6)	4.09
B	0.4027(9)	0.8115(14)	0.6124(9)	5.66
F(1)	0.3901(6)	0.9185(8)	0.5565(6)	10.67
F(2)	0.3340(5)	0.7266(8)	0.5715(5)	9.33
F(3)	0.4839(5)	0.7559(8)	0.6279(6)	9.47
F(4)	0.4018(6)	0.8519(8)	0.6925(5)	9.22

[a]Estimated standard deviations are given in parentheses.

[b]$B_{eq} = 4/3\Sigma_i\Sigma_j B_{ij} a_i a_j$.

Table A_{III}-2. Final Positional Parameters and Isotropic Temperature Factors ($Å^2$) for Hydrogen Atoms in [Cu(DL-topa)(bpy)(H_2O)]BF_4·3H_2O (**1**)[a]

Atom	*x/a*	*y/b*	*z/c*	*B*
H_{N3}(1)	0.408(6)	0.059(10)	0.759(6)	3(2)
H_{N3}(2)	0.402(6)	0.193(10)	0.822(7)	3(2)
H_{C1}(3)	0.375(6)	0.363(10)	0.740(6)	3(2)
H_{C2}(4)	0.354(6)	0.611(10)	0.725(6)	3(2)
H_{C3}(5)	0.200(6)	0.704(10)	0.662(6)	3(2)
H_{C4}(6)	0.068(6)	0.551(10)	0.612(6)	3(2)
H_{C7}(7)	-0.031(6)	0.408(10)	0.566(6)	3(2)
H_{C8}(8)	-0.144(6)	0.228(10)	0.528(7)	3(2)
H_{C9}(9)	-0.094(6)	-0.007(10)	0.571(6)	3(2)
H_{C10}(10)	0.073(6)	-0.050(10)	0.652(6)	3(2)
H_{C12}(11)	0.431(6)	-0.053(10)	0.890(6)	3(2)
H_{C13}(12)	0.423(6)	0.132(9)	0.981(6)	3(2)
H_{C13}(13)	0.351(6)	0.007(10)	0.988(6)	3(2)
H_{C16}(14)	0.243(6)	0.514(10)	0.883(6)	3(2)
H_{C19}(15)	0.184(6)	0.033(10)	0.898(7)	3(2)

[a]Estimated standard deviations are given in parentheses.

Table A_{III}-3. Anisotropic Temperature Factors ($\times 10^5$)[a] of Non-Hydrogen Atoms in [Cu(DL-topa)(bpy)(H_2O)]$BF_4 \cdot 3H_2O$ (1)[b]

Atom	B_{11}	B_{22}	B_{33}	B_{12}	B_{13}	B_{23}
Cu	397(6)	661(13)	445(7)	58(18)	-7(11)	165(18)
O(1)	418(35)	625(69)	573(40)	36(77)	-138(58)	256(85)
O(2)	513(38)	818(76)	647(45)	-14(89)	35(66)	549(98)
O(3)	371(33)	1010(81)	630(41)	-143(88)	159(59)	-28(99)
O(4)	369(33)	856(73)	548(40)	230(80)	136(58)	163(88)
O(5)	320(32)	868(74)	776(48)	-186(81)	214(63)	-124(100)
O(6)	739(51)	1934(126)	585(47)	778(133)	400(79)	169(128)
O(7)	432(34)	927(76)	567(40)	9(90)	39(59)	9(97)
O(8)	594(42)	831(79)	823(52)	12(96)	377(77)	-19(108)
O(9)	614(45)	841(79)	894(56)	-194(97)	455(81)	-214(111)
N(1)	449(43)	870(88)	349(41)	72(99)	59(68)	211(93)
N(2)	357(38)	722(86)	450(43)	39(93)	3(64)	153(99)
N(3)	297(35)	663(82)	433(41)	-126(84)	-32(60)	184(93)
C(1)	509(57)	831(114)	504(58)	-200(130)	108(91)	148(132)
C(2)	610(66)	899(125)	576(67)	-335(143)	99(104)	253(144)
C(3)	810(75)	549(106)	611(65)	-96(139)	232(111)	26(132)
C(4)	628(66)	769(112)	591(67)	240(141)	134(102)	200(143)
C(5)	538(53)	735(101)	369(49)	16(133)	156(80)	108(127)
C(6)	448(51)	814(106)	310(46)	275(122)	-60(77)	-57(119)
C(7)	514(62)	1137(135)	751(78)	272(154)	81(110)	196(173)
C(8)	371(57)	1609(172)	994(97)	307(165)	16(118)	155(216)
C(9)	432(59)	1392(152)	753(77)	-342(154)	58(104)	296(179)
C(10)	499(59)	819(117)	657(70)	-340(132)	-69(100)	20(145)
C(11)	359(47)	765(107)	522(56)	50(112)	170(81)	85(123)
C(12)	404(50)	628(97)	485(55)	72(114)	63(81)	223(123)
C(13)	329(46)	863(106)	432(52)	175(114)	-43(76)	322(125)
C(14)	395(47)	728(97)	302(44)	-113(111)	96(74)	-30(109)
C(15)	386(49)	686(97)	377(48)	-254(112)	-68(78)	15(116)
C(16)	432(50)	792(106)	372(49)	-152(118)	73(78)	79(117)
C(17)	425(48)	673(95)	421(50)	161(120)	87(78)	25(124)
C(18)	515(54)	769(103)	293(45)	-78(122)	97(80)	-59(115)
C(19)	602(56)	545(92)	354(47)	-46(125)	-3(82)	203(118)
B	654(81)	1134(158)	563(77)	-205(186)	191(127)	153(185)
F(1)	1385(75)	1578(107)	1242(68)	-25(143)	933(117)	1150(143)
F(2)	1023(55)	2263(127)	837(51)	-1594(143)	328(84)	-609(133)
F(3)	843(50)	2152(126)	1135(62)	708(131)	510(91)	-476(144)
F(4)	1063(57)	2167(127)	826(50)	157(138)	425(87)	-928(133)

[a] Temperature factor ($\times 10^5$) is expressed in the formura,
$T=1/\exp(B_{11} \times h \times h + B_{22} \times k \times k + B_{33} \times l \times l + 2B_{12} \times h \times k + 2B_{13} \times h \times l + 2B_{23} \times k \times l)$.

[b] Estimated standard deviations are given in parentheses.